STRUCTURING SILICONE ELASTOMERS

INTERCHAIN SILICONE INTERACTIONS: STRUCTURING SILICONE ELASTOMERS USING PHYSICAL, COVALENT, AND INTERFACIAL CHEMISTRY

By AMANDA SARA FAWCETT, H.B.Sc.

A Thesis

Submitted to the School of Graduate Studies

In Partial Fulfillment of the Requirements for the Degree of

Doctor of Philosophy

McMaster University Doctor of Philosophy (2013) Hamilton, Ontario (Chemistry)

TITLE: Interchain Silicone Interactions: Structuring Silicone Elastomers Using Physical, Covalent, and Interfacial Chemistry

AUTHOR: Amanda S. Fawcett, H.B.Sc. (McMaster University)

SUPERVISOR: Professor Michael A. Brook

NUMBER OF PAGES: xiv, 120

Abstract

Silicone polymers, particularly PDMS (poly(dimethylsiloxane)) exhibit a wide range of exceptional properties including optical transparency, biostability, hydrophobicity and excellent oxygen transmissibility that make them extremely useful in a wide range of applications, particularly as biomaterials. Current methods for the preparation of silicone elastomers have been well documented, however, silicone elastomers are thermoset materials and once cured, they cannot be reformed without chemical intervention. The properties of silicones that make them a popular material choice in a wide variety of industries also make them un-responsive and non-reusable often limiting their application to one primary purpose.

This thesis aims to further understand the mechanisms of silicone polymer chain interactions and how the chemistry of polymer modification can alter the mechanical and chemical properties of materials. The effects of distinctive functional groups (coumarin) on silicone chains to allow for both the formation of thermoplastic silicone elastomers and stimuli-responsive elastomers for reversible crosslinking are explored.

A companion study examined a different way to form silicone elastomers. The Piers-Rubinsztajn reaction was used to create elastomers and foams rapidly and under relatively mild conditions using very small quantities of the catalyst $B(C_6F_5)_3$. The factors required to create – on demand – a foam or an elastomer, and the strategies to control physical properties, including bubble density and modulus, are explored.

Silicone foams that were structured in a completely different way are described. Allyl-modified PEG (poly(ethylene glycol)) was found to structure foam mixtures precure. The product foam after cure was amphiphilic, due to the presence of both silicone and PEG constituents. The origins of bubble stabilization and the ability to control foam properties are described.

Acknowledgements

First and foremost I would like to thank my supervisor Dr. Mike Brook for all of his guidance, helpful advice (chemistry and otherwise), and quirky commentary during my years in his research group. I definitely would not have been able to become the researcher and person I am today without his excellent teaching ability. Thank you for providing me with so many unique experiences that I will never forget. I will always remember the effort and direction you gave so I could participate in and learn so many different research projects. Thank you for being such a wonderful supervisor!

I would like to thank all of the Brook Research Group members past and present: we have definitely had some amazing experiences together and I'm grateful for your friendship and support. I want to give a big thank you to Dan and Ferdinand for all of their help and guidance over the years. Thank you so much for taking the time to listen and help me sort through roadblocks whenever they came up. I also want to thank my summer students Meera and Tara, thank you for all your help and effort – I truly appreciated it!

I also want to thank my committee members Dr. Heather Sheardown for her advice and guidance on all things biomedical and Dr. Harald Stöver for his thoughts and guidance for the chemistry side of my projects. I would also like to thank the Department of Chemistry, in particular: Dr. Bob Berno for his help with my NOE experiments, Frank Gibbs for all his help with DSC, and Elizabeth Takacs for her help with rheology and Instron experiments. I'd also like to thank the 20/20: NSERC Ophthalmic Materials Network for financial support of my research, the stimulating research discussions, and great times.

I would like to thank my parents – Don and Linda – and my grandparents for all of their support along the way, challenging me and reading all of my published papers even though they had no idea what I was talking about. I want to thank my brother and the rest of my family and friends: I love you all so dearly and am grateful for having you in my life.

I want to give a giant thank you to John Grande. The start of our friendship in the early years of our Ph.D. gave me the push I needed to keep going even when nothing was working; everyday you make me a better person and I'm inspired by you to be the best I can be. I feel so lucky everyday to have you in my life and cannot wait to begin our lives together – I love you! Lastly, to my good friends Helen So and Casey Gardner: Thank you so much for always being there when I needed to vent and for all of the help and advice you've given for my graduate, chemistry and life problems – you are the best!

TABLE OF CONTENTS

LIST OF FIGURES AND TABLES

List of Abbreviations and Symbols

PDMS	Poly(dimethylsiloxane)
PEG	Poly(ethylene glycol)
C-PDMS	Coumarin-PDMS
MW	Molecular Weight
G’	Storage Modulus
G”	Loss Modulus
λ	Wavelength
TMOS	Tetramethyl orthosilicate
TEOS	Tetraethyl orthosilicate
TPOS	Tetrapropyl orthosilicate
MTES	Methyltriethoxysilane
IT	Iodopropyltrimethoxysilane
TV	Tetravinylsilane
D_4	1,1,3,3,5,5,7,7-octamethylcyclotetrasiloxane
NOE	Nuclear Overhauser effect

CHAPTER 1: Introduction

1.1 Silicone Polymers

Although the history of silicone polymers is relatively short in comparison to its carbon-based analogues, the sheer magnitude of its current production and uses indicates how truly unique and valuable the materials are. Silicones were discovered in the early 1900's by Fredrick S. Kipping, who coined the term silicone for compounds of molecular formula RR'SiO, which he thought at the time were similar in structure to analogous carbon-based ketones.[1, 2] A cheaper, more efficient method for manufacturing silicones was developed in the early 1940's,[3] which initiated the commercial production of silicones, today several billion kilograms are produced each year.[4] The silicon-oxygen backbone (Figure 1.1) provides the unique properties of silicone polymers that make them so attractive for so many industries: electrical resistance, optical clarity, flexibility, stability over a wide range of temperatures (-100 – 250 °C because of the low T_g of -127 °C), oxygen transmissibility, and stability to oxidation in chemical or biological environments.[5] There are several processes available for synthesizing and crosslinking silicone polymers.

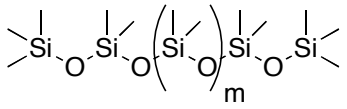

Figure 1.1. Poly(dimethylsiloxane) structure

1.1.1 Silicone synthesis

The starting material for silicone polymers is typically dimethyldichlorosilane, which hydrolyzes in the presence of water to give silanols that can dimerize to give a disiloxane. This procedure repeats to give cyclic oligomers such as D_4 (octamethylcyclotetrasiloxane) shown in Figure 1.2.

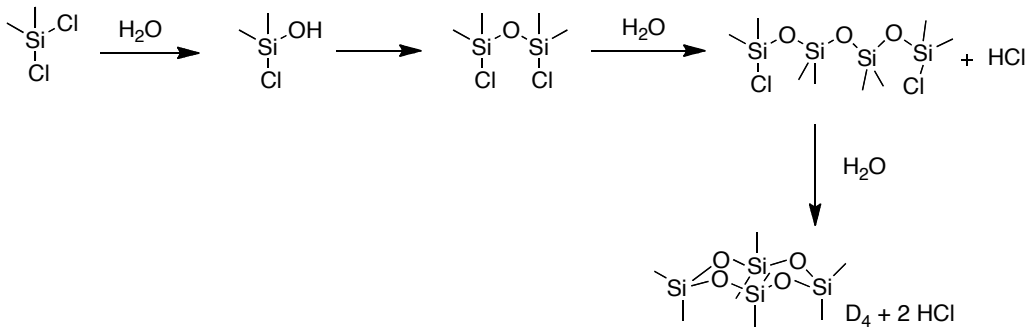

Figure 1.2. Typical cyclic oligomer precursor formation for linear silicone polymers

Longer silicone polymer chains can be synthesized from the cyclic precursors through an acid/base equilibrium reaction (Figure 1.3). Dimethylsilicone polymers exhibit low surface activity because of two structural properties: the flexible Si-O-Si backbone and the hydrophobic methyl groups.[1], When combined with the flexible Si-O-Si backbone the hydrophobic methyl groups can preferentially orientate at interfaces, promoting easy spreading of silicones across surfaces.[6]

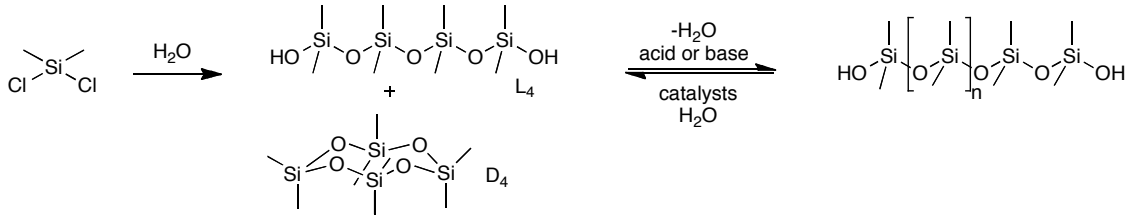

Figure 1.3. Typical industrial synthesis of silicone polymers[7]

1.1.2 Controlled silicone architecture

Over the last decade, new methods for silicone polymer synthesis have been developed utilizing the dehydrocarbonative condensation of alkoxysilanes and hydrosilanes with a catalytic amount of trispentafluorophenylborane – the Piers-Rubinsztajn reaction – to rapidly form controlled complex 3D structures (Figure 1.3).[7-10] The mechanism forms gaseous alkane byproducts while forming new Si-O bonds, and is thought to involve complexation of the Lewis acidic boron with the hydrosilane (Figure 1.3). Addition of the alkoxysilane produces the key intermediate for both the desired reaction products (b) and the metathesis product to form (c).[9]

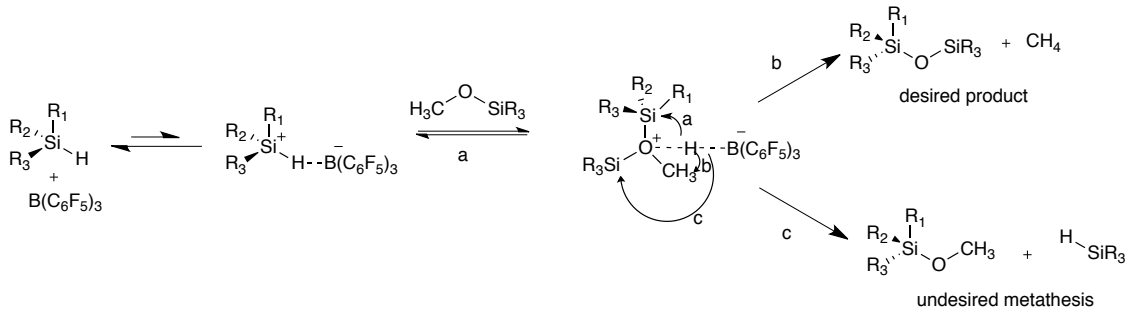

Figure 1.4. Mechanism for Piers-Rubinsztajn reaction[9]

The reaction has been used to create small functional molecules, as the reaction is tolerant to functional groups like halides and allyl or vinyl groups (with low catalyst loadings).[9] This allows molecules or polymers to be formed that contain reactive functional groups, which can undergo further chemistry after the Piers-Rubinsztajn reaction is complete.

1.1.3 Silicones as Ophthalmic Biomaterials

In ophthalmology, one important goal is to create devices that allow for the correct dosage of pharmaceutical drug to reach the required tissue without causing any damage to healthy tissues. In order for a material to be considered biocompatible it must fulfill the following requirements: no inflammatory, toxic, or allergic response, no protein denaturation, no immunological response, no carcinogenic effect, and no tissue damage.[11]

Silicones have an extensive history as ophthalmic biomaterials and, for example, have been used for contact lenses since 1966.[12] The properties that make silicones such excellent ophthalmic materials are their optical transparency, oxygen transmissibility, flexibility, low toxicity, thermal and oxidative stability, and moldability. There are a few problems with using solely silicone elastomers for anterior ophthalmic applications, for example, as contact lenses. In particular, the hydrophobic nature of the silicone surface causes the lens to not sit on the hydrophilic tear film but adhere directly to the cornea, which results in damage to the eye.[13] Modification of these silicone lenses was necessary in order to create a safe and successful material.

Besides improving impaired vision at the anterior segment of the eye, silicones have the potential to also help in restoring or preventing loss of vision in the posterior segment (the structure of the eye can be found in Figure 1.5A). Posterior disorders range from degenerative diseases such as age-related macular degeneration (AMD) and diabetic retinopathy to infections and traumas. AMD is the leading cause of irreversible blindness in the developed world for people 50 years of age or older.[14] The macula is responsible for central high-resolution visual acuity and is a part of the retina, it allows for individuals

to read and recognize faces. Over time, the degradation of the internal acellular matrix can cause the formation of focal deposits, called drusen. When the concentration of drusen in the eye is very high damage to the retinal pigment epithelium can occur which in turn can cause retinal atrophy and lead to choroidal neovascularization, and loss of vision.[14] Diabetic retinopathy (DR) is the leading cause of reversible blindness among adults in the United States, with over 20 million having diabetes and 50 million having prediabetes (this number is expected to double over the next 20 years). Almost all patients that have diabetes will have some form of DR, these staggering numbers and cost of healthcare leads to a drain on the national healthcare system.[15] Like AMD, diabetic retinopathy causes vision loss through vitreoretinal neovascularization; in this case from the release of growth factors because of retinal ischemia.

Standard treatment for DR includes retinal laser photocoagulation (very invasive, with adverse effects) in order to reduce the amount of neovascularization.[15] For both DR and AMD vascular endothelial growth factor (VEGF) is responsible for the loss of vision and promotion of blood vessel formation. By inhibiting VEGF vision loss can be slowed and the diseases managed. Bevacizumab or Avastin® is the current leading VEGF inhibitor that is injected into the vitreous humor to get to the retina.[16] Many drugs cannot make it through the blood-retinal and blood-aqueous barriers and therefore need to be injected intravitreally: eye drop formulations do not work with this drug. Aside from the unpleasant aspects of administration using a needle in the eye, the main disadvantage to intravitreal injections is the rapid clearance of the drug from the vitreous humor causing the available concentration to fall below therapeutic levels too quickly (drug dependent, the loss can be over a few days, Figure 1.5C), in addition to the risk of infection from repeated injections and patient compliance.[17] Several polymeric drug delivery mechanisms have been proposed to overcome the drawbacks of intravitreal injection.

In order to design materials and methods for drug delivery that are superior to intravitreal injections, not only does the rate and concentration of drug released need to be controlled but patient comfort and compliance need to be considered. Current devices release drug at a set rate over time either via biodegradation or diffusion, without the opportunity to change the release rate to coincide with patient requirements:[18-22] current methods for ocular drug delivery are shown in Figure 1.5B. There are several device designs that can be used to deliver controlled release of drug including: particulate systems and implantable solid release materials; these are subdivided into two categories: biodegradable and non-biodegradeable.[21] Particulate systems are advantageous due to their microscopic size, which allows for easy implantation into the vitreous body. The main disadvantage with these systems is extended release and ensuring the drug that is released goes to the retina where it is needed. The microparticules or capsules can float

freely in the vitreous space and therefore, there can be non-uniform drug delivery.[17]

Solid substrate drug delivery devices can overcome the drawbacks of particulate systems because the rate of drug release can be extended and the device can be strategically placed where it will remain in place for the duration of treatment. Biodegradable implants have the advantage of not needing to be removed from the eye after drug release and the rate of release is fairly controlled with the rate of degradation; however, the materials tend to usually only last for a few weeks to months and have a final uncontrolled burst of drug release. Non-biodegradable materials have a controlled release duration of 1 to ~3 years; however, the device requires surgical intervention to remove the device after the drug has been depleted. With these "one-time" implantation devices there is improved patient comfort and compliance.[21]

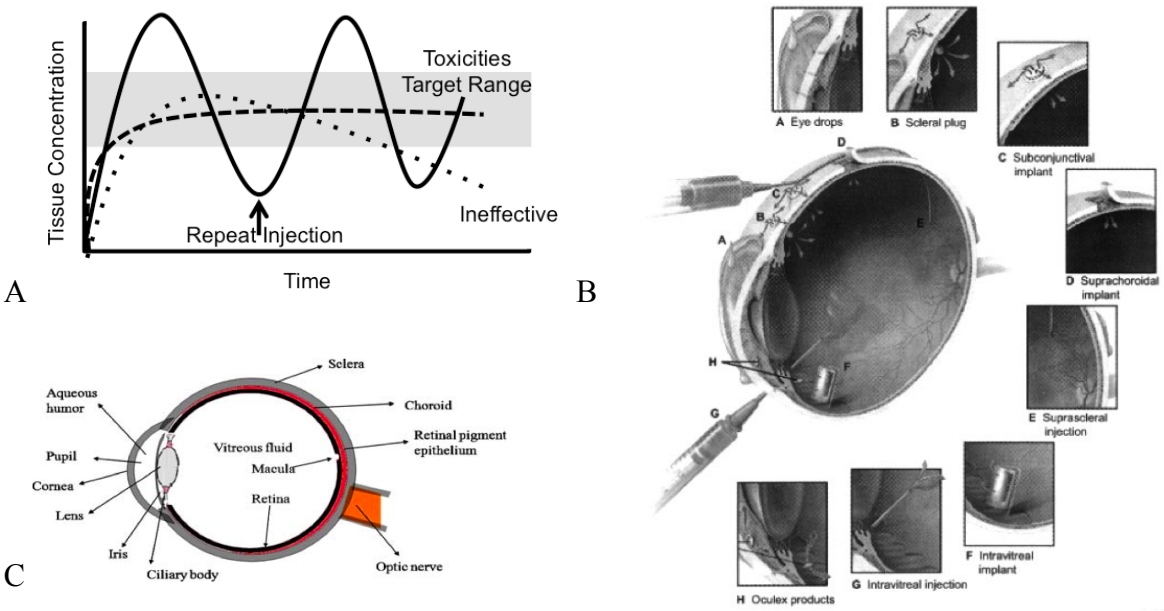

Figure 1.5. A: Structure of the eye.[22] B: Methods of ocular drug delivery.[23] C: Release profile for intravitreal injections

There are currently non-biodegradable materials on the market such as Retisert®, Vitrasert® and Iluvien®. Retisert® and Vitrasert® both are implanted surgically and require surgical explantation: both materials have had reported problems with either cataract formation or retinal detachment. Iluvien® can be inserted through a one-time injection due to its very small size, and is designed to deliver a specific daily dosage for 2-3 years after injection. The main disadvantages to the current drug delivery processes (besides their methods of implantation and explantation, are the rate of drug release. There is no process in place to change the concentration of drug delivered. It would be more beneficial to the patient and their disease management if there were a way to

control the rate of drug delivery on a medium timescale through a non-invasive method, while still having a long-term delivery device implanted through injection.

In order to design a more efficient and compatible ophthalmic drug delivery device the advantages and disadvantages of current systems can be examined to determine the best route to an optimal material. For example, a material that can be easily injected would be ideal, with the ability to externally control the rate of drug delivery, and easily remove the device after delivery is complete. Silicones provide an opportunity to create such materials and have also been used in the posterior segment of the eye for scleral buckles and vitreous substitutes, their flexibility and hydrophobicity could prove to be useful properties for the development of a non-biodegradable implant.

Creating materials from which drugs can be released non-invasively at a controlled rate over extended periods of time, with an option for altering the therapeutic range "on-demand" to coincide with patient needs, would overcome the short-comings of intravitreal injections. One method for "on-demand" drug release that would be non-invasive would be through the use of an external stimulus. Creating a material that would respond to a non-invasive stimuli for initiating drug release could be an effective way of ensuring patient compliance and efficient drug delivery, while minimizing side effects which exist with current drug delivery devices.

Previous work on stimulus-responsive materials for ophthalmic drug delivery has been done with a variety of stimuli such as ion-, pH-, and temperature-responsive polymers. Temperature-sensitive polymers that gel *in situ* are probably the most studied class of materials due to their ease of insertion into the eye. They can be injected as a liquid, and will gel into a solid at room temperature because of the lower critical solution temperature (LCST) of the polymer, for example poly(N-Isopropylacrylamide) (PNIPAAm), which has an LCST of 32 °C.[24] One disadvantage to these systems in regards to the properties outlined, compared to ideal ophthalmic drug delivery materials, is the inability to alter or change the amount of drug delivered "on-demand". The drug would be encapsulated during gelling and diffuse out at a controlled rate.

Recently, photoresponsive magnetic nanoparticles have been developed using coumarin as a two-photon phototrigger for targeted drug delivery of an anticancer drug.[25] The ability to perform two photon experiments to initiate controlled drug delivery would be ideal in the ophthalmic environment. In this way, light of the visible wavelength can pass through the cornea, without damaging it, and combine with another wavelength of visible light of the same wavelength and intensity to initiate a coumarin response and induce a specific concentration of drug to be released.[26-28]

The development of a light-activated delivery device that can change its internal structure to allow release would require the use of a flexible and biocompatible polymer. The properties of silicones make them an excellent candidate to create such delivery materials. Altering the structure of the silicone polymers with functional groups offers possibilities for change in both properties and how the polymers will behave when inserted into an ophthalmic environment. Specifically, the incorporation of photoresponsive groups onto the silicone backbone could allow for the formation of novel drug delivery materials that would not only overcome the issues with intravitreal injections, but would surpass problems associated with current drug delivery materials.

1.2 Functional Silicones

Silicones are extremely susceptible to rearrangement in the presence of acid or base and it is this susceptibility that allows for formation of larger functional polymer chains. When functional silicone end groups are combined with the cyclic oligomers and acid/base catalyst, the reaction proceeds in an equilibrium between cyclic and linear systems.[1] Functional linear silicone polymers (PDMS (poly(dimethylsiloxane))) can be synthesized from the cyclic products of this process (Figure 1.4). Using this method, many functional silicone polymers can be synthesized: halogenated, vinyl, allyl, etc. The placement of the functional groups can be on the termini of the polymers, along the polymer backbone, or a combination of the two (Figure 1.5).

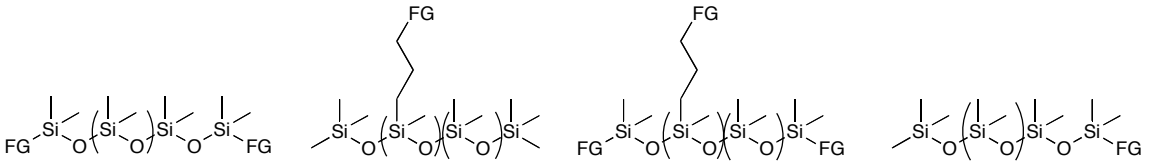

Figure 1.5. Possible functional group (FG) placement

1.2.1 Click Chemistry

The incorporation of particular functional groups onto silicones allows for a variety of chemical transformation reactions to occur. One reaction of interest, in particular, is the Huisgen 1,3-dipolar cycloaddition reaction of azides and alkynes. This reaction falls under the category of "click" chemistry, which was named by Barry Sharpless[29] and includes any reactions which can be done in the presence of water or air with no disagreeable by-products, and are high yielding with simple product isolation. The cycloaddition reaction of azides and alkynes is one of the most widely reported click reaction in literature to date.[29-36] The azide (4π electrons) acts as the dipole and the alkyne

(2π electrons) the dipolarophile; both participate in a thermally allowed [4+2] cycloaddition, forming a 1,2,3-trizaole. Using FMO theory it is known that the HOMO of the azide overlaps with the LUMO of the alkyne, if the alkyne is conjugated and made into an even better dipolarophile, the energy gap of the HOMO-LUMO can be overcome to favour the thermal reaction at room temperature (Figure 1.6).[37]

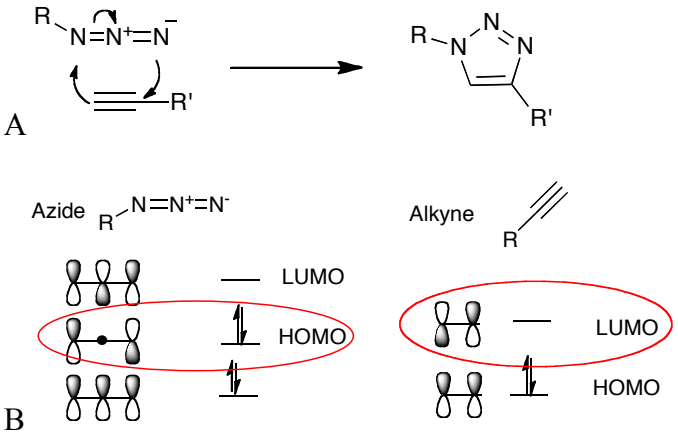

Figure 1.6. A: Thermal cycloaddition of an azide and alkyne, B: molecular orbitals of the azide and alkyne showing the correct orientation for cycloaddition with the HOMO of the azide and LUMO of the alkyne

Introducing functional groups onto silicones that allow for azide-alkyne click chemistry to occur has several advantages. The ease of reaction and simplicity of work up with no by-products permits the preparation of novel materials that can not only be synthesized reproducibly, but also introduces a relatively straightforward transition to industrial manufacturing.

1.2.2 Rheology

The incorporation of low molecular weight (< 1 kDa) functional groups onto silicone polymer chains will change how the polymer chains interact with one another and their mechanical properties; however, typically the extent to which various molecular substitutes will alter the properties is limited.[38] One change functional groups impose on silicone polymers can include a difference in viscosity, rheology is used to measure this change. Rheology measures the change in deformation resulting from an applied force, and is particularly useful when characterizing viscoelastic materials. Many polymers for biomedical applications exhibit viscoelastic behavior, meaning they exhibit both viscous and elastic behaviors in the liquid state. The viscosity of a polymer is proportional to its molecular weight (MW) when below a certain critical value (MC), the shear viscosity is

proportional to 3.4^{th} the power of the MW when greater than MC. When the MW is less than MC the polymer is considered to be unentangled, and when it is greater it is considered entangled. Entangled polymers are highly viscoelastic while unentangled polymers are not.[39]

When silicone oils are crosslinked, the polymer properties will change from being purely viscous to viscoelastic to elastic (a high concentration of crosslinks). When strain is applied, the response of the polymer is described by shear modulus (G). In a viscoelastic material when a strain is applied, some of the energy will be stored (elastic portion, G') and some will be dissipated (viscous portion, G"). When measuring the viscoelasticity of materials, as a strain is applied at a specific frequency, the G' response will be in phase, where as the G" response will be out of phase by 90°. The combination of the elastic and viscous responses provides information on the viscoelastic nature of the material (how much lag displays the quantity of viscous response in a viscoelastic material). It is possible to measure both the elastic and viscous nature of polymers and how small changes along the polymer backbone or within a material affect these two properties using parallel plate rheology.[40] In some cases the effect of polymer crystallinity can provide the effect of crosslinking. For example, when linear hydrocarbon polymers are cooled from the melt they can form crystallized, closely aligned, regions such that the van der Waal's interactions can be maximized.[40]

The elastic modulus is used to quantify how changes along the polymer backbone or how the concentration of crosslinks within a material affect its mechanical properties. When a strain is applied to a crosslinked elastomer the conformation of the polymer chains are confined by the crosslink sites, this causes the elastic modulus to increase with an increase in temperature – instead of decreasing like other materials (think of a solid melting vs. an elastomer becoming more springy).[40] The viscosity of dimethylsilicone polymers has less dependence on temperature than hydrocarbon analogues, due to silicone thermal stability; the lowest viscosities achievable at high temperatures are limited by chain entanglements when molecular weights are high.[6]

It is useful to measure how materials react to oscillating stress over time, in order to give an approximation of how they will behave in their potential applications. For instance, when interactive fillers are added to a polymer network, the change in the viscoelastic nature of the polymers over time provides information on how the material behaves under shear over time. Self-associating polymers will also demonstrate unique properties over time, as the change in chain entanglement under shear will provide useful information on the viscoelastic nature of the polymer.

1.2.3 Thesis Focus (I)

The low intermolecular interaction between silicone polymers gives silicones a high free volume. The incorporation of functional groups along the silicone backbone has potential to change the mechanics of how polymer chains interact with one another. The focus of Chapter 2 in this thesis is to better understand the effects of incorporating small functional groups along linear silicone polymers. It is hypothesized that the addition of small molecules that have an affinity for each other within the silicone chains will change how the polymers interact with each other, either increasing or decreasing the free volume of the chains.

This thesis focuses on determining the effect of incorporating 7-hydroxycoumarin onto the backbone of a linear silicone polymer. As will be discussed, coumarins can undergo a reversible [2+2] photocycloaddition, however, Chapter 2 examines only the effect on the silicone polymer chains when the coumarins are attached. Varying the concentration of coumarin along the silicone chain changes the polymer-polymer interactions, which were monitored by both rheology and NMR. The incorporation of coumarin onto silicone polymers could prove to be interesting for novel ophthalmic drug delivery applications. By changing the free volume of the modified polymers, the properties of the silicone chains will also be modified, this could allow for materials which, through an external stimuls such as heat or light, can change its crosslink density..

1.3 Chemical Crosslinking of Silicones

1.3.1 Elastomer Synthesis and Characterization

The crosslinking of silicone polymers allows one to take advantage of the polymer's properties to permit applications from biomaterials to the automotive industries. Because of the polymer's flexibility – crosslinked PDMS forms elastomers, resins, or coatings. Although a variety of different processes can be employed to crosslink silicones,[41] room-temperature vulcanization (RTV) methods have been examined in detail in the thesis and will be discussed here.

The platinum-catalyzed RTV of silicone elastomers takes advantage of the hydrosilylation reaction between the Si-H group and olefins, typically performed by combining vinyl-terminated PDMS with a poly(hydridomethylsiloxane-dimethylsiloxane) copolymer. In commercial systems, for example, Sylgard 184, the platinum catalyst is

combined with the vinyl-terminated PDMS "base" which is then mixed with the hydrosilane 'crosslinker' to initiate the crosslinking process. The pre-elastomer mixture is poured into a mold and left to cure at room temperature, or alternatively can be heated to encourage faster curing rates. The proposed mechanism for curing with Karstedt's platinum catalyst is shown in Figure 1.7A. A second possible cure mechanism can occur under these conditions. The Si-H bond can undergo hydrolysis in the presence of water and Pt catalyst to form silanols. A silanol and a silane can condense to form a new siloxane bond, and give off hydrogen gas ($R_3Si\text{-}OH + H\text{-}SiR'_3 \rightarrow R_3Si\text{-}O\text{-}SiR'_3 + H_2$). Loss of a limited concentration of Si-H will still allow for crosslinking, thus this process can be considered robust in slight humid environments.

A completely different process exploits the hydrolysis of functional silanes. Tin compounds catalyze the hydrolysis and condensation of functional silanes, and may be formulated as a two-part curing RTV system where one part is silanol-terminated PDMS and the other is the tin catalyst and crosslinker ($R_2Sn(O_2CR')_2 + MeSi(OR'')_3$), or a one part system in which the only missing ingredient is water: exposure to moisture starts the cure. There are several proposed mechanisms in which water acts as a co-catalyst, to initiate catalyst activation and nucleophilic substitution of the silicone (Figure 1.7B).

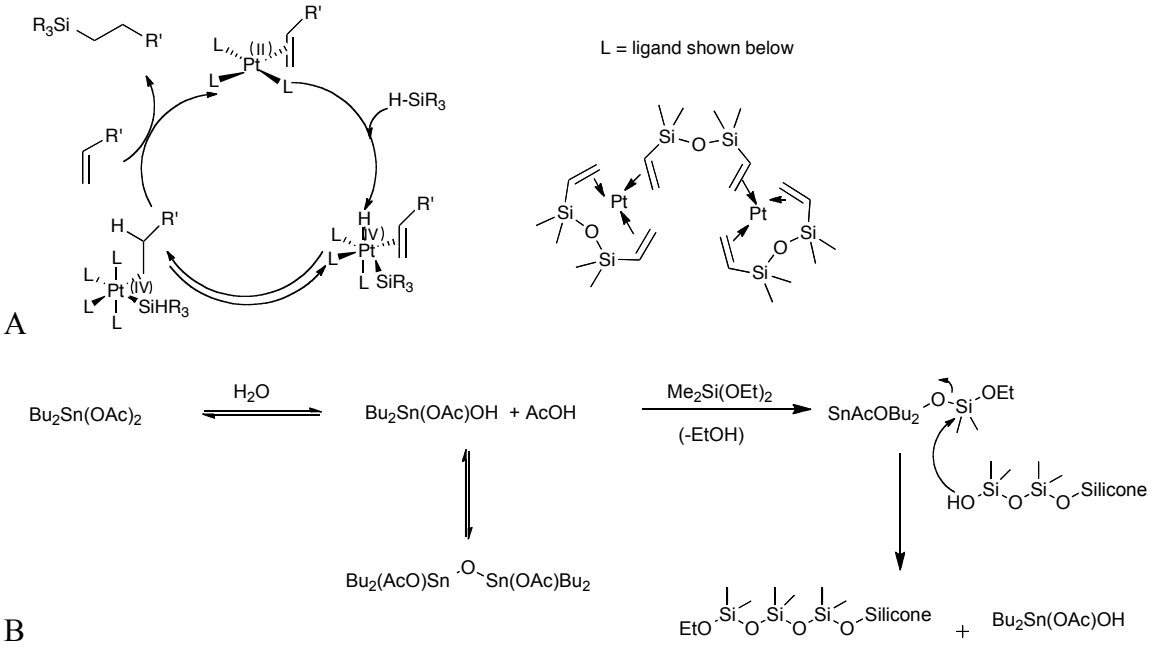

Figure 1.7 A: Proposed mechanism for platinum-catalyzed hydrosilylation. B: Proposed tin catalyst mechanism for formation of silicone elastomers[1]

1.3.1.1 Shore Hardness

The mechanical hardness of elastomers is often characterized by Shore A or other Shore hardness measurements. The relative deformation a material can withstand when deformed with a Shore A durometer can be indicative of the crosslink density of the elastomer. Shore A hardness from 20-90 can be obtained through RTV silicone elastomer synthesis, however, 50-70 has been shown to generally give optimal mechanical properties for many applications including the aerospace and automotive industry as well as for biomaterials.[41]

1.3.2 Stimuli-Responsive Materials

Stimuli-responsive materials have become a popular research topic over the last decade due to their unique ability to perform specific functions "on-demand". By incorporating functional molecules or groups onto polymer chains, the polymer properties can be modulated in response to stimuli.[42] The effects of the stimulus on the polymer can range from altering its solubility, structure and intermolecular associations to inducing bond formation or breakage.[43] For example, the synthesis of photo-responsive polymers would allow for a non-invasive chemical change within the polymeric material. This would be particularly useful for ophthalmic materials, since light can be focused with high accuracy on a specific site in the eye. There are several examples of photoactive small molecules that could be attached onto a silicone backbone to induce material change, however, the research in this thesis has focused on coumarin.

1.3.3 [2+2] Photocycloaddition of Coumarin

Coumarin is a lactone derivative of cinnamic acid, and can undergo a [2+2] photocycloaddition with wavelengths > 300 nm; the resulting cyclobutane rings can be photocleaved with wavelengths < 300 nm,[44] suggesting the materials have promise as reversibly responsive materials (Figure 1.8A). The 2 π electrons on the carbons of the α,β-unsaturated carbonyl are the electrons that participate in bonding.

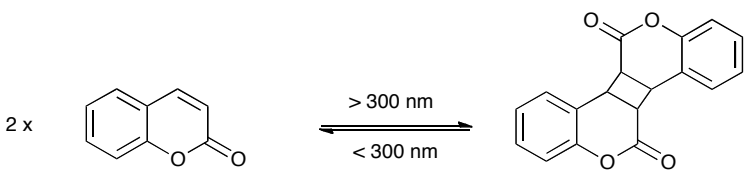

Figure 1.8. Photocycloaddition of coumarin

1.3.4 Self-Healing Materials

If covalent crosslinks in a reticulated material are broken during the application of stress, the material itself will partly (or completely) degrade. Self-healing materials are a new class of materials that are designed to respond to damage, undergoing repair when exposed to external stresses, lengthening the lifetime of these materials, improving their efficiency and saving costs.[45-47] There are two main types of self-healing polymers: capsular based healing and intrinsic healing.[46] Capsular healing mechanisms incorporate capsules within the polymeric material network that will break when external stress is applied releasing a low molecular weight "healing agent" that will fill the void and heal the material.[48] This mechanism has been used for creating self-healing silicone elastomers.[49-51] In these examples, capsular healing agent of crosslinker and catalyst are combined in some capsules and in others exist long polymer chains to promote entanglement of the current polymeric network. When a crack in the material begins to propagate the capsules are broken and the contents of the two different capsules will mix, encouraging cure and healing of the elastomer (Figure 1.10).

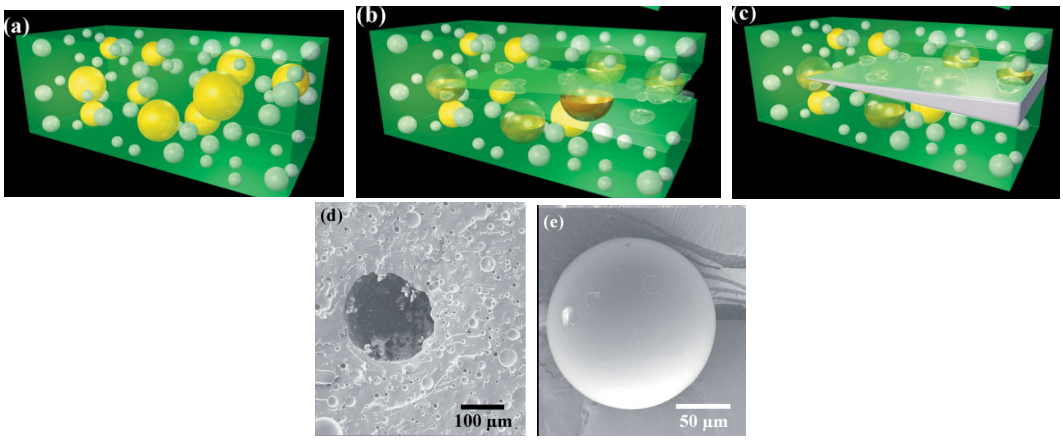

Figure 1.9. Diagram of capsular silicone self-healing mechanism from Cho et al.[49] A: silicone elastomer containing the two different capsules (catalyst/crosslinker (white) and polymer (yellow). B: crack propagation causes capsular breakage. C: polymer filling the crack, the two components mixing to initiate cure. D: an empty capsule. E: a filled capsule. Reprinted (adapted) with permission from Cho et al., Adv. Mater., 2006, 18, 997-1000. Copyright (2006) Wiley-VCH Verlag GmbH & Co. KGaA, Weinhelm

Intrinsic healing mechanisms take advantage of material changes at the molecular level: when a stress is applied to a material, the weakest bonds will break first. Creating a material that contains both covalent and non-covalent bonds will allow for self-healing by re-entangling the "broken" non-covalent bonds.[52] There are several reversible bonding mechanisms that can be used to create intrinsic self-healing materials: hydrogen-bonding, aromatic-stacking, [2+2] photoreactions, and [4+2] thermal reactions are a few

examples.[53-56] One example exists in the literature for an intrinsic healing mechanism for silicone elastomers. Zheng and coworkers[57] used an anionic polymerization reaction to create self-healing silicone materials, with a catalytic amount of bis(tetramethylammonium)oligodimethylsiloxanediolate, D_4 and a bis-D_4 crosslinker the rearrangement of the siloxane bonds occurs at 90 °C over 4 h (Figure 1.10). This intrinsic healing mechanism is thermally responsive, re-initiating anionic polymerization, however, in terms of application practicality, the healing time is about 24 h at 90 °C, which is not ideal.

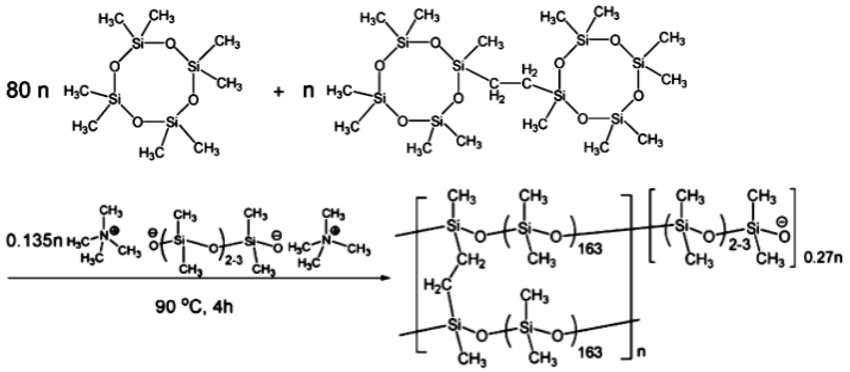

Figure 1.10. Self-healing crosslinking mechanism described by Zheng et al.[57] D_4 and a bis-D_4 crosslinker with an anionic catalyst are used to create a network. When heated anionic polymerization can be re-initiated. Reprinted (adapted) with permission from Zheng et al., J. Am. Chem. Soc., 2012, 134, 2024-2027. Copyright (2012) ACS

There are several examples of self-healing polymers that use hydrogen bonding or aromatic stacking to create reversible "weak links" within the polymer network. For example, Burattini et al. combined hydrogen bonding with isocyanate groups and aromatic π-π stacking with pyrene and a chain-folding diimide to create self-healing materials.[58-60] Their work demonstrated the increased strength and healing properties of the materials by combining two healing mechanisms together. Reversible covalent bonds can also be used to form self-healing materials. Crack propagation through a polymeric material comprised of photoactive moieties like coumarin or cinnamic acid has been shown to preferentially propagate at cyclobutane ring sites due to the stress imposed by the cyclobutane ring.[56] This allows the material to be self-healing in response to light due to the reformation of the photoactive double bonds (Figure 1.11). The incorporation of stimuli or responsive polymers or functional groups into a material initiates an interesting change in mechanical properties that can be followed using rheology.

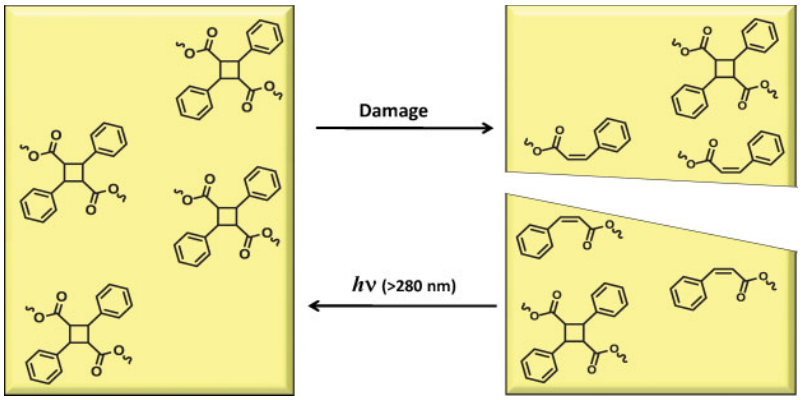

Figure 1.11. Diagram of crack propagation through a self-healing material containing photoactive molecules.[56] Adapted with permission from Chung et al., Chem. Mater., 2004, 16 (21), 3982-3984. Copyright (2004) ACS

1.3.5 Thesis Focus (II, III)

The incorporation of covalent crosslinks between silicone polymer chains leads to substantial changes in material properties. As previously mentioned, the rheological data of a crosslinked network will exhibit remarkably different properties than its non-covalently crosslinked equivalent. Chapter 3 explores the changes in material properties with various degrees of photocrosslinking of coumarin-functionalized PDMS chains. It also examines the thermal properties of the photocrosslinked materials and how the materials change in comparison to the non-photocrosslinked polymers. The ability to reverse the coumarin [2+2] photocycloaddition was also studied. The ability to reversibly control the specific concentration of crosslinks between silicone polymers, at any time, to afford novel materials with unique properties may be of use for ophthalmic drug delivery applications.

Chapter 4 examines covalently crosslinked networks as well, however, in this case novel synthetic routes, using the Piers-Rubinsztajn reaction, are used to create a variety of non-reversible PDMS materials. This chapter describes the use of a range of starting materials with different reactivities to control the rate of crosslinking and, the final material properties. In particular, we aim to utilize the reactivity rates of a variety of starting materials to control the speed of elastomer synthesis. Starting materials were chosen based on previous work with the Piers-Rubinsztajn reaction. From this previous work it is known what functional groups the reaction is tolerant to, and based on the proposed mechanism it is possible to understand which starting materials will be more reactive than others. Since silicones have many uses as ophthalmic biomaterials we suspect that a faster

synthetic method may be of use in the ophthalmic industry.

1.4 Control of silicone properties with polymer blends

1.4.1 Polymer Blends

The incredibly hydrophobic nature of silicones can sometimes be considered a disadvantage, for example, when used for biomaterial applications.[61] As previously mentioned, the hydrophilic nature of the eye does not have a healthy interaction with hydrophobic silicone contact lenses. By controlling the chemistry on the interior and exterior of an elastomer it can be functionalized to become more hydrophilic, while still maintaining the properties that make silicones such excellent materials. Creating a polymer blend will allow for control within the material and control of material properties: hydrophilicity, polymer structure, strength, elasticity, etc.[62-65] Utilizing what is known about how molecules interact, for example, through hydrogen-bonding or hydrophobic-hydrophlic interactions, a broad range of materials can be created.[66] The change in mechanical properties when silicones are blended with other polymers can be monitored by rheology and by changes in material hardness.

Control of polymer morphology by taking advantage of a secondary phase allows for potential improvement of the mechanical properties. For example, in the work by Lei et al.,[67] PDMS was blended with polyurethane to create thermoplastic vulcanizates. They noted an improvement of mechanical properties over PDMS alone. This secondary phase does not necessarily have to be a polymer it could also be air, for instance, when air stabilizes material structures in silicone foams.[68]

1.4.2 Silicone Foams

There are several advantages to using silicone foams over conventional polyurethane foams due to the excellent properties that silicones possess: electrical/thermal stability, resistance to decomposition by ozone and UV irradiation. Perhaps most important are their dramatically improved properties during combustion/heating processes.[41] These properties make silicone foams excellent candidates for mechanical shock absorbers for the aerospace industry. Siloxane foams also have applications as insulators and biomaterials (scleral buckles, wound dressings, etc.) among others. Silicone foams are typically prepared using routes analogous to those used to form silicone elastomers, with elastomer cure occurring at the same rate as bubble formation in order to entrap the gaseous bubbles within the elastomer. Typically blowing agents are added, however, foams can also be prepared through a secondary chemical reaction with the silicone

constituents that provide gaseous by-products, or through the use of surfactants to stabilize formed bubbles while cure takes place.[69-74] While there are several mechanisms for creating silicone foams or elastomers, their properties can be improved or changed with the incorporation of other polymers or attachment of functional small molecules within the silicone.

1.4.3 Thesis Focus (IV, V)

Chapter 5 explores novel methods for silicone foam formation with a focus on examining foam morphology. It was determined that the gaseous alkane byproducts of the Piers-Rubinsztajn reaction could be used as blowing agents to simultaneously blow a foam and crosslink the silicone polymers. We hypothesize that by controlling the reactivity of the starting materials different foam morphologies can be synthesized. Creating silicone foams, which can be synthesized quickly and with a range of foam densities, may allow for optimal mechanical properties for applications such as insulators or for wound dressings.

Creating a polymer blend of hydrophilic polymers into hydrophobic silicone medium will affect the properties of the silicone and potentially make them more biocompatible. Chapter 6 examines the effect of incorporating hydrophilic PEG (poly(ethyleneglycol)) polymers into silicone elastomers to make amphiphilic materials. We hypothesize that the incorporation of PEG will create more biocompatible materials, and the mechanical properties will be modified. It was determined that the simple incorporation of low molecular weight PEG chains with standard RTV PDMS curing materials afforded a substantial increase in viscosity that on degassing of the PDMS created stable silicone foams. Applications for silicone-PEG blended foams could include improved scleral buckles. Silicones have been shown to be a better, longer lasting option for scleral buckles, however, they have shown some signs of infection in a minority of patients.[20] Incorporating hydrophilic polymers may either reduce the incidence of infection, the foams could also potentially be used as drug delivery devices or for non-adherent wound dressings.

1.5 References

1. Brook, M. A. *Silicon in Organic, Organometallic, and Polymer Chemistry*. John Wiley & Sons: Toronto, 2000; p 680.
2. Klosowski, J. M.; Wolf, A. T. The Histrory of Sealants. In *CRC Handbook of Sealant Technology*, Mittal, K. L.; Pizzi, A., Eds. Boca Raton: CRC Press: 2009; pp 13-`17.
3. Rochow, E. G. *J. Am. Chem. Soc.* **1945,** *67* (6), 963-965.

4. Lane, T. H.; Burns, S. A. Silica, Silicon and Silicones...Unraveling the Mystery. In *Immunology of Silicones*, Potter, M.; Rose, N., Eds. Springer Berlin Heidelberg: 1996; Vol. 210, pp 3-12.
5. Odian, G. G. *Principles of Polymerization*. 4th ed.; Wiley-Interscience: Hoboken, N.J., 2004; p xxiv, 812 p.
6. Owen, M. J. *Chemtech* **1981,** *11* (5), 288-292.
7. Brook, M. A.; Grande, J. B.; Ganachaud, F. New Synthetic Strategies for Structured Silicones Using B(C6F5)3. In *Silicon Polymers*, Muzafarov, A. M., Ed. Springer Berlin Heidelberg: 2011; Vol. 235, pp 161-183.
8. Grande, J. B.; Gonzaga, F.; Brook, M. A. *Dalton Trans.* **2010,** *39* (39), 9369-9378.
9. Grande, J. B.; Thompson, D. B.; Gonzaga, F.; Brook, M. A. *Chem. Commun.* **2010,** *46* (27), 4988-4990.
10. Brook, M. A.; Thompson, D. B. *J. Am. Chem. Soc.* **2008,** *130* (1), 32-+.
11. Kalman, P. G.; Ward, C. A.; McKeown, N. B.; McCullough, D.; Romaschin, A. D. *J. Biomed. Mater. Res.* **1991,** *25* (2), 199-211.
12. Becker, W. E. Corneal Contact Lens Fabricated From Transparent Silicone Rubber. US3228741, 1966.
13. Keogh, P. L.; Kunzler, J. F.; Niu, G. C. C. Hydrophilic contact lens made from polysiloxanes which are thermally bonded to polymerizable groups and which contain hydrophilic sidechains. US4260725 A, 1981.
14. Jager, R. D.; Mieler, W. F.; Miller, J. W. *N. Engl. J. Med.* **2008,** *358* (24), 2606-2617.
15. Ali, T. K.; El-Remessy, A. B. *Pharmacotherapy* **2009,** *29* (2), 182-192.
16. Xu, X.; Weng, Y.; Xu, L.; Chen, H. *Inter. J. Bio. Macromol.* **2013,** *60*, 272-6.
17. Colthurst, M. J.; Williams, R. L.; Hiscott, P. S.; Grierson, I. *Biomaterials* **2000,** *21* (7), 649-665.
18. Weiner, A. L.; Gilger, B. C. *Vet. Ophthalmol.* **2010,** *13* (6), 395-406.
19. Choonara, Y. E.; Pillay, V.; Danckwerts, M. P.; Carmichael, T. R.; Du Toit, L. C. *J. Pharma. Sci.* **2010,** *99* (5), 2219-2239.
20. Colthurst, M. J., Williams, R. L., Hiscott, P. S., Grierson, I. *Biomaterials* **2000,** *21* (7), 649-65.
21. Eljarrat-Binstock, E.; Pe'er, J.; Domb, A. J. *Pharm. Res.* **2010,** *27* (4), 530-543.
22. Gaudana, R., Jwala, J., Boddu, S. H. S., Mitra, A. K. *Pharm. Res.* **2009,** *26* (5), 1197-1216.
23. Davis, J. L.; Gilger, B. C.; Robinson, M. R. *Curr. Opin. Mol. Ther.* **2004,** *6* (2), 195-205.
24. Agrawal, A. K.; Das, M.; Jain, S. *Expert Opin. Drug Deliv.* **2012,** *9* (4), 383-402.
25. Karthik, S.; Puvvada, N.; Kumar, B. N. P.; Rajput, S.; Pathak, A.; Mandal, M.; Singh, N. D. P. *ACS Appl. Mater. Interfaces* **2013,** *5* (11), 5232-5238.
26. Buckup, T.; Southan, A.; Kim, H. C.; Hampp, N.; Motzkus, M. *J. Photochem. Photobio., Part A: Chem.* **2010,** *210* (2-3), 188-192.
27. Kehrloesser, D.; Behrendt, P. J.; Hampp, N. *J. Photochem. Photobio., Part A: Chem.* **2012,** *248*, 8-14.
28. Liese, J.; Hampp, N. A. *J. Photochem. Photobio., Part A: Chem.* **2011,** *219* (2-3),

228-234.
29. Kolb, H. C.; Finn, M. G.; Sharpless, K. B. *Angew. Chem. Int. Ed.* **2001,** *40* (11), 2004-21.
30. Binauld, S.; Damiron, D.; Hamaide, T.; Pascault, J. P.; Fleury, E.; Drockenmuller, E. *Chem. Commun.* **2008,** (35), 4138-40.
31. Gragert, M.; Schunack, M.; Binder, W. H. *Macromol. Rapid Commun.* **2011,** *32* (5), 419-425.
32. Kavitha, A. A.; Singha, N. K. *ACS Appl. Mater. Interfaces* **2009,** *1* (7), 1427-1436.
33. Malkoch, M.; Vestberg, R.; Gupta, N.; Mespouille, L.; Dubois, P.; Mason, A. F.; Hedrick, J. L.; Liao, Q.; Frank, C. W.; Kingsbury, K.; Hawker, C. J. *Chem. Commun.* **2006,** (26), 2774-2776.
34. Pietrzik, N.; Schmollinger, D.; Ziegler, T. *Beilstein J. Org. Chem.* **2008,** *4*, -.
35. Rambarran, T.; Gonzaga, F.; Brook, M. A. *Macromolecules* **2012,** *45* (5), 2276-2285.
36. Sheng, X.; Mauldin, T. C.; Kessler, M. R. *J. Polym. Sci., Part A: Polym. Chem.* **2010,** *48* (18), 4093-4102.
37. Gonzaga, F.; Yu, G.; Brook, M. A. *Chem. Commun.* **2009,** (13), 1730-1732.
38. Butts, M.; Cella, J.; Wood, C. D.; Gillette, G.; Kerboua, R.; Leman, J.; Lewis, L.; Rubinsztajn, S.; Schattenmann, F.; Stein, J.; Wicht, D.; Rajaraman, S.; Wengrovius, J. Silicones. In *Kirk-Othmer Encyclopedia of Chemical Technology*, John Wiley & Sons, Inc.: 2000.
39. Han, C. D. *Polymer Rheology*. Oxford: Oxford University Press, 2007.
40. Goodwin, J. W.; Hughes, R. W.; Royal Society of Chemistry (Great Britain). *Rheology for Chemists : An Introduction*. Royal Society of Chemistry: Cambridge, 2000; p x, 290 p.
41. Noll, W. J. *Chemistry and Technology of Silicones*. Academic Press: New York, 1968.
42. Cabane, E.; Zhang, X.; Langowska, K.; Palivan, C. G.; Meier, W. *Biointerphases* **2012,** *7* (1-4).
43. Roy, D.; Cambre, J. N.; Sumerlin, B. S. *Prog. Polym. Sci.* **2010,** *35* (1-2), 278-301.
44. Kehrloesser, D.; Baumann, R. P.; Kim, H. C.; Hampp, N. *Langmuir* **2011,** *27* (7), 4149-4155.
45. Kessler, M. R. *Proc. Inst. Mech. Eng., Part G: J. Aerosp. Eng.* **2007,** *221* (G4), 479-495.
46. Mauldin, T. C.; Kessler, M. R. *Int. Mater. Rev.* **2010,** *55* (6), 317-346.
47. Syrett, J. A.; Becer, C. R.; Haddleton, D. M. *Polym. Chem.* **2010,** *1* (7), 978-987.
48. White, S. R.; Sottos, N. R.; Geubelle, P. H.; Moore, J. S.; Kessler, M. R.; Sriram, S. R.; Brown, E. N.; Viswanathan, S. *Nature* **2001,** *415* (6873), 817-817.
49. Cho, S. H.; Andersson, H. M.; White, S. R.; Sottos, N. R.; Braun, P. V. *Adv. Mater.* **2006,** *18* (8), 997-+.
50. Keller, M. W.; White, S. R.; Sottos, N. R. *Adv. Funct. Mater.* **2007,** *17* (14), 2399-2404.
51. Leir, C. M.; Galkiewicz, R. K.; Kantner, S. S.; Mazurek, M. *J. Appl. Polym. Sci.* **2010,** *117* (2), 756-766.

52. Yuan, Y. C.; Yin, T.; Rong, M. Z.; Zhang, M. Q. *Express Polym. Lett.* **2008,** *2* (4), 238-250.
53. Blaiszik, B. J.; Kramer, S. L. B.; Olugebefola, S. C.; Moore, J. S.; Sottos, N. R.; White, S. R. *Annu. Rev. Mater. Res.* **2010,** *40*, 179-211.
54. Luo, X.; Ou, R.; Eberly, D. E.; Singhal, A.; Viratyaporn, W.; Mather, P. T. *ACS Appl. Mater. Interfaces* **2009,** *1* (3), 612-620.
55. Murphy, E. B.; Bolanos, E.; Schaffner-Hamann, C.; Wudl, F.; Nutt, S. R.; Auad, M. L. *Macromolecules* **2008,** *41* (14), 5203-5209.
56. Chung, C.-M.; Roh, Y.-S.; Cho, S.-Y.; Kim, J.-G. *Chem. Mater.* **2004,** *16* (21), 3982-3984.
57. Zheng, P.; McCarthy, T. J. *J. Am. Chem. Soc.* **2012,** *134* (4), 2024-2027.
58. Burattini, S.; Greenland, B. W.; Hayes, W.; Mackay, M. E.; Rowan, S. J.; Colquhoun, H. M. *Chem. Mater.* **2011,** *23* (1), 6-8.
59. Burattini, S.; Greenland, B. W.; Merino, D. H.; Weng, W. G.; Seppala, J.; Colquhoun, H. M.; Hayes, W.; Mackay, M. E.; Hamley, I. W.; Rowan, S. J. *J. Am. Chem. Soc.* **2010,** *132* (34), 12051-12058.
60. Greenland, B. W.; Burattini, S.; Hayes, W.; Colquhoun, H. M. *Tetrahedron* **2008,** *64* (36), 8346-8354.
61. Berthier, E.; Young, E. W. K.; Beebe, D. *Lab on a Chip* **2012,** *12* (7), 1224-1237.
62. Lai, W. Y., Baccei, L.J. Prepolymers Useful in Biomedical Devices. 2001.
63. Valint, P. Plasma Surface Treatment of Silicone Hydrogel Contact Lenses. 2001.
64. Lucas, P.; Robin, J. J. Silicone-based polymer blends: An overview of the materials and processes. In *Functional Materials and Biomaterials*, 2007; Vol. 209, pp 111-147.
65. Koning, C.; Delmotte, A.; Larno, P.; Van Mele, B. *Polymer* **1998,** *39* (16), 3697-3702.
66. Barnes, G.; Gentle, I. *Interfacial Science : An Introduction*. 2nd ed.; Oxford University Press: Oxford ; New York, 2011; p xxii, 325 p.
67. Lei, C. H.; Li, S. L.; Xu, R. J.; Xu, Y. Q. *J. Elast. Plast.* **2012,** *44* (6), 563-574.
68. So, H.; Fawcett, A. S.; Sheardown, H.; Brook, M. A. *J. Coll. Interface Sci.* **2013,** *390* (1), 121-128.
69. Liu, P. B.; Liu, D. L.; Zou, H. W.; Fan, P.; Xu, W. *J. Appl. Polym. Sci.* **2009,** *113* (6), 3590-3595.
70. Lee, C. L.; Homan, G. R. *J. Cell. Plast.* **1982,** *18* (4), 233-239.
71. Zhang, X. D., Macosko, C. W., Davis, H. T., Nikolov, A. D., Wasan, D. T. *J. Coll. Interface Sci.* **1999,** *215* (2), 270-279.
72. Zhang, X. D.; Davis, H. T.; Macosko, C. W. *J. Cell. Plast.* **1999,** *35* (5), 458-+.
73. Chrusciel, J. J.; Lesniak, E. *J. Appl. Polym. Sci.* **2011,** *119* (3), 1696-1703.
74. Modic, F. J. Foamable organopolysiloxane composition and foamed product obtained therefrom. 3425967, General Electric Company, 1969.

CHAPTER 2: Self-Association of Pendant Coumarin Groups Converts Silicone Oils into Thermoplastic Silicone Elastomers[†]

2.1 Abstract:

Although there are many benefits associated with self-healing, thermoplastic elastomeric silicones, very few examples exist: silicone elastomers are normally thermoset materials. We have discovered that the simple incorporation of coumarin groups on linear silicone polymer backbones creates physical silicone polymeric networks that exhibit thermoplastic elastomeric properties in the absence of covalent crosslinks. A range of materials was prepared by incorporating four different concentrations of coumarin along the silicone backbone using thermal azide/alkyne cycloaddition reactions: higher coumarin concentrations lead to more tightly crosslinked, higher modulus materials. Intermediate properties could be obtained by mixing silicones with different coumarin loadings in the melt and then cooling. The physical interactions between coumarin-triazoles on the silicone polymers could be temporarily overcome thermally as shown by tensile, rheometry and thermal remolding experiments. The simple expedient of grafting coumarin groups, which crosslink reversibly through head-to-tail π-stacking, to silicone chains allows one to tailor the mechanical properties of these the thermoplastic elastomers, enhancing their utility.

2.2 Introduction

Elegant strategies have been developed to create polymeric materials that are able to respond to a variety of stimuli.[1-6] One area of special focus has been the development of self-healing polymers that, through a variety of mechanisms, can in-fill voids or reinforce interfaces generated by physical damage.[7-19] There is also interest in repurposing polymeric systems, or in developing processes that facilitate recycling: both of these are particularly difficult with reticulated systems. The ability to repurpose/recycle polymers

[†] Fawcett performed all synthesis and experiments with the guidance and advice from Dr. Brook. Fawcett also wrote the manuscript with edits and guidance from Dr. Brook. The chapter is currently a manuscript submitted to Macromolecules.

is generally inconsistent with the self-healing polymers just noted. There is one class of polymers that can fulfill both objectives: thermoplastic elastomers.[12, 13]

Many of the strategies exploited for self-healing polymers utilize dispersed depots of polymers/catalysts that, upon rupture, are released to form new polymers or elastomers.[8, 11, 20] The high mobility of silicone polymers in this context has been utilized to repair polyolefins, including epoxies and silicone elastomers themselves.[8, 17, 21, 22] Crosslinkers and polymers/catalysts are typically stored in separate packages that crosslink on combination: both condensation and hydrosilylation cure mechanisms have been shown to be successful. These silicone-based elastomers, however, are thermoset polymers, which are, at best, difficult to recycle or repurpose.

The initial motivation of this research was to develop silicone-based materials that could undergo controlled, reversible photohealing. As a consequence, coumarin moieties that undergo [2+2] cyclizations,[23-27] a reaction that has been exploited for the reversible crosslinking of polymers[28-32] at $\lambda > 300$ nm and retrocyclization at $\lambda < 300$ nm, respectively, were incorporated on the backbone of silicone polymers chains (**C-PDMS**).[33-35] Surprisingly, prior to any photochemistry, the properties of coumarin-modified silicones were shown to be dramatically different from their precursors. In particular, there were enormous increases in viscosity that could be tailored, including the ability to create elastomeric materials. Importantly, these behaviors were temperature sensitive: the compounds are thermoplastic silicone elastomers. The low surface activity of silicones enables easy surface spreading. The low T_g of silicones allows even high molecular weight polymers to remain as liquids at room temperature. The addition of coumarin onto linear silicone polymer chains created solid thermoplastic elastomers that exhibited no shape change over extended periods of time. While a few examples of silicone-modified thermoplastic polymers, such as polyurethane, poly(butylene terephthalate) or polystyrene[36-39] have been reported, this class of polymers is almost unknown in the literature for pure silicones.

2.3 Results and Discussion

Linear silicone polymers were functionalized with azidoalkyl groups by reacting a chloropropylmethylsiloxane-co-dimethylsiloxane polymer with sodium azide and a catalytic amount of *tert*-butylammonium azide (Figure 2.1A).[40] At most, approximately every 6th monomer carried an azide, with Me_2SiO units in between, however, lower concentrations of azide were prepared simply by controlling the stoichiometry during

azidation (Figure 2.1A): final azide concentrations along the chain ranged from 3-14%, with the remaining monomers being Me_2SiO or unmodified $Me(ClCH_2CH_2CH_2)SiO$.

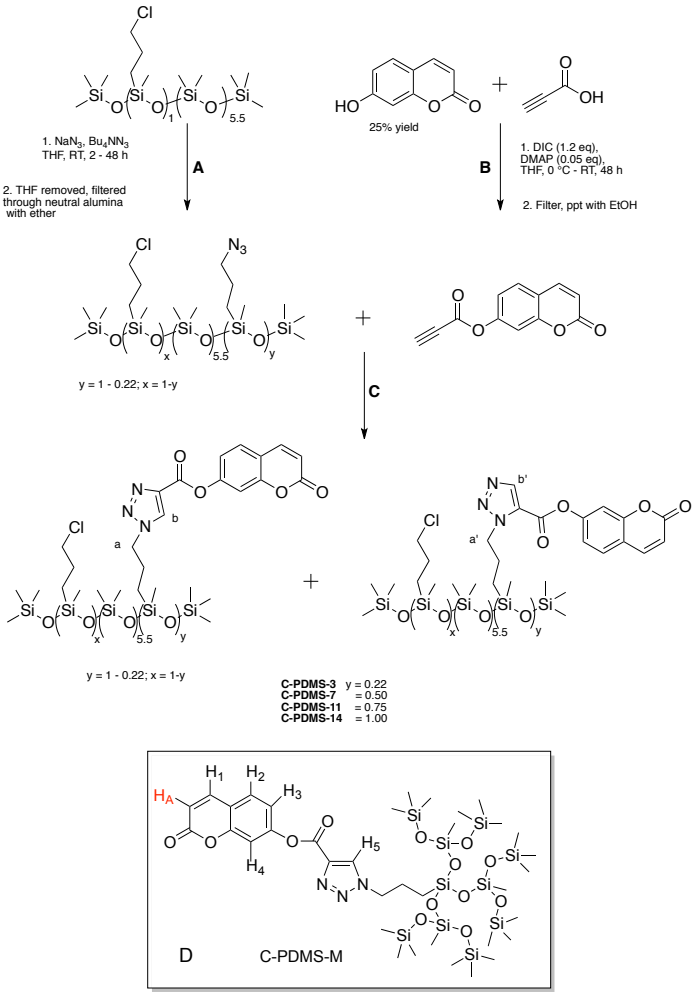

Figure 2.1. Preparation of coumarin-modified silicones **C-PDMS:** A: Azide-functional PDMS with varying concentrations of azide, B: Formation of coumarin propiolates, C: Coumarin-PDMS after Huisgen cyclization. D: **C-PDMS-M** for NOE studies

Coumarin groups could be introduced onto the azidoalkylsilicone backbone using the Huisgen cyclization,[41] a metal free version of the popular CuAAC 'click' reaction between alkynes and azides.[42] To do so, the propiolate ester of 7-hydroxycoumarin was prepared using propiolic acid with DIC-mediated coupling (Figure 2.1B). Four different silicone polymers were prepared with coumarin densities along the chain ranging from 3-14% (3% **C-PDMS-3**, 7% **C-PDMS-7**, 11% **C-PDMS-11** and 14% **C-PDMS-14**; y = 0.22, 0.50, 0.75, 1.0 respectively, Figure 2.1C) at 72 °C over 24 – 96 hours. One other

azidoalkylsilicone was synthesized, a precise, highly branched silicone dendron containing a single azide moiety **C-PDMS-M** (Figure 2.1D). The Huisgen cyclization was followed in the ^{1}H NMR by the loss of the alkyne proton and appearance of the aromatic proton on the triazole ring (Figure 2.1C): quantitative cyclization was observed, as is common with this reaction.

A surprising accompaniment to the formation of the coumarin-modified silicones was a dramatic increase in viscosity, in elasticity or embrittlement: the products **C-PDMS** were solids with varying degrees of elastic response. Although no covalent crosslinks were present, the linear **C-PDMS** samples exhibited stress/strain relationships consistent with crosslinked silicones, as was shown by comparison with unfilled commercial silicone rubbers (limited capacity for stress, but high strain tolerance) and silica filled elastomers (excellent elongation at break, but a significantly reduced strain tolerance) (Figure 2.2A). The highly (physically) crosslinked sample **C-PDMS-14** was brittle, while samples **C-PDMS-11** and **C-PDMS-7** were elastic; **C-PDMS-3** was a non-flowing soft material (like Brie cheese). The product formed from melting and cooling a 1:1 mixture of **C-PDMS-14** and **C-PDMS-7**, exhibited properties in between the two starting materials, but not identical to **C-PDMS-11** (see below). The Young's moduli of the **C-PDMS** samples were all much higher than the starting azidoalkyl/chloroalkylsilicones and increased with increasing coumarin concentration on the silicone backbone (Table 2.).

Table 2.1. Summary of Mechanical Properties of Coumarin Crosslinked Silicone Elastomers

Sample	Young's Modulus (MPa)	Strength-at-break (MPa)	Strain-at-break (%)[a]	Max Strength (Mpa)	Upper yield strength (MPa)
Control	8.2 ± 0.7	5 ± 1	133 ± 7	5 ± 1	5 ± 1
Unfilled PDMS Control	0.37 ± 0.07	0.4 ± 0.1	313 ± 131	0.5 ± 0.1	-[b]
C-PDMS-7	13 ± 1	0.6 ± 0.2	26 ± 5	0.87 ± 0.04	0.7 ± 0.2
C-PDMS-11	39 ± 9	2.6 ± 0.9	30 ± 6	3.7 ± 0.9	3 ± 1
C-PDMS-14	63 ± 7	3.2 ± 0.4	12 ± 3	3.2 ± 0.4	1.47 ± 1.4
C-PDMS-7 + C-PDMS-14	21 ± 4	1.0 ± 0.3	33 ± 3	2.1 ± 0.3	0.5 ± 0.1

[a] Strain rate = 5 mm/min, 50 N load, 25 °C. [b] Could not be determined by the instrument.

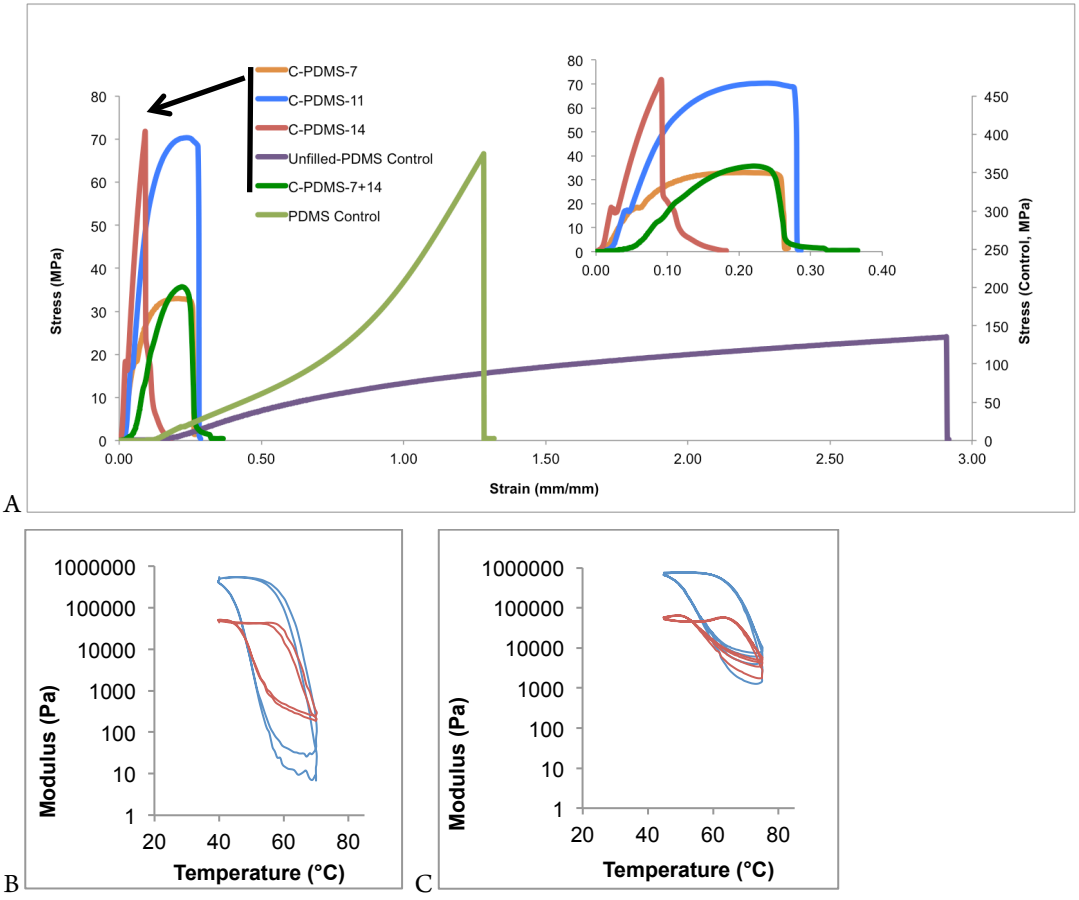

Figure 2.2. A: Tensile tests for PDMS elastomer controls with and without silica fillers ('unfilled'); **C-PDMS-7**, **-11**, **-14**; and a 1:1 mixture of **C-PDMS-7** and **-14** (more clearly seen on the inset). All coumarin-containing silicones exhibit thermoplastic properties. Only the commercial silicone was plotted on the secondary axis. Rheometer thermal cycling of B: **C-PDMS-7** and C: **C-PDMS-11** (see also Appendix – Section 8.1)

Rheological studies of the silicones, which possessed the same degree of polymerization but had four different concentrations of coumarin on the backbone, showed that viscosity correlated with the coumarin density along the silicone chain: values increased from ~3500 to ~90,000 Pa s as the coumarin loading increased from 3 to 14% (Appendix – Section 8.1), while the starting unfunctionalized copolymer had a dynamic viscosity of only 0.4 Pa s. Cycled dynamic temperature ramp tests ranging from room temperature up to 80 °C showed the viscosity decreased with temperature. In all cases, the storage modulus (G') was significantly higher for all samples at lower temperatures, demonstrating their elastomeric nature, whereas at higher temperatures the loss modulus (G") was more prevalent, clarifying the thermoplastic nature of the materials (Figure 2.2B,C, Appendix 8.1): all the materials were fluids above 90 °C.

Physical evidence of the thermoplastic nature of these materials and the ability to thermally reform is depicted in Figure 2.3. A circular mould was created and a small amount of **C-PDMS-11** was melted at 85 °C and placed in the mould and left to cool. It was straightforward to cut the elastomer into pieces, melt and then reform an elastomeric object (Figure 2.3). The yellow colour of the elastomers is attributed to the light brown colour of the coumarin starting material and the triazole ring from the thermal click reaction.[43] Elastomers with higher coumarin concentrations contain more colour. Similar behaviour was exhibited by **C-PDMS-14** and **C-PDMS-7**, respectively (Appendix – Section 8.1). More importantly, it was possible to tune the properties of the polymers simply by dissolving, mixing and evaporating (a combination of different materials could also be done through melting, however, with the viscous nature of the materials, even mixing could not be ensured, Appendix – Section 8.1).

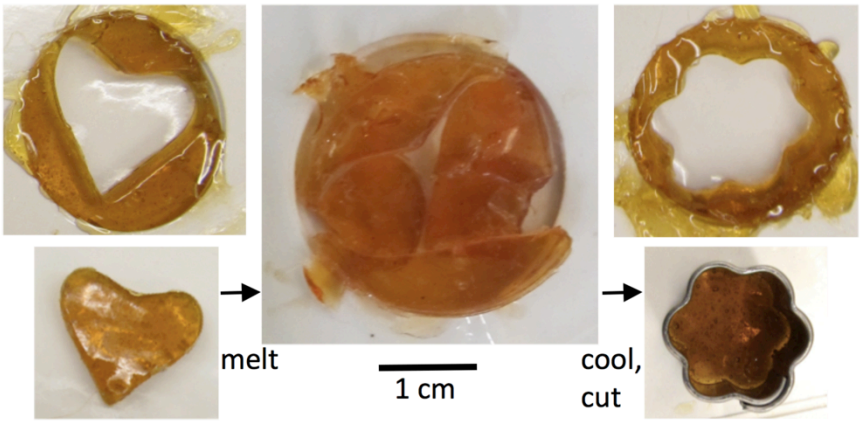

Figure 2.3. Photographic images showing the thermoplastic nature of the coumarin-silicones. A: An elastomeric heart shaped object, and its parent made from moulded **C-PDMS-11** were B: cut into small pieces, melted at 85 °C and C: remoulded to a give a body from which a flower shaped elastomer object was cut (cutter shown in bottom right)

The origins of the increase in viscosity could arise from simple physical separation of the coumarin groups with the silicone matrix, or result from a more organized type of association, such as aromatic pi stacking, which would allow coumarin rings to affiliate.[44] A highly branched silicone model structure **C-PDMS-M** containing one coumarin per molecule (Figure 2.1D, Figure 2.5A) was used to probe the nature of the interactions: in this case, only intermolecular interactions are possible. ^{1}H NMR spectra and NOE (nuclear Overhauser effect) experiments were undertaken at a series of concentrations and solvents including neat, diluted in low viscosity silicone oil $(Me_2SiO)_4$ and diluted in $CDCl_3$. There were large differences in the NOE spectra as a function of concentration. Under dilute conditions no NOE was evident (Figure 2.4 – third spectrum from top). By

contrast, there was a strong NOE relation between H_A and $H_{1\text{-}5}$ in the concentrated (neat) sample (Figure 2.4B – top spectrum). When the concentrated sample was diluted with non-functional, low molecular weight silicone an NOE effect was also observed, however, at a lower intensity, as would be expected (Figure 2.4B – second spectrum from top; slight chemical shifts occur due to the high sample concentration and lack of reference solvent – spectra were referenced to the silicone peak at 0.1 ppm). Thus, in a poor solvent for coumarin – low or higher molecular weight silicone oil – the coumarin molecules associate initially building viscosity and, at higher concentrations, developing first elasticity and then brittleness through these physical crosslinks.

To the degree that the studies with **C-PDMS-M** reflect the polymer behavior, the NOE relationship between H_A and H_4 and H_5 suggests a head-to-tail pi stacking arrangement that bring these protons into proximity (Figure 2.4A): other orientations will leave H_A and H_5 too distal for an observed NOE. A head-to-tail arrangement of stacked coumarin rings is found in the crystal structure of the parent compound. The NMR data of **C-PDMS-M**, which indicates that the triazole ring interacts with the lactone ring in a head-to-tail arrangement, this is consistent with the benzene-lactone ring association in the X-ray structure of coumarins.[34]

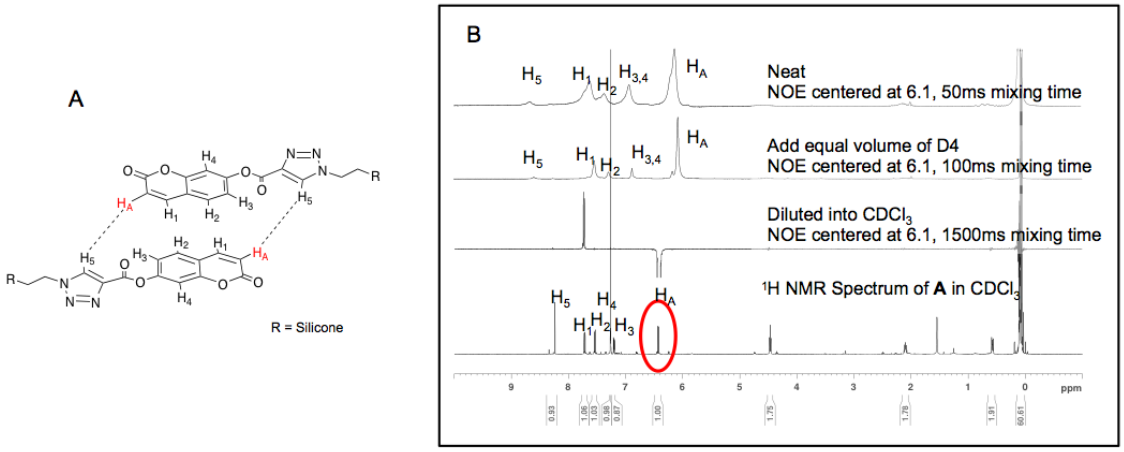

Figure 2.4. A: Potential stacking arrangements between the triazole and coumarins. B: NOE experiment with **C-PDMS-M**; proton H_A at 6.1 ppm was irradiated for the NOE measurements

The incorporation of coumarin through a carbonyltriazole linker leads to increases in viscosity that may be attributed to oriented coumarin-coumarin interactions that likely involve head to tail pi stacking based on a model compound. Simple control over the coumarin density along the polymer chain allows for the formation of viscous,

viscoelastic or brittle materials, all of which can be thermally reformed: viscosity increases of several orders of magnitude are possible. More importantly, combining the materials, melting and cooling, allows the preparation of materials with intermediate physical properties. For example, the product obtained by mixing **C-PDMS-14** and **C-PDMS-7** was similar, but not identical to **C-PDMS-11**: the concentration of coumarin is identical, the crosslink densities should be similar, but the network structures are different. Thus, these coumarin-modified silicones hold the promise of acting as masterbatch materials from which a wide variety of thermoplastic elastomers with desired properties can be predictably prepared.

2.4 Conclusions

Thermoset silicone elastomers have broad utility. There are few examples of thermoplastic elastomeric silicones and, in essentially all of them, the silicone plays role as diluent rather than the 'active ingredient.' The benefits of pure silicone elastomers would be enhanced by the capacity to reuse the materials; such "green" silicones have many attractive advantages over their thermoset counterparts including the ability to tailor the silicone physical properties on first synthesis and to modify it for subsequent uses simply by adding other materials with different coumarin loadings. The authors are currently examining the photoactivity of the thermoplastic coumarin-siloxane polymers, to further understand the effects of incorporating covalent crosslinks into the material. It is hoped the advantages that accrue from physical crosslinks can be further enhanced by reversible photostimulated chemical crosslinking.

2.5 Experimental

2.5.1 Materials

Tetrabutylammonium azide, *N,N'*-diisopropylcarbodiimide (DIC), 4-(dimethylamino)pyridine (DMAP), dimethylformamide (DMF), propiolic acid, tetraethyl orthosilicate (TEOS), trispentafluorophenylborane, sodium azide, trispentafluorophenylborane and umbelliferone (7-hydroxycoumarin) were purchased from Sigma-Aldrich and were used as received. Bis(trimethylsiloxy)methylsilane, chloropropylmethylsiloxane-dimethylsiloxane copolymer, 1000 cSt (28,000 MW) hydride-terminated PDMS and iodopropyltrimethoxysilane were purchased from Gelest and used as received. Sylgard 184 was purchased from Dow Corning as a two-part kit. Tetrahydrofuran and toluene was purchased from Caledon and dried before use over an

activated alumina column. Ethanol, chloroform and hexanes were purchased from Caledon and used as received.

2.5.2 Methods

NMR Analysis. ^{1}H NMR experiments were performed on a Bruker Avance 500 or AV600 spectrometer. NOE experiments were undertaken with irradiation at 6.1ppm.

DSC Analysis. DSC analysis was performed on a TA Instruments DSC2910 with the standard DSC cell and we used the hermetic pans. For the T_g determinations, manual liquid nitrogen (LN2) cooling was used to get to -150 °C and then the sample was heated at 15 °C/min. In some instances modulated DSC was used to determine T_g.

Rheological Analysis. Rheometry was performed on an ARES 3ARES-9A rheometer (TA Instruments, USA) with parallel plate geometry and a plate diameter of 7 mm or 20 mm. A dynamic temperature step test was performed at oscillatory frequencies of 10 rad s^{-1} and a strain of 1% and a temperature step time of 3 °C/min to obtain data for the change in dynamic viscosity as a function of temperature.

Instron Analysis. The tensile tests were performed on an Instron 3366 (Table model), USA, tensile testing machine at room temperature with a 50 N load cell. The specimen gauge length was 8.00 mm and a crosshead speed of 5 mm/minute was used. All reported mechanical properties are based on an average of a minimum of three to five specimens.

Digital Photography. Images were taken with a Canon PowerShot SX130 IS. The gridlines are 1 cm^2.

2.5.3 Synthesis of unfilled-PDMS Control for Instron Studies.[45]

In one vial, hydride-terminated PDMS (3.0 g, 0.12 mmol) was placed, while in another, TEOS (0.013 g, 0.06 mmol), $B(C_6F_5)_3$ catalyst (20 μL, of a 40 mg/mL solution in dry toluene), and hexanes (1 mL) were combined. The contents of the second vial were added to the hydride and mixed vigorously for 5 s, 2.5 g was poured into a Teflon-lined Petri dish (15 mm x 100 mm) and placed under vacuum (571 Torr) for 5 minutes until cure was complete. The dish was then moved to a 50 °C oven for 48 h to remove any remaining hexanes.

2.5.4 Synthesis of Sylgard PDMS Control for Instron Studies.

In a beaker, Sylgard 184 base (5.5 g) and Sylgard 184 curing agent (0.5 g) were combined and mixed vigorously by hand for 5 min and 5.0 g were transferred to a 15 mm x 100 mm Petri dish. The dish was left to cure on a level surface at room temperature after which it was moved to a 70 °C oven for post-cure for 24 h.

2.5.5 Synthesis of propargyl coumarin

7-Hydroxycoumarin (25.00 g, 154.1 mmol) was partially dissolved in 75 mL of THF. Propiolic acid (16.20 g, 231.2 mmol), and DMAP (50.02 mg, 0.409 mmol) were added and the temperature lowered to -0 °C. DIC (29.18 g, 231.2 mmol) was slowly added to the cold coumarin solution. The mixture was allowed to slowly warm to room temperature overnight, after which the solution was heated to 60°C and left to stir for another 24 h. The reaction was monitored by ^{1}H NMR. When complete, the reaction mixture was filtered through a fritted funnel to remove the urea precipitate, and washed with 40 mL chloroform. The THF-chloroform mixture was then exposed to reduced pressure to remove the solvent and excess propiolic acid and DIC. The residue was then re-dissolved in chloroform and filtered through a silica pad to remove any remaining urea and DMAP. The mixture was then evaporated *in vacuo* and re-solubilized into hot ethanol and placed into the freezer to precipitate overnight. Following this the precipitate was filtered and washed with cold ethanol. The final product was a light brown powder. Yield (6.2 g, 25%).

^{1}H NMR ($CDCl_3$, 500 MHz): δ 7.69 (d, 1 H, J = 9.5 Hz), 7.52 (d, 1 H, J = 8.5 Hz), 7.19 (d, 1 H, J^3 = 2 Hz), 7.11 (dd, 1 H, J = 8.5 Hz, J^3 = 2.2 Hz), 6.42 (d, 1 H, J = 9.6 Hz), 3.15 (s, 1 H) ppm; ^{13}C NMR: ($CDCl_3$, 600 MHz): δ 160.15, 154.79, 152.10, 150.15, 142.74, 128.91, 118.06, 117.42, 116.77, 110.40, 77.90, 73.86 ppm ; HRMS (EI Positive mode): m/z [M^+] calculated = 214.0266, found = 214.0265.

2.5.6 Synthesis of azidopropylmethylsiloxane-dimethylsiloxane co-polymer: 22-100 % conversion of chloroalkyl groups (9 kDa, PDMS-3 -14)

Following the procedure from Gonzaga et al.[40] Chloropropylmethylsiloxane-dimethylsiloxane co-polymer (25.0 g, 50 mmol) was placed in a round-bottomed flask with 50 mL of THF and sodium azide (4.9 g, 75 mmol). To help speed up the reaction time, a catalytic amount of tetrabutylammonium azide (0.1 g, 0.3 mmol) was added. The reaction was left stirring at 60 °C for 48 h, and monitored by ^{1}H NMR. Based on the NMR data a fraction of the reaction mixture was removed at appropriate times to give 22, 50, 75 or 100 % conversion, respectively, of the chloro-species to the azido-species. The

work up for each stage of conversion consisted of removal of the THF, addition of neutral alumina and diethyl ether followed by stirring for approximately 30 min, and filtration. Finally the solvent was evaporated under vacuum, the product was a clear oil with a yield of approximately 6 g per conversion species.

^{1}H NMR ($CDCl_3$, 600 MHz):

100% of chloropropyl groups converted to azides δ 3.24 (m, 2 H), 1.64 (m, 2 H), 0.56 (m, 2 H), 0.11-0.07 (m, 38 H); DSC: T_g = -122 °C

75% of chloropropyl groups converted to azides (25% chloropropylsiloxane remain) δ 3.49 (m, 0.5 H), 3.23 (m, 1.5 H), 1.82 (m, 0.5 H), 1.64 (m, 1.5 H), 0.63 (m, 0.5 H), 0.56 (m, 1.5 H), 0.11-0.07 (m, 33 H);

50% of chloropropyl groups converted to azides (50% choropropylsiloxane remain) δ 3.50 (m, 1 H), 3.24 (m, 1 H), 1.82 (m, 1 H), 1.64 (m, 1 H), 0.62 (m, 1 H), 0.56 (m, 1 H), 0.11-0.07 (m, 32 H);

22% of chloropropyl groups converted to azides (78% choropropylsiloxane remain) δ 3.50 (m, 1.64 H), 3.24 (m, 0.36 H), 1.82 (m, 1.64 H), 1.64 (m, 0.36 H), 0.62 (m, 1.64 H), 0.56 (m, 0.36 H), 0.11-0.07 (m, 32 H).

2.5.7 Synthesis of coumarin-click-silicones (C-PDMS-14 – 3)

Shown for **C-PDMS-14**. Propargyl coumarin (1.42 g, 6.65 mmol) and azide-copolymer (100%) (3.00 g, 6.65 mmol) was placed in a round-bottomed flask (RBF) containing THF (10 mL). The mixture was left stirring at 75 °C for 4 d. The reaction was monitored by ^{1}H NMR, and on completion remaining THF was removed *in vacuo*. The final product(s) were yellow-brown in color and, depending on the concentration of coumarin, were either elastomeric (lower coumarin content) or quite brittle (high coumarin content). The products were formed in quantitative yield.

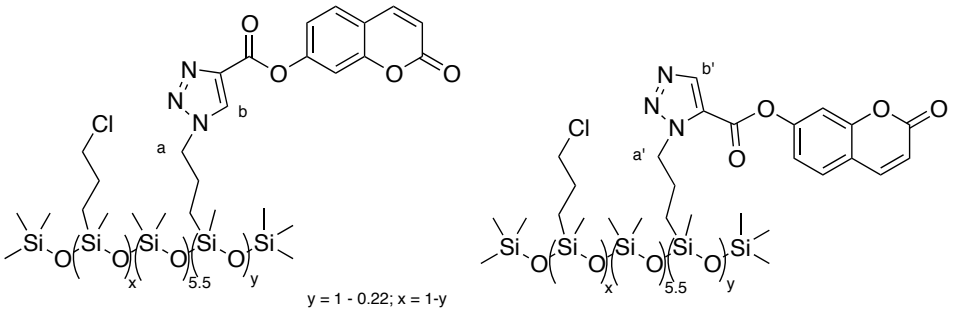

C-PDMS-14 – Major isomer (1,4 ~75%), minor isomer (1,5 ~25%): ^{1}H NMR ($CDCl_3$, 600 MHz): δ 8.25 (m, 1 H, b, b'), 7.73 (d, 1 H, *J* = 6.0 Hz), 7.54 (d, 1 H, *J* = 6.0 Hz), 7.29-7.20 (m, 2 H), 6.42 (d, 1 H, *J* = 9.6 Hz), 4.73, 4.46 (m, 2 H, a, a'), 2.03 (m, 2 H), 0.54 (m, 2 H), 0.11-0.07 (m, 38 H). DSC: T_g = -97 °C

C-PDMS-11 – Major isomer (1,4 ~75%), minor isomer (1,5 ~25%): ^{1}H NMR ($CDCl_3$, 500 MHz): δ 8.25 (m, 0.75 H, b, b'), 7.71 (d, 0.75 H, *J* = 8.5 Hz), 7.54 (m, 0.75 H), 7.29-7.20 (m, 1.5 H), 6.42 (m, 0.75 H), 4.72, 4.46 (m, 1.5 H, a, a'), 3.49 (m, 0.5 H), 2.03 (m, 1.5 H), 1.79 (m, 0.5 H), 0.61 (m, 0.5 H), 0.54 (m, 1.5 H), 0.11-0.06 (m, 33 H). DSC: T_g = -105 °C

C-PDMS-7 – Major isomer (1,4 ~75%), minor isomer (1,5 ~25%): ^{1}H NMR ($CDCl_3$, 600 MHz): δ 8.25 (m, 0.5 H, b, b'), 7.72 (m, 0.5 H), 7.54 (m, 0.5 H), 7.28-7.20 (m, 1 H), 6.42 (m, 0.5 H), 4.72, 4.45 (m, 1 H, a, a'), 3.50 (m, 1 H), 2.03 (m, 1 H), 1.81 (m, 1 H), 0.62 (m, 1 H), 0.54 (m, 1 H), 0.13-0.07 (m, 32 H). DSC: T_g = -110 °C

C-PDMS-3 – Major isomer (1,4 ~75%), minor isomer (1,5 ~25%): ^{1}H NMR ($CDCl_3$, 500 MHz): δ 8.25 (m, 0.22 H, b, b'), 7.72 (d, 0.22 H, J = 9.5 Hz), 7.54 (dd, 0.22 H, J = 8.5 Hz, J^3 = 3.5 Hz), 7.28 (s, 0.22 H), 7.20 (m, 0.22 H), 6.43 (dd, 0.22 H, J = 9.5, J^3 = 2), 4.72, 4.45 (m, 0.5 H, a, a'), 3.50 (m, 1.5 H), 2.03 (m, 0.5 H), 1.80 (m, 1.5 H), 0.63 (m, 1.5 H), 0.54 (m, 0.5 H), 0.08-0.04 (m, 32 H). DSC: T_g = -115 °C

2.5.8 Synthesis of iodopropyltris(1,1,1,3,5,5,5-heptamethyltrisiloxy)silane[46]

Bis(trimethylsiloxy)methylsilane (6.90 g, 31.0 mmol) was combined with iodopropyltrimethoxysilane (2.0 g, 6.9 mmol) in dry hexanes (20 mL). Trispentafluorophenylborane (60 μL of a 40 mg/1 mL dry toluene stock solution) was added and the solution was left to stir overnight. On completion, neutral alumina was added and the mixture was left to stir for 30 min. The mixture was filtered and any remaining solvent and starting materials were removed *in vacuo,* using a Kugelrohr (88% yield).

^{1}H NMR ($CDCl_3$, 500 MHz): δ 3.18 (t, 2 H, *J* = 7.5 Hz), 1.93 (m, 2 H), 0.63 (m, 2 H), 0.10 (m, 54 H), 0.04 (s, 9 H).

2.5.9 Synthesis of azidopropyltris(1,1,1,3,5,5,5-heptamethyltrisiloxy)silane

Iodopropyltris(1,1,1,3,5,5,5-heptamethyltrisiloxy)silane (2.50 g, 2.74 mmol) was combined with sodium azide (0.36 g, 5.48 mmol) in 10 mL of dry DMF and left stirring at 45 °C overnight, the reaction was monitored by ^{1}H NMR. On completion it was extracted 3 times with hexanes and water, dried over magnesium sulfate and the solvent was removed *in vacuo* (74% yield).

^{1}H NMR ($CDCl_3$, 600 MHz): δ 3.24 (t, 2 H, *J* = 9.0 Hz), 1.71 (m, 2 H), 0.58 (m, 2 H), 0.10 (m, 54 H), 0.05 (s, 9 H).

2.5.10 Synthesis of coumarin-click-propyltris(1,1,1,3,5,5,5-heptamethyltrisiloxy)silane (C-PDMS-M)

Azidopropyltris(1,1,1,3,5,5,5-heptamethyltrisiloxy)silane (1.58 g, 1.91 mmol) was combined with propargyl coumarin (0.41 g, 1.91 mmol) in 3 mL of dry THF and left stirring at 75 °C for 2 d, the reaction was monitored by ^{1}H NMR (quantitative yield).

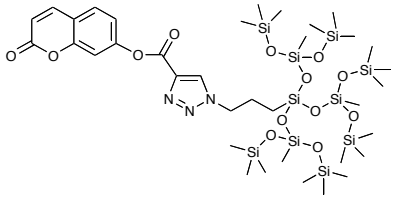

^{1}H NMR ($CDCl_3$, 600 MHz): δ 8.24 (d, 1 H, *J* = 12.0 Hz), 7.72 (d, 2 H, *J* = 12.0 Hz), 7.27-7.19 (m, 2H) 6.43 (d, 1 H, *J* = 6.0 Hz) 4.47 (t, 2 H, *J* = 3.0 Hz), 2.10 (m, 2 H), 0.58 (m, 2 H), 0.08 (m, 54 H), 0.03 (s, 9 H); ^{13}C NMR: ($CDCl_3$, 600 MHz): δ 160.41, 158.52, 154.85, 142.94, 138.73, 128.80, 128.54, 118.60, 117.10, 116.43, 110.77, 53.24, 24.50, 11.10, 1.89, -1.89. HRMS (EI Positive mode): m/z [M^+] calculated = 1038.3071, found = 1038.3044.

2.5.11 Synthesis of C-PDMS-7 + C-PDMS-14

C-PDMS-7 (0.42 g, 0.76 mmol) was combined with C-PDMS-14 (0.42 g, 0.61 mmol) in a 1:1 by mass ratio. The two polymers were dissolved in 2.5 mL THF, thoroughly mixed, and allowed to evaporate to form a film.

2.6 Acknowledgements

The authors would are grateful to the 20/20: NSERC Ophthalmic Materials Network for financial support and would like to thank Dr. Bob Berno for his assistance with the NOE experiments, Frank Gibbs for his assistance with DSC, and Dr. Lina Liu and Elizabeth Takacs for their assistance with the Instron experiments.

2.7 References

1. Bergman, S. D.; Wudl, F. *J. Mat. Chem.* **2008,** *18*, 41-62.
2. Cabane, E.; Zhang, X.; Langowska, K.; Palivan, C. G.; Meier, W. *Biointerphases* **2012,** *7*, 1-4.
3. Li, W.; Yan, D.; Gao, R.; Lu, J.; Wei, M.; Duan, X. *J. Nanomat.* **2013**.
4. Pasparakis, G.; Vamvakaki, M. *Polym. Chem.* **2011,** *2* (6), 1234-1248.
5. Roy, D.; Cambre, J. N.; Sumerlin, B. S. *Prog. Polym. Sci.* **2010,** *35* (1-2), 278-301.
6. Sun, L.; Huang, W. M.; Ding, Z.; Zhao, Y.; Wang, C. C.; Purnawali, H.; Tang, C. *Mater. Design* **2012,** *33*, 577-640.
7. Esser-Kahn, A. P.; Odom, S. A.; Sottos, N. R.; White, S. R.; Moore, J. S. *Macromolecules* **2011,** *44* (14), 5539-5553.
8. Keller, M. W.; White, S. R.; Sottos, N. R. *Adv. Funct. Mater.* **2007,** *17* (14), 2399-2404.
9. Urban, M. W. *Nat. Chem.* **2012,** *4* (2), 80-82.
10. White, S. R.; Blaiszik, B. J.; Kramer, S. L. B.; Olugebefola, S. C.; Moore, J. S.; Sottos, N. R. *Am. Sci.* **2011,** *99* (5), 392-399.
11. White, S. R.; Sottos, N. R.; Geubelle, P. H.; Moore, J. S.; Kessler, M. R.; Sriram, S. R.; Brown, E. N.; Viswanathan, S. *Nature* **2001,** *415* (6873), 817-817.
12. Chen, Y.; Kushner, A. M.; Williams, G. A.; Guan, Z. *Nat. Chem.* **2012,** *4* (6), 467-472.
13. Jalali-Arani, A.; Katbab, A. A.; Nazockdast, H. *J. Appl. Polym. Sci.* **2003,** *90* (12), 3402-3408.
14. Ghosh, S. K. Self-Healing Materials: Fundamentals, Design Strategies, and Applications. In *Self-Healing Materials*, Wiley-VCH Verlag GmbH & Co. KGaA: 2009; pp 1-28.
15. Blaiszik, B. J.; Kramer, S. L. B.; Olugebefola, S. C.; Moore, J. S.; Sottos, N. R.; White, S. R. Self-Healing Polymers and Composites. In *Annu. Rev. Mater. Res.*, Clarke, D. R.; Ruhle, M.; Zok, F., Eds. 2010; Vol. 40, pp 179-211.
16. Caruso, M. M.; Delafuente, D. A.; Ho, V.; Sottos, N. R.; Moore, J. S.; White, S. R. *Macromolecules* **2007,** *40* (25), 8830-8832.
17. Cho, S. H.; Andersson, H. M.; White, S. R.; Sottos, N. R.; Braun, P. V. *Adv. Mater.* **2006,** *18* (8), 997–1000.

18. Cordier, P.; Tournilhac, F.; Soulie-Ziakovic, C.; Leibler, L. *Nature* **2008,** *451* (7181), 977-980.
19. Gragert, M.; Schunack, M.; Binder, W. H. *Macromol. Rapid Commun.* **2011,** *32* (5), 419-425.
20. Blaiszik, B. J.; Sottos, N. R.; White, S. R. *Composites Sci. Tech.* **2008,** *68* (3-4), 978-986.
21. Mangun, C. L.; Mader, A. C.; Sottos, N. R.; White, S. R. *Polymer* **2010,** *51* (18), 4063-4068.
22. Cho, S. H.; White, S. R.; Braun, P. V. *Chem. Mater.* **2012,** *24* (21), 4209-4214.
23. Anet, R. *Can. J. Chem.* **1962,** *40* (7), 1249-1257.
24. Morrison, H.; Curtis, H.; McDowell, T. *J. Am. Chem. Soc.* **1966,** *88* (23), 5415-5419.
25. Muthuramu, K.; Ramamurthy, V. *J. Org. Chem.* **1982,** *47* (20), 3976-3979.
26. Ramasubbu, N.; Row, T. N. G.; Venkatesan, K.; Ramamurthy, V.; Rao, C. N. R. *Chem. Commun.* **1982,** (3), 178-179.
27. Lewis, F. D.; Howard, D. K.; Oxman, J. D. *J. Am. Chem. Soc.* **1983,** *105* (10), 3344-3345.
28. Chung, C.-M.; Roh, Y.-S.; Cho, S.-Y.; Kim, J.-G. *Chem. Mater.* **2004,** *16* (21), 3982-3984.
29. Kim, H. C., Kreiling, S., Greiner, A., Hampp, N. *Chem. Phys. Lett.* **2003,** *372* (5-6), 899-903.
30. Kim, H. C.; Hartner, S.; Behe, M.; Behr, T. M.; Hampp, N. A. *J. Biomed. Opt.* **2006,** *11* (3), 34024.
31. Hartner, S.; Kim, H. C.; Hampp, N. *J. Photochem. Photobio., Part A: Chem.* **2007,** *187* (2-3), 242-246.
32. Trager, J.; Heinzer, J.; Kim, H. C.; Hampp, N. *Macromol. Biosci.* **2008,** *8* (2), 177-83.
33. Lai, Y. S.; Long, Y. Y.; Lei, Y.; Deng, X.; He, B.; Sheng, M. M.; Li, M.; Gu, Z. W. *J. Drug. Target.* **2012,** *20* (3), 246-254.
34. Seth, S. K.; Sarkar, D.; Jana, A. D.; Kar, T. *Cryst. Growth Des.* **2011,** *11* (11), 4837-4849.
35. Madsen, F. B.; Dimitrov, I.; Daugaard, A. E.; Hvilsted, S.; Skov, A. L. *Polym. Chem.* **2013,** *4* (5), 1700-1707.
36. Schaefer, O.; Kneissl, A.; Delica, S.; Weis, J.; Csellich, F. *Abst. Pap. Am. Chem. Soc.* **2004,** *227*, U445-U445.
37. Lei, C.-H.; Li, S.-L.; Xu, R.-J.; Xu, Y.-Q. *J. Elast. Plast.* **2012,** *44* (6), 563-574.
38. Gornowicz, G. A.; Lupton, K. E.; Romenesko, D. J.; Struble, K.; Zhang, H. Thermoplastic Silicone Elastomers. US 6,013,715, 2000.
39. Lautenschlager, H.; Dauth, J.; Keller, W.; Mayer, T.; Stark, K. Thermoplastic Silicone Block Copolymers, the Production Thereof and the use of the Same. US App 2004/0054115, 2004.
40. Gonzaga, F.; Yu, G.; Brook, M. A. *Chem. Commun.* **2009,** (13), 1730-1732.
41. Huisgen, R.; Szeimies, G.; Moebius, L. *Chem. Ber.* **1967,** *100*, 2494-2507.

42. Kolb, H. C.; Finn, M. G.; Sharpless, K. B. *Angew. Chem. Int. Ed.* **2001,** *40* (11), 2004-21.
43. Rambarran, T.; Gonzaga, F.; Brook, M. A. *J. Polym. Sci., Part A: Polym. Chem.* **2013,** *51* (4), 855-864.
44. Burattini, S.; Greenland, B. W.; Merino, D. H.; Weng, W. G.; Seppala, J.; Colquhoun, H. M.; Hayes, W.; Mackay, M. E.; Hamley, I. W.; Rowan, S. J. *J. Am. Chem. Soc.* **2010,** *132* (34), 12051-12058.
45. Fawcett, A. S.; Grande, J. B.; Brook, M. A. *J. Polym. Sci., Part A: Polym. Chem.* **2013,** *51* (3), 644-652.
46. Grande, J. B.; Gonzaga, F.; Brook, M. A. *Dalton Trans.* **2010,** *39* (39), 9369-9378.

CHAPTER 3: Phototunable Silicone Crosslinks‡

A.S. Fawcett,[a] Tim C. Hughes[b] and Michael A. Brook[a]

3.1 Abstract

Silicone elastomers are normally thermoset materials. While their properties make them highly valuable, it would be of interest to develop stimuli-responsive silicones whose properties could be reversibly tuned at will. A particularly interesting trigger is light, since silicone elastomers can readily be formulated to be transparent. We describe the utilization of coumarin-modified silicones for this purpose. On their own, addition of the coumarin groups converts silicone oils into thermoplastic elastomers. Photolysis permits covalent crosslinking through a [2+2] cycloaddition. Higher energy photons permit, in part, photoinitiated retrocycloaddition and a subsequent decrease in crosslinking. It is thus possible to tailor the physical properties of the elastomer to either increase or decrease the modulus using light.

3.2 Introduction

The wide utility of silicone elastomers is constrained somewhat by the inability to tune properties after curing: silicones are thermoset materials.[1] Stimuli-responsive materials have become a popular research focus over the last decade due to their ability to use external sources such as heat or light to induce structural or property changes within the material.[2-9] As a consequence of precise, localized control over polymer morphology, the properties of light-responsive polymers, particularly those that allow for reversible transitions, can be tuned at will.[10] In spite of the broad use of silicones in a variety of applications, there are very few examples of stimuli responsive silicone polymers.[11-13]

Previously, we reported the ability of coumarin-modified silicone polymers to self-assemble. Thermoplastic silicone elastomers result, with the crosslink density directly

‡ Fawcett performed all synthesis and experiments with the guidance and advice from Dr. Hughes and Dr. Brook. Fawcett also wrote the manuscript with edits and guidance from Dr. Brook. This work was performed in collaboration with CSIRO in Melbourne, Australia. This manuscript is being prepared for submission to Polymer.

proportional to the concentration of coumarin groups on the polymer backbone.[14] The incorporation of coumarin into the silicone also means these materials are photoresponsive and this response can be reversible in principle: coumarin undergoes a reversible [2+2] photocycloaddition with $\lambda > 300$ nm and photocleaves with $\lambda < 300$ nm (Figure 3.1).[15]

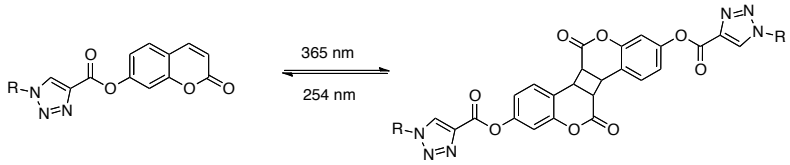

Figure 3.1. Photodimerization/cleavage of coumarin. R = silicone

We have developed strategies to control the number of coumarin functional groups along the PDMS (poly(dimethylsiloxane)) backbone (Figure 3.2). In this paper, we examine the ability to manipulate the crosslink density – both through pi-pi stacking and covalent interactions - by photocrosslinking the coumarin groups, turning a thermoplastic into a thermoset. In addition, the ability to initiate retrocycloaddition, therefore reducing the covalent crosslink density, was explored.

3.3 Results

A variety of coumarin-functional PDMS polymers (**C-PDMS**) were prepared by the Huisgen-1,3-thermal-cycloaddition reaction between alkyne functionalized 7-hydroxycoumarin (Figure 3.2B) and various azide-functional PDMS (~9kDa, Figure 3.2A) to give copolymers with 3, 7, 11 and 14% coumarinylpropylmethyl-co-dimethylsilicones (**C-PDMS-3**, **C-PDMS-7**, etc. Figure 3.2C.).[14] For one of the samples, the azide backbone was modified with coumarin and thermally crosslinked with an alkyne-terminated PDMS of approximately 1 kDa. **SC-PDMS-1.5** was formed by reacting half of the available azides on **1a** (y = 22) with coumarin and the other half were used to form chemical crosslinks (Figure 3.2D).

Prior to photocuring, silicone polymers with pendant coumarin groups are thermoplastic elastomers because of the coumarin/coumarin stacking interactions. These interactions can be overcome at elevated temperatures:[14] heating-cooling cycles of the non-crosslinked materials led to circular plots of modulus against temperature (e.g., **C-PDMS-14**, Figure 3.4D) because of the re-organization of self-assembled coumarin groups that occurred as temperatures were increased or decreased.[14]

Coumarin-functionalized PDMS were photocured on a photorheometer using a 365 nm light source (**C-PDMS→PC-PDMS**). Changes in viscosity were followed over time of UV irradiation. Optimal temperatures for the photocuring reaction were obtained through preliminary temperature sweep tests of each material such that every sample would cure with approximately the same initial viscosity (**C-PDMS-3**: 40 °C, **C-PDMS-7**: 62 °C, **C-PDMS-11**: 74 °C, **C-PDMS-14**: 74 °C): the final viscosities of the **PC-PDMS** materials were more easily compared when all four compounds had the same initial viscosity. Over time, each polymer becomes more elastomeric as seen from the storage modulus G', which crosses over the loss modulus, G" (Figure 3.3A, B, D, E).

The partly crosslinked polymer **SC-PDMS-1.5** was also exposed to UV light to initiate photocrosslinking. The photorheological response was similar to that of its precursor **C-PDMS-3**, although the crossover of the storage and loss moduli occurred earlier (Figure 3.3A vs C).

In order to confirm that the viscosity increase with exposure to light was a direct consequence of photodimerization, rather than thermal side reactions, the lamp was cycled on and off to cure **C-PDMS-3** (Figure 3.5). Identical behavior to the continuous photodimerization study (Figure 3.2A) was observed, except that the viscosity plateaued after each 18 minute irradiation. This behavior is consistent with photodimerization as the only cause of viscosity changes.

The unique properties of **SC-PDMS-1.5** can be seen from Figure 3.3C. By incorporating a second type of crosslinking (covalent silicone crosslinks through 'click' chemistry) the mechanical properties of the elastomer are quite different than the physically crosslinked analogue. The covalent silicone crosslinks within the material cause the material to possess more elastomeric properties prior to UV irradiation. When the lamp is turned on and [2+2] photocycloaddition begins, more crosslinks are formed within the elastomer. In contrast to **C-PDMS-3**, the storage modulus (G'), which describes the elastic nature of the material, crosses over the loss modulus (G'') much earlier, showing the effect the permanent 'clicked' crosslinks have on the system. The overall trend of the curve is similar to that of **C-PDMS-3**, demonstrating how the physical coumarin-coumarin interactions also play a role in the material viscosity.

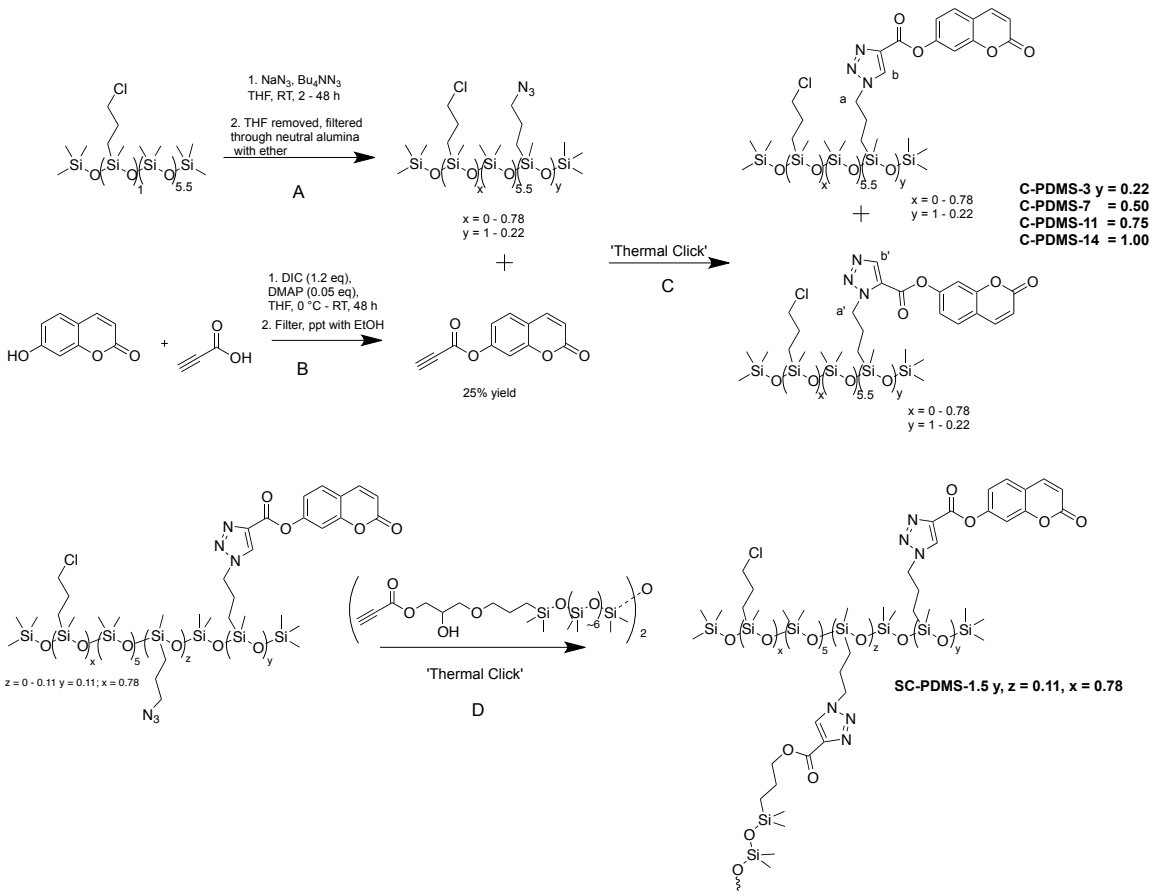

Figure 3.2. Synthesis of **C-PDMS** and **SC-PDMS** A: synthesis of azide-functional silicone. B: synthesis of alkyne-coumarin. C: click reaction to create **C-PDMS** containing different concentrations of coumarin. D: thermal crosslinking to form **SC-PDMS-1.5** using alkynylsilicones. Note: an approximately 75:25 mixture of 1,4 and 1,5 triazole isomers is produced in the Huisgen cyclization. Both isomers are shown in these model structures

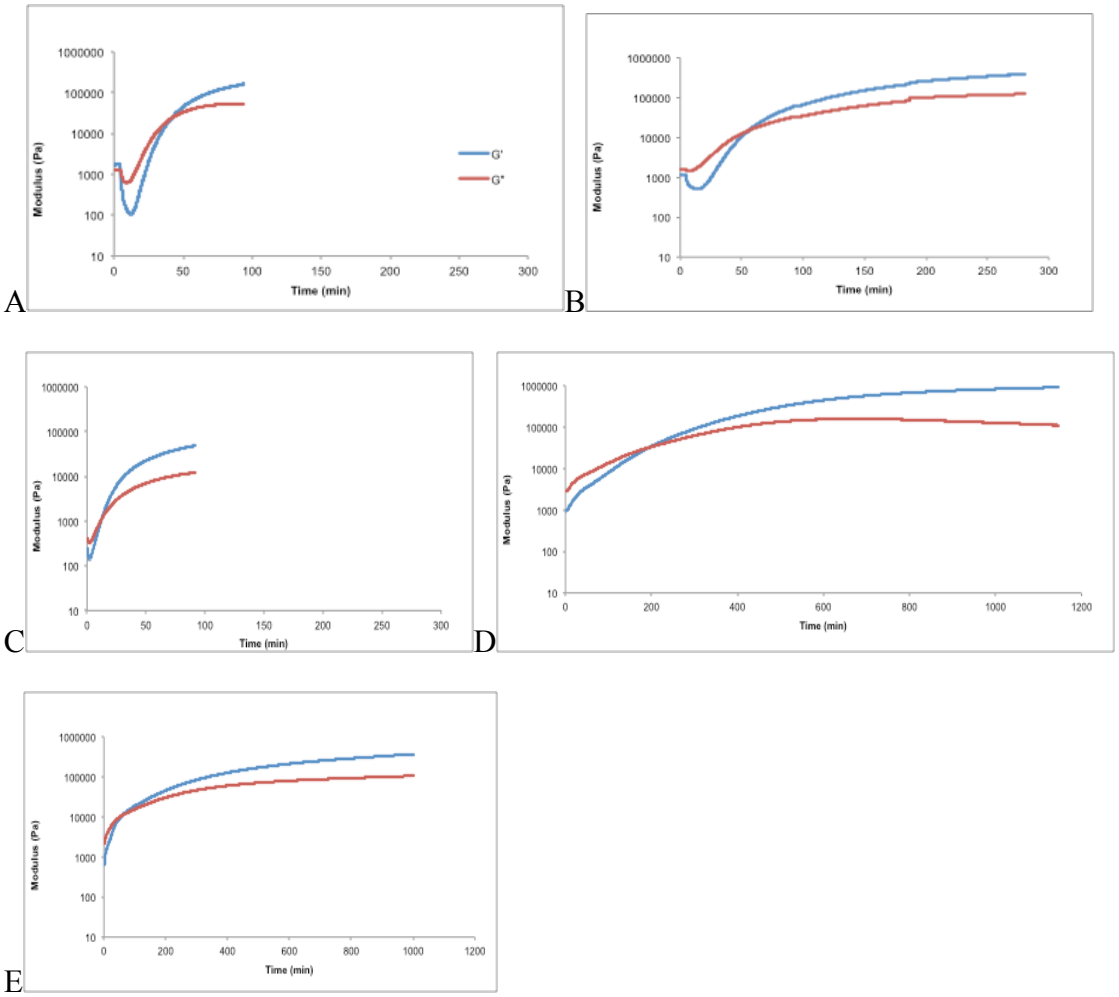

Figure 3.3. Photocuring of **C-PDMS → PC-PDMS** A: **PC-PDMS-3** at 40 °C, B: **PC-PDMS-7** at 62 °C, C: **SC-PDMS-1.5** at 40 °C (A, B and C have a time scale of 300 minutes) D: **PC-PDMS-11** at 74 °C, and E: **PC-PDMS-14** at 74 °C (Both C and D have a time scale of 1200 minutes)

Once a plateau was reached on the rheometer, i.e., once photocuring had been maximized, the **PC-PDMS** samples were tested to confirm cure completion using thermal cycling (Figure 3.4A-F). As seen by comparing **C-PDMS-14** with **PC-PDMS-14**, little change occurred in modulus with temperature in the latter case. All photocured materials followed a straight line with temperature showing that there are insufficient free-coumarin groups left to permit any additional physical coumarin/coumarin crosslinks. **PC-PDMS-11** is the only sample that still showed some cycling, even after 18 hours of curing. This may be due to incomplete photocuring as a consequence of structural orientations of coumarin groups within the polymer, such that there is insufficient chain

mobility to permit photodimerization – leaving a fraction of free coumarin groups that can respond to temperature changes.

The photoreversibility of the system was examined in a UV-Vis spectrometer using two light sources: 365 nm for dimerization and 254 nm for retrocycloaddition (the available light intensity on the photorheometer was insufficient to show any change in viscosity). The experiment was designed such that the temperature within the spectrometer was constant at 20 °C and there was gentle stirring to ensure even mixing of the material throughout the cuvette rather than simply where the light was directed. In the first cycle, the sample was irradiated with 365 nm light (Figure 3.6: red to purple). Next, the retro-cycloaddition reaction was run at 254 nm light for two hours (Figure 3.6: purple to orange): after the first hour further changes were negligible. The final cycle was re-dimerization with 365 nm light (Figure 3.6: orange to green). It can be seen that recovery after each cycle is less than 100%. This suggests the formation of a photostationary state for the polymer, a phenomenon that is typical when photoactive molecules are incorporated into polymeric materials.[16-20]

Instron studies were undertaken on the photocured samples after removal from the rheometer (Figure 3.7, **PC-PDMS-7** could not be recovered from the rheometer to produce a pristine sample for testing). The samples followed typical elastomeric tensile curves similar to commercial PDMS elastomer controls. To demonstrate this, two controls were tested: a commercial sample that contained the silica fillers that are commonly used to reinforce PDMS (the control containing silica is plotted on the secondary right hand axis) and an unfilled PDMS control. The latter compound shows substantially lower stress and corresponds closely to **PC-PDMS-3**, indicating that at certain concentrations dimerized coumarin crosslinks are as effective as traditional silicone crosslinks in silicone rubber. When the number of crosslink sites is further increased with the presence of additional coumarin, e.g., **PC-PDMS-11** and **-14**, the compounds show much higher stress and a lower strain – they are much more brittle. The strength of the photocured materials is much higher in comparison to the un-cured thermoplastic starting material.[14] Comparisons of **C-PDMS-11** and **PC-PDMS-11** as well as **C-PDMS-14** and **PC-PDMS-14** are shown in Figure 3.7. A substantial difference can be seen between **C-PDMS-14** before dimerization and after. Before dimerization, **C-PDMS-14** was very brittle, whereas, after photodimerization, the stress it could withstand more than doubled. The incorporation of covalent crosslinks into the material increased the elasticity of the compound, which corresponds with what is observed from the rheology measurements. Both **PC-PDMS-11** and **-14** exhibit more elastic tensile behavior in comparison to their thermoplastic, non-irradiated analogues.

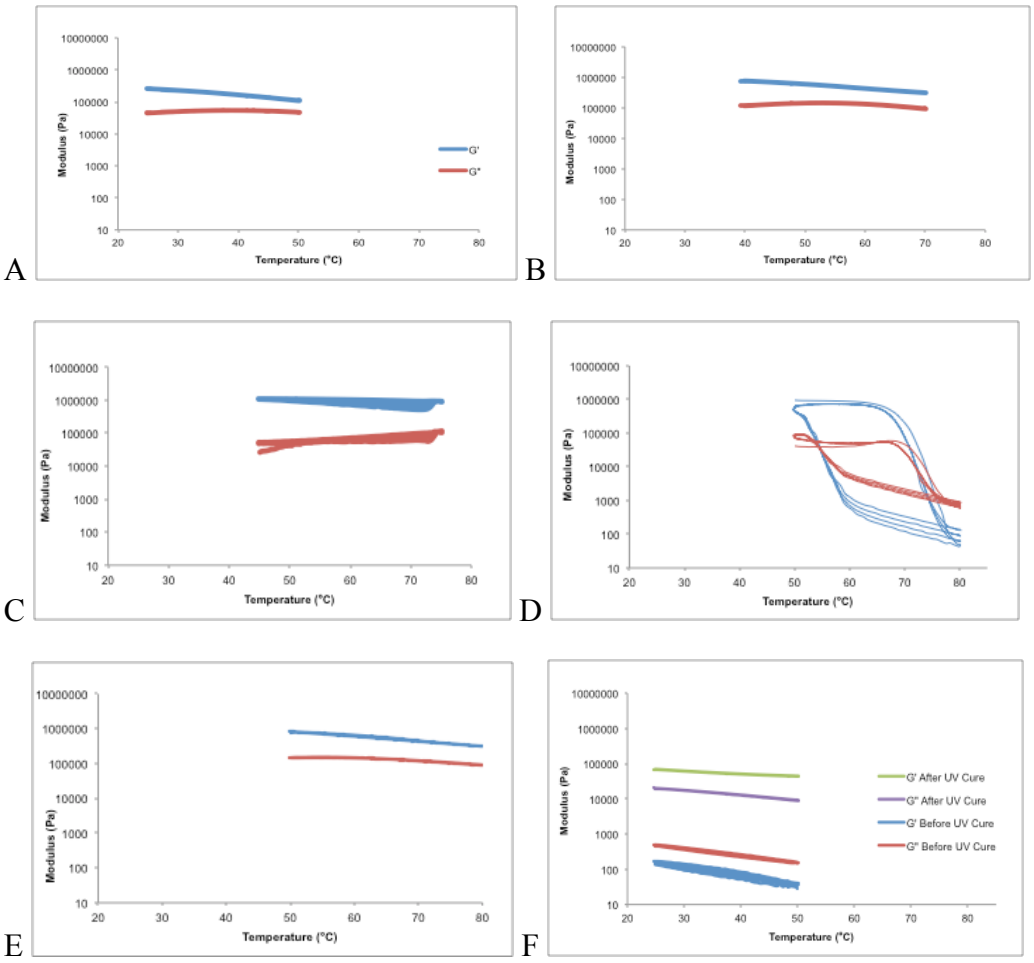

Figure 3.4. Thermal cycling rheology data after the **C-PDMS** samples have been photocured. A: **PC-PDMS-3**, B: **PC-PDMS-7**, C: **PC-PDMS-11**, D: **C-PDMS 14**, E: **PC-PDMS-14**, F: **SC-PDMS-1.5** and **PSC-PDMS-1.5**

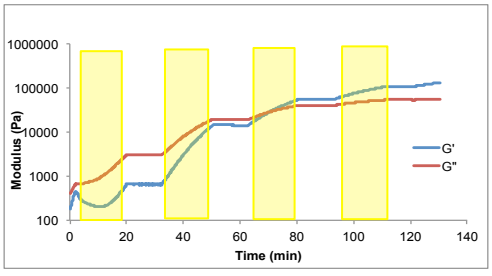

Figure 3.5. **C-PDMS-3** photocure to give P**C-PDMS-3** with lamp on/off cycling. In each cycle the lamp is on for 18 minutes (yellow), then off for 12 minutes, on for 18 minutes, etc.

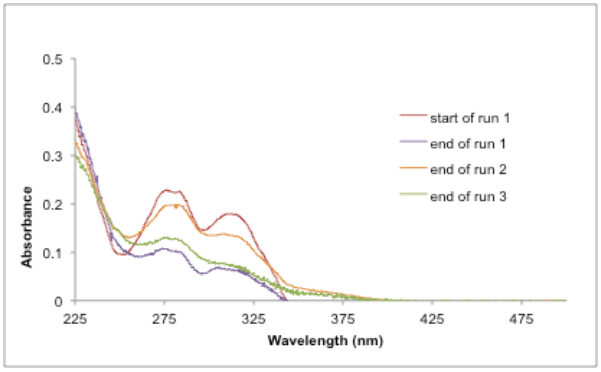

Figure 3.6. UV-Vis of **PC-PDMS-3** after 365 nm irradiation (red to purple), then 254 nm irradiation (purple to orange), and then 365 nm irradiation again (orange to green)

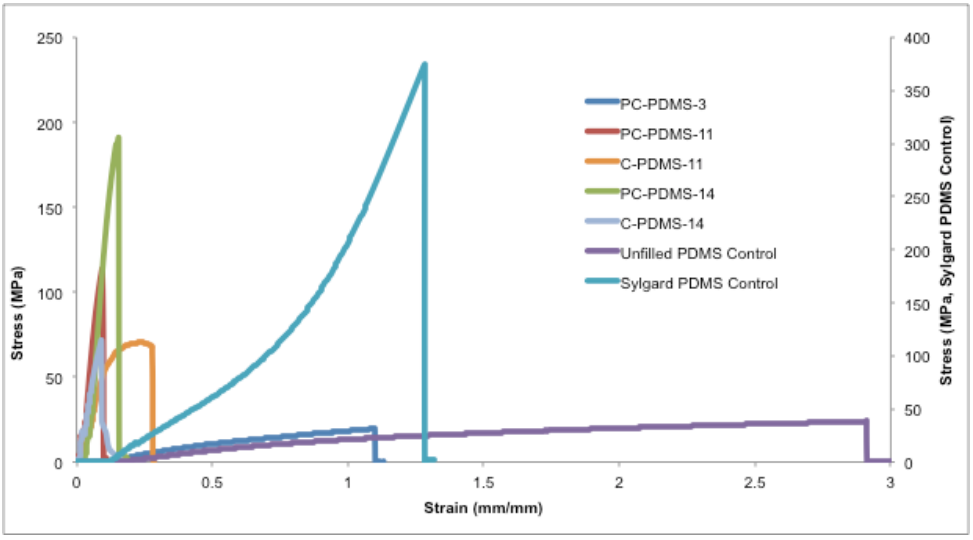

Figure 3.7. Instron results of the **PC-PDMS** samples (based on a minimum of 3 repeats) and results for comparison of **C-PDMS-11** and **-14**. The silica-containing Sylgard control is plotted on the secondary (right hand) axis

3.4 Discussion

The presence of coumarin molecules on a silicone backbone leads to dramatic increases of viscosity: fluids become thermoplastic elastomers or even rigid resins at higher loading.[14] However, the affinity between coumarin molecules is easily overcome simply by heating. For many applications, that level of resilience is insufficient for practical purpose. Photochemistry provides a reversible process to tune the elastomeric properties of the polymer.

Previously, we showed that alkyne coumarin groups, clicked onto linear low molecular weight PDMS chains, led to novel thermoplastic elastomers through coumarin self-assembly. The thermal response on the viscoelasticity of the materials was shown to vary with the concentration of coumarin along the backbone. A higher concentration of coumarin required higher temperatures to achieve comparable viscosities to lower coumarin-containing materials. In other words, higher coumarin backbone density gave higher physical crosslink densities. Thermal cycling was completed on all physically crosslinked materials demonstrating the response of the various polymers to heat. All polymers exhibited reproducible changes in viscosity as the temperature was cycled; **SC-PDMS-1.5** showed the least change in viscosity with temperature, which is due to the permanent crosslinks incorporated into the material. Since **SC-PDMS-1.5** is already crosslinked, the polymer chain movement with changing temperatures is limited, although slight cycling is noted from the effect of the coumarin self-assembly (Figure 3.4F).

The [2+2] photoactivity of all **C-PDMS** samples was explored using real-time viscosity measurements during 365 nm UV irradiation. The temperature of the dimerization experiment was different for each sample, depending on the concentration of coumarin, in order to maintain constant initial viscosities across all samples. Except for **PC-PDMS-14**, polymers with higher coumarin backbone concentrations had a higher modulus after longer irradiation times: the viscosity of **PC-PDMS-14** did not exceed that reached by **PC-PDMS-11**. Increases in viscosity are a consequence of crosslinking through [2+2]-cycloaddition reactions: The deviation by **PC-PDMS-14** is likely a consequence of too high a density of coumarin moieties. At these higher loadings, we rationalize that complete dimerization of coumarin along the polymer backbone may not be possible due to the conformational restraints placed within the material during crosslinking: there are insufficient degrees of freedom to permit more than a small fraction of coumarin to attain the geometry necessary for photocycloaddition.

The polymers possessing lower coumarin concentration along the backbone, **PC-PDMS-3** and **PC-PDMS-7**, exhibited an unexpected initial decrease in viscosity when the lamp was turned on at 2 minutes (Figure 3.3A-B). We postulate this decrease in viscosity is due to the conformational changes that occur when dimerization begins Figure 3.8A. When the polymer is initially placed on the rheometer, the coumarin molecules are stacked in a favorable head-to-tail conformation that leads to the viscosity increase previously reported.[14] When the lamp is turned the associated coumarin groups must first dissemble – leading to lower viscosity materials – prior to the orientation permitting them to undergo cycloaddition. Note that thermal association of the coumarin molecules was found to arise from head to tail arrangements in model studies. By contrast, the photodimer can arise from either head to tail or head to head interactions (Figure 3.8B).[20]

Photocure of all of the compounds tested led to increases in modulus. **PC-PDMS-3** had the lowest final viscosity, which is expected as it contains the lowest concentration of coumarin and therefore the lowest possible concentration of coumarin photocrosslinks. **PC-PDMS-7** and **PC-PDMS-14** increased by the same degree in modulus, just over double the final modulus for **PC-PDMS-3**. In comparison to **PC-PDMS-3**, **PC-PDMS-7** contains just over double the percentage of coumarin moieties, and so the increase in modulus follows with what would be expected. **PC-PDMS-14** contains double the coumarin moieties of **PC-PDMS-7**, however, as previously mentioned, it is thought that the concentration of coumarin groups may be too high to allow for the conformational changes to occur to allow for further coumarin crosslinking, leading to maybe only half of the coumarin moieties being able to photocrosslink. **PC-PDMS-11** displays the largest degree of modulus increase, a 130% increase in modulus over **PC-PDMS-7**, despite having 4% more coumarin groups along the silicone chain. This demonstrates an optimal coumarin concentration along the PDMS chain for maximum crosslinking efficiency. There appears to be no loss in viscosity during initial irradiation, which suggests there are free coumarins that are not pi-stacked, and in a conformation to initiate the [2+2] photoreaction (this is true also for **PC-PDMS-14**).

The partly cured material **SC-PDMS-1.5** did not yield, on photolysis, the same magnitude of modulus change as its **C-PDMS-3** counterpart. The photorheology was run at 40 °C, the same as for **C-PDMS-3**. However, in this instance the polymer starts with a lower number of coumarin physical crosslinks, and thus has a lower initial viscosity. The covalent crosslinks initially prepared by azide-alkyne ‘click’ chemistry with a silicone chain of 1,000 MW did not significantly change the crosslink density because of the length of the spacer. As the physical coumarin crosslinks became chemical crosslinks the material quickly becomes more elastomeric and the storage modulus increased. The viscosity in the **SC-PDMS-1.5** samples thus plateaued more quickly than the **C-PDMS-3** samples. These results are interesting because they demonstrate the ability to independently utilize physical, irreversible covalent and reversible covalent interactions to tailor the silicone elastomer properties.

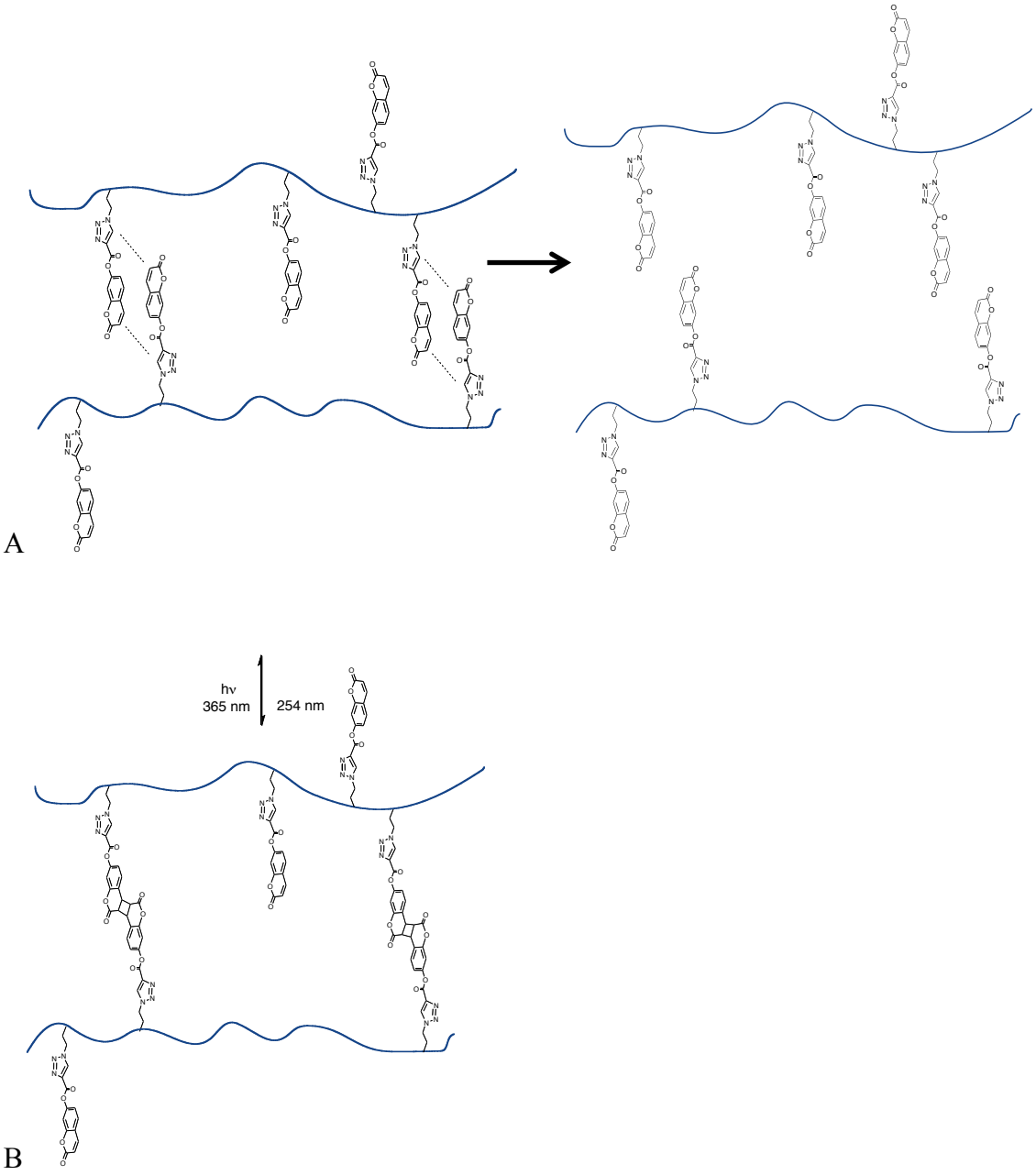

Figure 3.8. Photocure involves dissociation of A: dissociation of stacked coumarin molecules and B: reversible photodimerization of the coumarin molecules

Thermal cycling experiments were completed on all photocrosslinked samples and can be compared to previously reported thermally cycled unphotodimerized, self-associated materials. In Figure 3.4D and E, the storage and loss moduli of **C-PDMS-14** during heating were the same as **PC-PDMS-14**, which suggests 1:1 coumarin crosslinks are

occurring in both cases. In the case of **PC-PDMS-14**, two coumarin groups are required to make a crosslink, in **C-PDMS-14**, if there were multiple coumarin groups involved in crosslinking, it can be extrapolated that the viscosity of the material would be higher than when it is photodimerized. The similar behavior of the photodimerized materials to their non-photocrosslinked analogues suggests only two coumarin groups are required to give one crosslink in both cases. The thermal cycling for **PC-PDMS** materials no longer exhibits circular changes in the flow of the material after UV irradiation due to the presence of covalent crosslinks within the network.

Instron studies further reflect the changes between **C-PDMS** and **PC-PDMS** materials. The thermoplastic nature of **C-PDMS-11** and **-14** are shown in the curves of Figure 3.7. However, once photodimerized, the materials exhibit a typical thermoset tensile strength curve. The changes to **PC-PDMS-11** and **-14** show an increase in stress over their physically crosslinked analogues, which is expected considering the incorporation of stronger chemical crosslinks within the material. **PC-PDMS-3** exhibits a tensile strength that is very similar to the unfilled-PDMS control, which demonstrates that there is a concentration of coumarin photocrosslinks that can produce materials with a similar tensile strength as silicones containing alkyl crosslinks.

The main advantage to these materials is the ability to incorporate a specific concentration of crosslinks within the network that are reversible. The temperature sensitive nature of the **C-PDMS** samples can be overcome by incorporating a controlled amount of covalent crosslinks into the material. The crosslink density of the materials can be controlled below the temperature threshold for C-PDMS with physical and a specific concentration of chemical crosslinks. In some cases the concentration of chemical crosslinks within the material can supersede the effect of physical crosslinking. The photoactivity of **C-PDMS** materials allows for the development of silicone elastomers with a reversibly controllable crosslink density at a variety of temperatures.

3.5 Conclusions

Coumarin-modified silicones provide two distinct methods to control elastomeric properties. The concentration of coumarin incorporated along the silicone backbone controls the initial viscosity and thermal properties of the material. In addition, the dimerization of coumarin within PDMS allows the thermoplastic silicone polymers to be converted by light into thermosets of the desired modulus. To a degree, the process can be reversed to reduce the permanent density.

3.6 Experimental

3.6.1 Materials

Sylgard 184 was purchased from Dow Corning as a two-part kit. Tetrahydrofuran and toluene was purchased from Caledon and dried before use over an activated alumina column. Ethanol, acetonitrile, chloroform and hexanes were purchased from Caledon and used as received. Glycidylether-terminated PDMS and propiolic acid were purchased from Aldrich.

All materials for the synthesis of C-PDMS materials were obtained, synthesized and characterized following previously reported experimental procedures.

3.6.2 Methods

Rheological Analysis. Rheometry was performed on an ARES 3ARES-9A rheometer (TA Instruments, USA) with parallel plate geometry and a 0.3 mm gap. The top plate was a 20 mm quartz plate with the bottom a Peltier plate. A dynamic temperature step test was performed at oscillatory frequencies of 10 rad s^{-1} and a strain of 1% and a temperature step time of 3 °C/min to obtain data for the change in dynamic viscosity as a function of temperature. Photocrosslinking reactions were performed using oscillatory frequencies of 10 rad s^{-1} and a strain of 1%, with a 365 nm light source at an intensity of 96 mW/cm^2 at temperatures that gave a starting modulus of ~1000 Pa. The UV light source was an EXFO Acticure 4000.

Reversible UV Studies. The UV studies were performed using a Varian Cary 50 Bio UV-Vis Spectrometer with a Single Cell Peltier Accessory to ensure even mixing and controlled temperature during irradiation. The 254 nm light source was a UVP PenRay. Experiments were run in acetonitrile at a concentration of 10^{-4}M. Each irradiation experiment was run for an hour, followed by an extra 15-60 minutes to ensure complete reaction.

Instron Analysis. The tensile tests were performed on an Instron 3366 (Table model), USA, tensile testing machine at room temperature with a 50 N load cell. The specimen gauge length was 8.00 mm and a crosshead speed of 5 mm/minute was used. PC-PDMS samples were removed from the rheometer and punched into Instron testing strips following procedures used for contact lens tensile testing. All reported mechanical properties are based on an average of a minimum of three to five specimens.

3.6.3 Synthesis of di-alkyne terminated PDMS

Glycidylether terminated PDMS (5.0 g, 5.1 mmol) was combined with propiolic acid (1.42 g, 20 mmol) in 10 mL THF and stirred at 50 °C over 4 days. The reaction was monitored by NMR and on completion any remaining acid and solvent were removed *in vacuo*.

^{1}H NMR ($CDCl_3$, 600 MHz): δ 4.21 (t, 1 H, J = 9.0), 3.53-3.42 (m, 4 H), 2.96 (s, 1 H), 1.76-1.74 (m, 1 H), 1.69-1.65 (m, 1 H), 1.62-1.58 (m, 2 H), 0.52-0.50 (m, 2 H), 0.07-0.0.02 (m, 32 H); ^{13}C NMR: ($CDCl_3$, 600 MHz): δ 155.10, 75.98, 74.56, 70.96, 69.69, 68.49, 66.26, 23.32, 14.14, 1.28, 0.20.

3.6.4 Synthesis of SC-PDMS-1.5

Azide-functional PDMS-3 (synthesis described in previous chapter) (5.0 g, 11 mmol) was combined with propargyl coumarin (1.19 g, 5.5 mmol) and dialkyne-terminated PDMS (3.5 g, 2.7 mmol) with 10 mL THF and stirred at 50 °C for 4 days. The reaction was monitored by NMR, and on completion the THF was removed using a rotary evaporator.

^{1}H NMR ($CDCl_3$, 500 MHz): δ 8.36-8.25 (m, 0.11 H), 8.13-8.05 (m, 0.11 H), 7.36 (d, 0.11 H, J = 9.5 Hz), 7.54 (dd, 0.11 H, J = 9.0 Hz, J^3 = 3 Hz), 7.28 (s, 0.11 H), 7.22-7.18 (m, 0.11 H), 6.42 (d, 0.11 H, J = 9.5 Hz), 4.63-4.43 (m, 0.22 H), 4.38 (t, 0.22 H, J = 7 Hz), 3.52-3.47 (m, 2.22 H), 2.87 (d, 0.11 H, J = 7.0 Hz), 2.07-1.91 (m, 0.22 H), 1.88-1.78 (m, 1.78 H), 1.66-1.55 (m, 0.22 H), 0.65-0.60 (m, 1.56 H), 055-0.50 (m, 0.66 H), 0.13-0.02 (m, 32 H).

3.7 Acknowledgement

The authors would like to thank the 20/20 NSERC Ophthalmic Materials Network for funding and the Natural Sciences and Engineering Research Council (NSERC) for provision of travel funds (SNEI program) to visit CSIRO, Melbourne Australia. We would also like to express our gratitude to CSIRO for helpful discussions and the use of their photorheometer. [1]

3.8 References

1. Noll, W. J. *Chemistry and Technology of Silicones*. Academic Press: New York, 1968.

2. Jiang, H. Y.; Kelch, S.; Lendlein, A. *Adv. Mater.* **2006,** *18* (11), 1471-1475.
3. Dong, R.; Liu, Y.; Zhou, Y.; Yan, D.; Zhu, X. *Polym. Chem.* **2011,** *2* (12), 2771-2774.
4. Jin, Y.; Paris, S. I. M.; Rack, J. J. *Adv. Mater.* **2011,** *23* (37), 4312-4317.
5. Kloxin, C. J.; Scott, T. F.; Park, H. Y.; Bowman, C. N. *Adv. Mater.* **2011,** *23* (17), 1977-1981.
6. Wells, L. A.; Brook, M. A.; Sheardown, H. *Macromol. Biosci.* **2011,** *11* (7), 988-998.
7. Yagai, S.; Ohta, K.; Gushiken, M.; Iwai, K.; Asano, A.; Seki, S.; Kikkawa, Y.; Morimoto, M.; Kitamura, A.; Karatsu, T. *Chem. Eur. J.* **2012,** *18* (8), 2244-2253.
8. Cabane, E.; Zhang, X.; Langowska, K.; Palivan, C. G.; Meier, W. *Biointerphases* **2012,** *7* (1-4).
9. Elisseeff, J.; Anseth, K.; Sims, D.; McIntosh, W.; Randolph, M.; Yaremchuk, M.; Langer, R. *Plast. Reconstr. Surg.* **1999,** *104* (4), 1014-1022.
10. Biyani, M. V.; Foster, E. J.; Weder, C. *Macro Letters* **2013,** *2* (3), 236-240.
11. Clarson, S. J.; Semlyen, J. A. *Siloxane Polymers*. Prentice Hall: Englewood Cliffs, NJ, 1993; p 673.
12. Keller, M. W.; White, S. R.; Sottos, N. R. *Adv. Funct. Mater.* **2007,** *17* (14), 2399-2404.
13. Zheng, P.; McCarthy, T. J. *J. Am. Chem. Soc.* **2012,** *134* (4), 2024-2027.
14. Fawcett, A. S.; Brook, M. A. *Macromolecules* **2013**, submitted.
15. Kehrloesser, D.; Baumann, R. P.; Kim, H. C.; Hampp, N. *Langmuir* **2011,** *27* (7), 4149-4155.
16. Zheng, Y. J.; Mieie, M.; Mello, S. V.; Mabrouki, M.; Andreopoulos, F. M.; Konka, V.; Pham, S. M.; Leblanc, R. M. *Macromolecules* **2002,** *35* (13), 5228-5234.
17. Chen, Y.; Chen, K. H. *J. Poly. Sci., Part A: Polm. Chem.* **1997,** *35* (4), 613-624.
18. Chen, Y.; Chou, C. F. *J. Poly. Sci., Part A: Polm. Chem.* **1995,** *33* (16), 2705-2714.
19. Chen, Y.; Jean, C. S. *J. Appl. Polym. Sci.* **1997,** *64* (9), 1749-1758.
20. Chen, Y.; Jean, C. S. *J. Appl. Polym. Sci.* **1997,** *64* (9), 1759-1768.

CHAPTER 4: Rapid, Metal-Free Room Temperature Vulcanization Produces Silicone Elastomers[§]

4.1 Abstract

Silicone room temperature vulcanization elastomers are usually formed through either a platinum-catalyzed hydro- silylation or tin-catalyzed moisture cure. In this article, we show that it is possible to create robust, transparent silicone elastomers without the need for metal catalysts. Hydrogen-terminated silicone polymers are crosslinked by tri- or tetraalkoxysilane crosslinkers in a condensation process catalyzed by the presence of trispentafluorophenylborane catalyst to give elastomers and alkane by-products. This procedure allows for very fast cure times (< 30 s to a tack free state): the process is more conveniently controlled with the addition of a small amount of solvent. Physical and mechanical properties are readily modified by control of the chain length of the starting polymer, the functionality and nature of the alkoxy group on the crosslinker. Organofunctional groups, useful for further polymer modification, can optionally be incorporated by judicious choice of readily available starting materials.

4.2 Introduction

Silicone elastomers are widely used in many applications ranging from biomaterials[1-3] to coatings and sealants, and so forth.[4-6] Although there are several methods available for their synthesis,[5, 7, 8] the most common of these are high-temperature radical cure, room-temperature vulcanization using either tin- or titanium-derived hydrolysis/condensation catalysts, or platinum-catalyzed hydrosilylation.[9] Each of these processes has its own disadvantages: for example, it can be difficult to control high-temperature curing to give reproducible networks. Although exquisite control over network structure is possible

---

[§] This chapter is reproduced from A.S. Fawcett, J.B. Grande, M.A. Brook, in *Journal of Polymer Science Part A: Polymer Chemistry*, **2013**, *51*, 644-652 with permission from Wiley Periodicals, 2012. Fawcett designed the experimental procedure with assistance from Grande. Fawcett performed all experiments with assistance from Grande. Fawcett also wrote the majority of the manuscript with additions, edits and guidance provided by Grande and Brook.

using metal-catalyzed crosslinking, for reasons of cost (platinum catalyst) or environmental concerns (tin catalysts are currently under scrutiny by regulatory agencies in many parts of the world[10]), there is a desire to avoid metals in room or elevated temperature crosslinking processes.

We have previously described the ability to make complex silicone structures, optionally containing functional groups, using the dehydrocarbonative coupling of alkoxysilanes with hydrosilanes ($R_3SiH + R'OSiR''_3 \rightarrow R_3SiOSiR''_3 + R'H$), a process catalyzed by $B(C_6F_5)_3$ (Figure 4.1A, B).[11-13] Others have also reported the synthesis of siloxane resins[14, 15] and polymers[16, 17] using this strategy. The reaction offers several advantages in the preparation of small molecules that include: rapid reaction times, simple removal of (gaseous) by-products, lower catalyst concentrations than Sn-based systems and the simplicity with which the 3D structures can be controlled by appropriate use of simple starting materials: complex structures can be prepared that are not available by traditional routes.[13] It seemed likely that this reaction could similarly offer benefits to the preparation of silicone polymers and elastomers (Figure 4.1C). We have therefore examined the ease with which α,ω-hydride-functional silicone polymers can be crosslinked with various alkoxysilanes as a function of molecular weight of the starting polymer, siloxane and catalyst concentrations, alkoxysilane reactivity, and choice of solvent to prepare uniform silicone elastomers.

4.3 Experimental

Tetraethyl orthosilicate (TEOS), tetrapropyl orthosilicate (TPOS), 1-pyrenemethanol, and tris(pentafluorophenyl)borane were purchased from Sigma-Aldrich and used as received. Methyltriethoxysilane (MTES), tetramethyl orthosilicate (TMOS), vinyltrimethoxysilane (VT), iodopropyltrimethoxy-silane (IT), tetravinylsilane (TV), 1,1,3,3-tetramethyldisiloxane, 1,1,3,3,5,5,7,7-octamethylcyclotetrasiloxane (D4), α,ω-hydride-terminated poly(dimethylsiloxane) (H-PDMS-H) 100, and 1000 centiStokes (cSt, ~ MW 5900 and 28,000, respectively)[18, 19] were purchased from Gelest; hexanes, dichloromethane, diethyl ether, tetrahydrofuran, and toluene were purchased from Caledon.

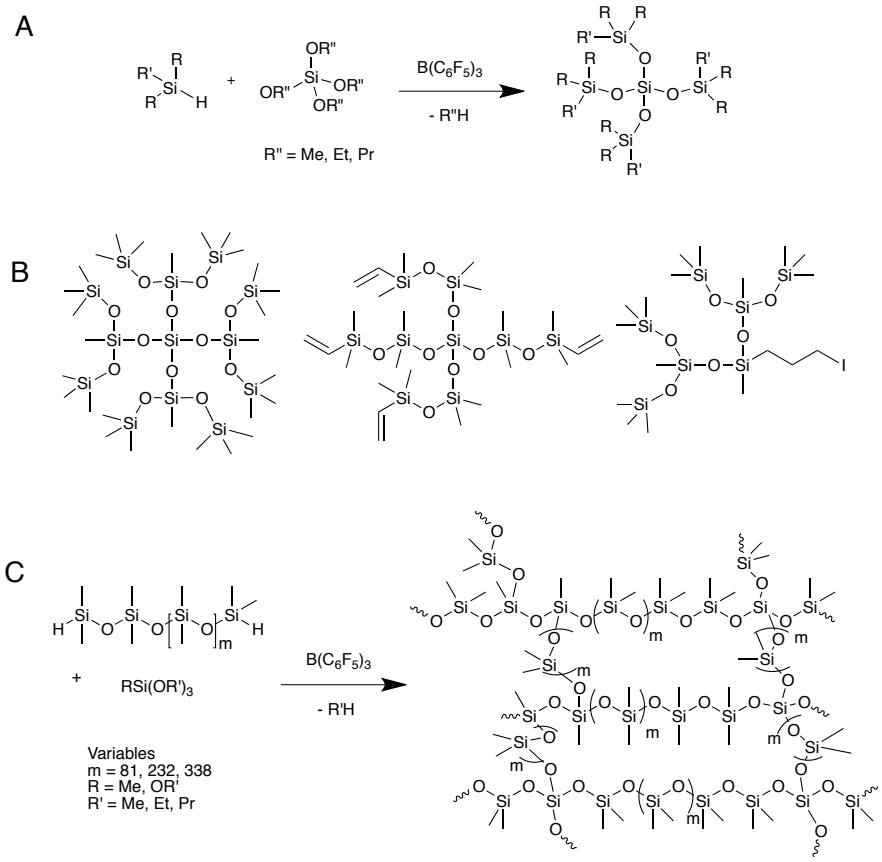

Figure 4.1. A: Reaction scheme depicting the dehydrocarbonative coupling used to synthesize PDMS elastomers. R = Me, OR'; R' = Me, Et, Pr. B: Examples of explicit silicones that can be synthesized using this process. C: Elastomer formation; product shown for R = OR'

NMR spectra were recorded using a Bruker Avance500 or AV600 spectrometer. Shore A hardness measurements were made using a Durometer Hardness type ''A2'' from The Shore Instrument & Mfg. Co., NY. Shore OO experiments were taken using a Rex Durometer, Type OO, Model 1600 from Rex Gauge Co.

4.3.1 Synthesis of 500 cSt PDMS (Poly(dimethylsiloxane), ~16,000 MW)

To a mixture of 1,1,3,3,5,5,7,7-octamethylcyclotetrasiloxane, D4 (50.0 g, 0.158 mol Me_2SiO unit), and 1,1,3,3-tetramethyldisiloxane (0.483 g, 3.59 mmol) was added trifluoromethanesulfonic acid (0.05 mL, 0.085 g, 0.57 mmol) at room temperature. The mixture was then heated at 100 °C for 5 h, cooled to room temperature, and magnesium oxide (~2 g) was added to quench the acid. After 30 min, tetrahydrofuran (200 mL) was added to the mixture. The solution was then filtered and concentrated under reduced

pressure. The residue was purified by removal of small molecular weight silicones using Kugelrohr distillation at 180 °C under vacuum (0.1 mmHg) for 5 h yielding a colorless oil (26.5 g, yield 62.8%).

1H NMR ($CDCl_3$, 600 MHz, δ): 4.70 (m, 2 H), 0.18 (d, 12 H), 0.08–0.05 (m, 1296 H).

4.3.2 General Synthesis of PDMS Elastomers

In a typical synthesis (shown for 1000 cSt SiH terminated PDMS with TEOS, 1:1 eq SiOEt:SiH, Table 4.2, Entry 6), TEOS (0.009 g, 0.04 mmol) was placed in a 25.0 mL vial with $B(C_6F_5)_3$ (15 μL of a 0.078 M solution, 239 ppm) and hexanes (2.0 mL). The contents of the vial were added to H-PDMS-H (1000 cSt, 2.50 g, 0.04 mmol SiH groups) that had been preweighed in a beaker, followed by rapid mixing. The contents were then poured into a Teflon-lined Petri dish (10 mm thick x 35 mm diameter) and placed under vacuum (571 Torr) to degas the mixture. The mixture was allowed to cure for 5 min at room temperature (20 °C) at which time the reaction was complete. The dish was then moved to a 50 °C oven overnight to remove any excess solvent.

Table 4.1 and Table 4.2 show the variables that were examined in an effort to correlate reagent types, concentrations, and reaction conditions with the ability to form uniform elastomers. Factors including: solvent volume (Table 4.1); catalyst concentration (a catalyst stock solution, 0.078 M, used to increase catalyst concentration in the elastomers, was prepared by dissolving the catalyst (40 mg, 0.07 mmol) in dry toluene (1 mL)); H-PDMS-H MW; type of crosslinker; molar ratio of crosslinker (SiOR) to SiH functional groups; and the effects of vacuum were examined (Table 4.1 and Table 4.2). The materials appeared to go to complete cure normally within 1–10 min (for example, bubble evolution ceased): hardnesses of the elastomers were measured after 24 h. In some instances, the elastomers required oven cure at 50 °C for 24 h to give a ‘‘tack-free’’ elastomer. An assessment of whether tack was coming from residual solvent or incomplete cure was not made.

4.3.3 A Comparison with Karstedt’s Catalyst

A 30 ppm Pt solution was prepared by taking 10 μL of Karstedt’s Catalyst (2.5% Pt in xylenes) and diluting in 1 mL of hexanes. A total of 0.33 mL of this stock solution was placed added to a vial containing $Si(CH{=}CH_2)_4$ (6.0 mg, 0.04 mmol) and 1.67 mL of hexanes. This solution was then quickly added to the hydrogen-terminated silicone, stirred, and poured into a Petri dish to cure following the protocol above (29, Table 4.2). The experiment was repeated at 50 °C to give 30.

Table 4.1. Solvent Effects on Reaction Time[a]

Exp#	Hexane (mL)	Reaction Time (s)
1	0	20
2	0.1	32
3	0.5	38
4	1.0	43
5	2.0	43

[a] for 5,900 MW silane with TMOS (1:1) with 15μL/236ppm catalyst.

Table 4.2. Preparation of Silicone Elastomers

Parameters						Outcome			
Exp #	Silane MW (g)[a]	X-linker (g)[b]	Ratio [SiOR]:[SiH]	Catalyst (μL/ppm)	Hexane (mL)	Rubber (Y/N)	Reaction Time (min:s)[c]	Shore A	Shore OO
6	28000 (2.5)	TE (0.009)	1:1	15/239	2.0	Y	1:42	18	67
7	28000 (2.5)	TE (0.014)	1.5:1	15/238	2.0	Y	2:00	13	63
8	16000 (2.5)	TE (0.024)	1.5:1	12/237	2.0	Y	1:10	21	70
9	5900 (2.5)	TE (0.066)	1.5:1	15/236	2.0	Y	1:20	25	68
10	28000 (2.5)	Me (0.006)	0.5:1	15/239	2.0	Y	4:48	20	78
11	5900 (2.5)	TE (0.022)	0.5:1	15/237	2.0	N[d]	-	-	-
12	16000 (2.5)	TE (0.008)	0.5:1	12/239	2.0	N[d]	-	-	
13	28000 (2.5)	Me (0.011)	1:1	15/238	2.0	Y	4:55	21	67
14	28000 (2.5)	Me (0.016)	1.5:1	15/238	2.0	Y	4:52	18	62
15	28000 (2.5)	Me (0.021)	2:1	15/238	2.0	Y	10:00	10	53
16	16000 (2.5)	TM (0.018)	1.5:1	12/238	2.0	Y	1:52	23	70
17	16000 (2.5)	TM (0.023)	2:1	12/237	2.0	Y	1:55	14	51
18	16000 (2.5)	TP (0.030)	1.5:1	12/237	2.0	Y	1:52	18	63
19	16000 (2.5)	Me (0.027)	1.5:1	12/237	2.0	Y	3:45	18	65
20	5900 (2.5)	VT (0.083)	2:1	15/232	2.0	Y	-	15	68
21	5900 (2.5)	IT (0.163)	2:1	15/225	2.0	Y	-	21	66
22	5900 (2.5)	TM (0.016)	0.5:1	15/238	2.0	N[d]	-	-	-
23	5900 (2.5)	TM (0.016)	0.5:1	9/143	5.0	Y	-	-	11
24	16000 (2.5)	TP (0.041)	2:1	12/236	2.0	Y	1:44	-	15
25	5900 (2.5)	Me (0.075)	1.5:1	15/233	2.0	Y	5:10	30	80
26	5900 (2.5)	TM (0.032)	1:1	15/236	2.0	Y	0:43	22	75
27	5900 (2.5)	TM (0.032)	1:1	1.9/30	0	Y	78:00	22	78
28	28000 (2.5)	TM (0.009)	1.5:1	15/239	2.0[e]	Y		8	60
29	28000 (2.5)	TV[f] (0.006)	1:1	30ppm	2.0	Y	19:08	12	62
30	28000 (2.5)	TV[g] (0.006)	1:1	30ppm	2.0	Y	9:00	12	62

[a] 28000 MW = 1000 cSt; 16000 MW = 500 cSt; 5900 MW = 100 cSt. [b] Me (methyltriethoxysilane), TM (tetramethyl orthosilicate), TE (tetraethyl orthosilicate), TP (tetrapropyl orthosilicate), IT (iodopropyltrimethoxysilane), VT (vinyltrimethoxysilane). [c] Small variations in temperature (2-4 °C) led to noticeable changes in reaction time; these values are thus reported ± 20 s. [d] The elastomers contained large bubbles. [e] 1.4 mL hexane with 0.6 mL toluene + 1-pyrenemethanol (0.001 g). [f] TV = $Si(CH=CH_2)_4$; these conditions match those of entry 6 (crosslinker is present in the same molar concentration), but using a 30ppm Pt solution to replace the boron catalyst. [g] The conditions reported in e were used, except the reaction was performed at 50 °C.

4.3.4 Synthesis of Fluorescent PDMS (Includes 10 mol % 1-Pyrenemethanol.)

1-Pyrenemethanol (0.001 g, 6.0 x 10^{-6} mol) was dissolved in toluene (0.6 mL) and added to H-PDMS-H (2.5 g, 8.9 x 10^{-5} mol) in a 20 mL vial. TMOS (0.009 g, 6 x 10^{-5} mol) and catalyst (15 μL, 239 ppm) were combined in a vial with hexane (1.4 mL). The crosslinker/catalyst solution was added to the silane, rapidly mixed, and poured into a Teflon- lined Petri dish and placed under vacuum to cure. After the initial curing reaction, 3 min, the Petri dish was placed into a 50 °C vacuum oven for 3 more days to remove any remaining toluene. A 1.27 cm disk was punched from the elastomer and placed in a cellulose thimble for a Soxhlet extraction, which was performed over 16 h with toluene as solvent. Following extraction and drying, images were taken using a Canon PowerShot SX120 IS camera, with irradiation by 365 nm light.

4.4 Results

Synthetic protocols for siloxane bond synthesis using dehydrocarbonative coupling[11, 12, 20, 21] simply involve mixing—often with a small amount of solvent (see below)—the hydrosilane, alkoxysilane, and a catalytic amount of $B(C_6F_5)_3$. After a short induction period, the reaction occurs with an exotherm and, occasionally (particularly with methoxysilanes) with vigorous release of an alkane gas. No protection from the local environment was needed. Normally, a small excess of the more volatile reagent is used, such that work-up (in the case of fluid products) is limited to addition of a small amount of neutral alumina to complex the catalyst, filtration, and evaporation of the residual volatile reagent (Figure 4.1). Although $B(C_6F_5)_3$ is normally removed from fluid silicones, we have not observed any evidence of silicone depolymerization/metathesis, even when the catalyst is left in the silicone over extended periods of time.

Preliminary experiments demonstrated that some procedural modifications would be necessary to evenly cure polymers into elastomers. Important process parameters to

control included the order of addition of the reactants, the concentration of the $B(C_6F_5)_3$ catalyst, and the need to add small amounts of solvent to enhance the dispersion of $B(C_6F_5)_3$ and alkoxysilane crosslinker within the hydride-terminated PDMS silicone. A more important effect that speaks to the efficiency of the reaction was the slower reaction time observed when solvent was present, which permitted transfer of the pre-elastomer mixture to the curing vessel, typically a Petri dish. If solvent was not used, the reaction was sufficiently fast that cure often occurred to a significant degree during mixing, including partial or complete setting, which frequently led to inhomogeneous materials (e.g., less than 30 s, see Table 4.1). This suggests, however, that it may be possible to use the reaction in extrusion or injection molding processes where high-speed production is particularly important.

Early experiments also demonstrated that the order of addition of the reagents was important for clean elastomer formation. The optimal addition order involved combining the alkoxysilane crosslinker with the catalyst and then adding this mixture to H-PDMS-H. If the catalyst was added to the hydrosilane first, crosslinking immediately proceeded, making reproducible reactions difficult. Evenly cured materials formed more readily if the pressure was reduced shortly after mixing the ingredients: degassing silicone elastomers during cure is a common practice to avoid entrained bubbles.[4] In this reaction, the likelihood of bubbles in the product is exacerbated by the formation of alkane by-products. In some cases, it was not possible to form bubble-free elastomers unless significant deviations were made from standard formulations (see below).

A wide range of elastomeric materials could be prepared once these factors had been optimized, as described in Table 4.2 (Figure 4.1C, Appendix Section 8.3). The factors that most influenced the mechanical properties of the product elastomers were: H-PDMS-H MW, crosslinker concentration, crosslinker reactivity, and solvent volume, which will be discussed in turn.

4.4.1 Reaction Rate, Use of Solvent, and Bubble Suppression

The rate of the reaction depended on a variety of factors including base polymer molecular weight, catalyst concentration, the character of the alkoxysilane crosslinker, and the use of hexane as diluent. Early explorations with the more reactive formulations (Table 4.1: 1) demonstrated that solvent-free elastomers could be formed completely in 20 s. This exceptionally rapid rate was frequently disadvantageous as, in many cases, the elastomers were relatively inhomogeneous because it was not possible to efficiently mix the starting materials before the onset of cure. Only hand mixing was possible: the use of

10 static mixer syringe tips with either 5 or 10 elements was unsuccessful because cure occurred in the mixer.

As would be expected, lowering the catalyst concentration led to increases in reaction time. For example, using 30 ppm instead of 239 ppm of catalyst increased the reaction time to 78 min (Table 4.2: 27). Although further manipulation of catalyst loading was possible, it proved to be more convenient both to facilitate mixing and moderate reaction times by addition of a small amount of solvent.

The first benefit of solvent addition was an increased level of control in the process as a consequence of mediation of cure kinetics: there was a concomitant reduction in reaction rate with decreasing reagent concentration (Table 4.1). Addition of hexanes also facilitated both catalyst and crosslinker dispersion and allowed the viscosity of the curing mixture to remain lower for longer periods of time, which led to a reduction in the incidence of entrapped bubbles. The addition of an appropriate amount of solvent could thus change outcomes from bubble containing to the desired uniform, bubble-free elastomers. For example, in an otherwise identical formulation containing 2.5 g of silicone, the use of 5 mL hexane instead of 2 mL, avoided the presence of bubbles in the product (Table 4.2: 22 vs. 23, Figure 4.2A, B). Bubble formation was also controlled by crosslinker type and silicone MW as is discussed further below.

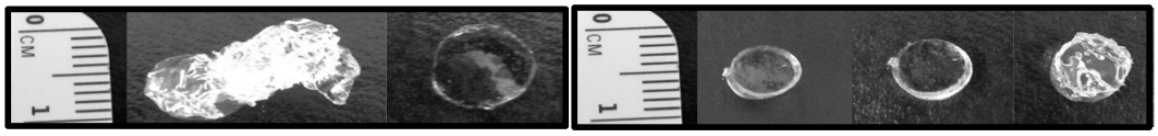

Figure 4.2. A: A foamed material (Table 4.2: 22); B: The corresponding elastomer arises from changing the amount of added solvent and/or catalyst concentration (Table 4.2: 23). Effect of PDMS MW on elastomer formation: entries on Table 4.2. C: entry 7 (1000 cSt), D: entry 8 (500 cSt), E: entry 9 (100 cSt) at a fixed [SiOR]:[SiH] ratio of 1.5:1

4.4.2 H-PDMS-H Molecular Weight

As with any rubber, elastomeric properties were associated with the crosslink density that could be optimized by changing the molecular weight of the base silicone polymer. More rigid/brittle materials formed when shorter silicone chains were used, due to the shorter distance between crosslinks. For example, at a fixed crosslinker ratio of 1.5:1 [SiOEt]:[SiH] functional groups (from TEOS crosslinker and linear H-PDMS-H, respectively), the hardness of the elastomer products increased as the molecular weight of the silicone was decreased from 28,000 to 16,000 and 5900 MW H-PDMS-H: the Shore

A hardness of the materials were 13, 21, and 25, respectively (Table 4.2: 7, 8, 9, respectively; Appendix Section 8.3, Figure 4.2C–E).

The lower MW starting H-PDMS-H (100 cSt, ~5900 MW) was more reactive than longer silicone chains due to a higher SiH concentration in the reaction mixture, causing some of the alkane by-products to be entrapped in the resulting elastomer. For instance, the reaction time for a 5.9 kDa MW H-PDMS-H with reactive crosslinker TMOS with 2 mL of hexane is 43 s (Table 4.1: 5, Figure 4.2E), while when the same conditions were used with a higher 28 kDa MW silicone hydride, the total reaction time increased to 1.4 min (Table 4.2: 6). Performing the reaction under vacuum, to facilitate removal of the alkane gases, avoided the trapping of bubbles in most cases. With shorter H-PDMS-H chains (100 cSt), particularly with lower concentrations of crosslinker, bubble-containing materials were almost always formed demonstrating that the rate of cure is faster than the rate of bubble removal.[22]

4.4.3 Ratio of $Si(OR)_4$:H-PDMS-H

The final properties of the elastomer can also be manipulated by changing the concentration of crosslinker present. At lower crosslinker concentrations, for example, at a 0.5:1 molar ratio of [SiOR]:[SiH], the materials formed were softer and more elastic (Figure 4.3A,B) than elastomers formed with higher crosslinker concentrations (Table 4.2: Entry 10, Appendix Section 8.3). Even if complete reaction occurs with the four reactive sites on the crosslinker, residual unreacted silicone chains, or chains only tethered at one terminus, convey gel-like properties onto the material. At this low ratio, the products formed with 100 and 500 cSt H-PDMS- H, entry 11 and 12 respectively, generally contained large bubbles that could not be removed before the elastomer cured. With the optimal crosslink density resulting from a [SiOR]:[SiH] 1:1 ratio, harder elastomers formed for each given H-PDMS-H MW (Figure 4.3C). As the crosslinker ratio was further increased from 1:1 to 1.5:1 [SiOR]:[SiH], the elastomers became softer (Shore A decreased from 21 to 18, respectively, for 1000 cSt H-PDMS-H with MTES crosslinker, Table 4.2: 13, 14, Figure 4.3D). With yet higher crosslinker concentrations, 2:1, the crosslink density is further decreased and a much softer elastomer resulted (Shore A decreases to 10, Table 4.2: 15, Figure 4.3E). In this case, the stoichiometry leads to a lightly crosslinked polymer that exhibits enhanced chain extension and crosslinker-capped chains, at the expense of crosslinks. The effect of both chain length and reduced crosslinker concentration can be seen by comparing Shore hardness values of the elastomers produced at 1.5:1 and 2:1 ratios with different H-PDMS-H MW: for 500 cSt H-PDMS-H MW the Shore A hardness decreased from 23 to 14, respectively, while for 1000 cSt hardnesses of 18 and 10 were observed (Table 4.2: 16, 17, Appendix Section 8.3

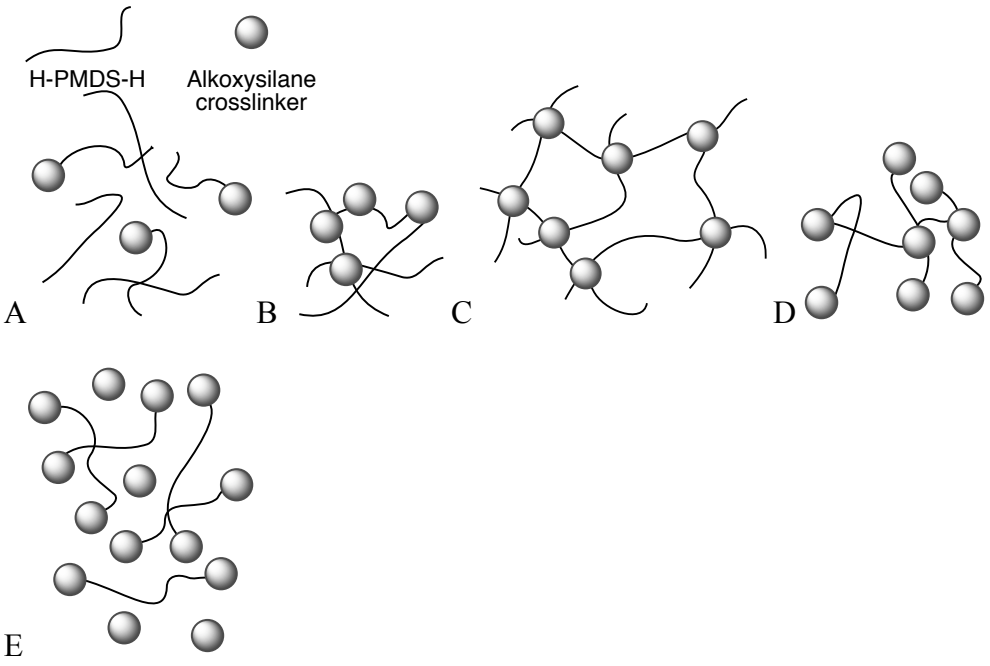

Figure 4.3. Models showing crosslink density changes associated with an increase in the concentration of alkoxysilane crosslinker. A: excess H-PDMS-H. B: [SiOR]:[SiH] ratio of 0.5:1. C: [SiOR]:[SiH] ratio of 1:1. D: [SiOR]:[SiH] ratio of 1.5:1. E: [SiOR]:[SiH] ratio of 2:1

4.4.4 Alkoxysilane Crosslinker

The type of alkoxysilane crosslinker also affects the rate of the dehydrocarbonative coupling reaction: more sterically congested alkoxy groups react more slowly.[13] We examined a range of silicone crosslinkers to see if the rate effects were manifested during elastomer formation and, more importantly, if they led to significant changes in the properties of the resulting elastomers. It was found that more reactive crosslinkers, such as TMOS ($Si(OMe)_4$), led to elastomers that contained relatively high densities of bubbles or were less transparent, or both (e.g., Table 4.2: 16, Figure 4.4B). The reaction process was too fast to allow bubbles to escape the curing material, even if solvent was used to slow the process. By contrast, use of the less reactive crosslinker, TPOS, slowed the reaction down to such an extent that in some instances the elastomers did not fully cure, and remained ‘‘tacky’’ (e.g., Table 4.2: 18, Figure 4.4D), but no bubbles were entrained. MTES and TEOS were thus determined to be the optimal crosslinkers, as the ethoxy groups were large enough to retard the reaction such that clear, uniform elastomers formed that contained few or no bubbles, but reactive enough for the reaction to go to completion in a convenient time period (Figure 4.4A,C, respectively). An additional

advantage of these two crosslinkers is that they can be used in different ratios: changing the ratio of tri- to tetra-functional silanes facilitates control of final elastomer hardness within a fixed [SiOR]:[SiH] ratio regime.

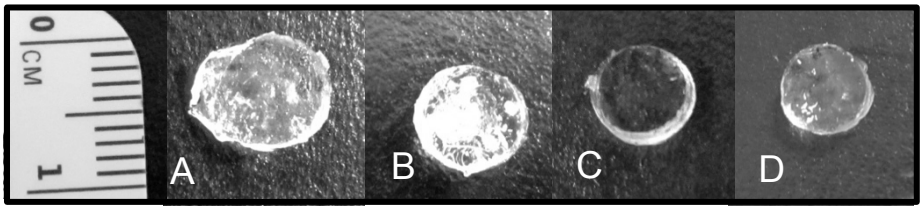

Figure 4.4. All elastomers were synthesized with 500 cSt PDMS, in a 1.5:1 ratio of [SiOR]:[SiH] in crosslinker:H-PDMS-H. Pictures show the effect of changing crosslinker reactivity: A: MTES 19; B: TMOS 16; C: TEOS 8, D: TPOS 18 (see Table 4.2)

4.4.5 The Effect of Humidity

$B(C_6F_5)_3$ is a strong Lewis acid, which is known to efficiently complex with water and other Lewis bases.[23, 24] The complexation with water leads to the formation of a relatively strong Brønsted acid. It was posited that the complexation would retard the coupling reaction and, possibly, the Brønsted acid could compromise the elastomer by catalyzing hydrolytic de-polymerization. As a consequence, the reaction was examined at various humidity levels. One of the most reactive formulations reacted in a chamber set at 75% humidity (Table 4.2: 26). When the components were mixed and immediately placed into the humidity chamber there was only a slight delay (+5 s) in the total elastomer cure time. However, when the components of the reaction were left in the humidity chamber for 1 h before mixing, the elastomer cure time was significantly delayed (from 43 s to 16 min). The final hardness of the bubble-containing elastomer was the same as previously reported.

4.4.6 Comparison with Traditional Catalysts

As noted above, platinum catalysts are frequently used to prepare silicone elastomers from precursors functionalized with SiH and Si-vinyl groups, respectively. To provide some comparison[24] between the process described above and traditional platinum-catalzyed addition cure, a formulation was prepared with 30 ppm of a platinum catalyst used to cure 28,000 MW hydrogen-terminated silicone with $Si(Vi)_4$ as crosslinker in hexane as diluent. As the molecular weight of silicone chains and functionality of the crosslinker are the same, the resulting network should be identical to formulation (6, Table 4.2). The initial experiment (29, Table 4.2) showed that cure took about an order of

magnitude longer under comparable conditions with the $B(C_6F_5)_3$-catalyzed process, a situation only slightly improved by heating to 50 °C, entry 30.

4.4.7 Functional Elastomers

Although the main focus of the research was the development of alternative routes to silicone elastomers, the $B(C_6F_5)_3$-catalyzed process conveniently allows incorporation of functional group synthetic handles: the chemistry used to form siloxane linkages does not affect some organic functional groups, including alkenes or alkyl halides (Figure 4.1B).[11] To demonstrate this premise, vinyltrimethoxysilane was used as a crosslinker to provide an elastomer bearing vinyl groups that are available for hydrosilylation reactions (Figure 4.5A, Table 4.2: 20], the most common way to modify silicones.[5] Note that, while hydrosilylation can be catalyzed by $B(C_6F_5)_3$,[25] it was not observed with the low concentration of catalysts used. Similarly, iodopropyltriethoxysilane was incorporated in the silicone elastomer to provide a reactive site that could be used to create available sites for azide functionalization that can be used to react with alkynes in a click reaction (Figure 4.5B, Table 4.2: 21).[26] The ability to incorporate synthetic functionality was further demonstrated by adding a fluorescent label which, through the Piers reduction,[27] becomes incorporated in the final elastomer. In the low [SiH] regime, reductive cleavage to methylpyrene was not observed, and the fluorescent label remained in the elastomer after Soxhlet extraction with toluene (Table 4.2: 28, Figure 4.5D).

4.5 Discussion

Silicone elastomers are normally cured by one of three means: high-temperature radical cure; tin-catalyzed moisture (condensation) cure; or platinum-catalyzed hydrosilylation (addition) cure. Each of these processes exhibits benefits and detriments.

Tin-catalyzed moisture cure is an efficient, but slow, elastomer-forming process. However, the tin catalysts are set for removal from commerce in Europe because of concerns about their environmental behavior.[10] From a materials' perspective, the challenge with this process is managing the moisture that is a co-constituent of the vulcanization process. As moisture is provided by the environment, cure always occurs from the ‘‘outside-in,’’ and complete and homogeneous cure is not always easy to attain: it is typically slow.

Radical cure, which is very rapid, provides little control over network structure and requires postcure baking to (attempt to) remove residuals from the radical initiators. Platinum-based addition cure is typically associated with the highest level of network

control. Elevated temperatures are frequently required to elicit cure and it is quite common to use a ‘‘postcure’’ thermolysis to finish the curing process, and to drive off residual volatile compounds. Platinum catalysts—even at the low concentrations at which they are used—are expensive. Over time, the residual platinum in the silicone elastomer can aggregate to form colloidal platinum particles that cast a yellow tinge to the elastomer.

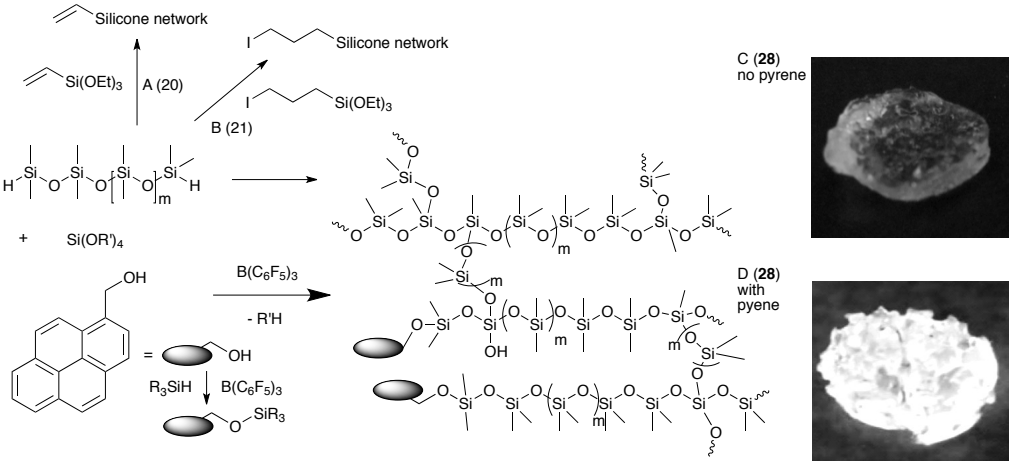

Figure 4.5. Functional silicones are readily prepared by use of functional crosslinkers A (Table 4.2: 20), B (Table 4.2: 21), C and D: non-functional (C: formulated without pyrenemethanol), and pyrene-modified silicone (D: Table 4.2: 28). The rippling in the elastomers occurred after Soxhlet extraction with toluene and drying

The outcome of the use of platinum catalysts under the optimized conditions used for the $B(C_6F_5)_3$-catalyzed process were instructive. The catalyst concentration—30 ppm—falls within the normal range of commercial elastomers. Platinum-catalyzed hydrosilylation is an efficient process in hexane as solvent, although the use of a solvent diluent is atypical for elastomer formation. As shown in Table 4.2, the reactions were significantly slower than the $B(C_6F_5)_3$, nearly an order of magnitude slower and, even at 50 °C, were about five times slower. This head-to-head comparison demonstrates the remarkable efficiency of the $B(C_6F_5)_3$-catalyzed condensation to give siloxanes.

The mechanism of the dehydrocarbonative coupling of hydrosilanes and alkoxysilanes involves the complexation of the Lewis acidic boron in $B(C_6F_5)_3$ with the silicon hydride.[12] The reaction proceeds efficiently despite the multitude of other Lewis bases present—silicone-based oxygens in particular: it is known that strong Lewis bases, including those based on nitrogen, completely suppress the process. Initially, there was concern that ambient water would intervene in the reaction as has been observed in other

reactions catalyzed by $B(C_6F_5)_3$. At high levels of humidity, the process was retarded, which is attributed to a fraction of the catalyst being tied up with water and therefore unable to facilitate the coupling process. However, we did not observe any acid-catalyzed degradation[5] of the silicone backbone in previous work,[11,12,20] nor with the materials prepared here. We attribute this to the hydrophobic silicone environment. The water:$B(C_6F_5)_3$ complex will be comparably very polar and therefore likely of low solubility in the silicone environment: if the complex forms, it will not be sufficiently soluble in the silicone to catalyze silicone decomposition. This observation is particularly important for elastomers: it is impractical to remove catalysts from rubber and the presence of catalyst in the final product cannot compromise its integrity, as is the case here.

When the dehydrocarbonative coupling reaction was performed at ambient humidity and temperature, it was exceptionally rapid—much more rapid than the other silicone cure methodologies. For many applications, the rate of cure was actually impractically fast in a normal laboratory setting. However, this fast cure could be extremely beneficial in an industrial environment, such as with extrusion or injection molding, where speed and use of low temperatures is particularly advantageous.

In practice, it was necessary to slow the reaction down, both to avoid capturing bubbles formed from alkane byproducts and to facilitate mixing of the starting materials. The former aspect is most important because significant amounts of alkane are produced as by-products during the curing process. When the rate of bubble formation is comparable with the rate of cure (increasing viscosity leading to bubble capture), bubble-containing elastomers can result. However, to a large degree, the production of bubble free elastomers can be achieved simply by applying a small vacuum during elastomer production, by decreasing the viscosity of the elastomer body early on with the addition of a small amount of solvent, or slowing down the cure rate by reducing the amount of catalyst such that bubbles are better able to escape the curing material. However, it should also be noted that for certain formulations, bubble capture is not problematic, and rapid reaction occurs at room temperature to give transparent silicone elastomers (Table 4.2, Appendix Section 8.3). Of course, foam formation can be a desirable outcome.[26]

The dehydrocarbonative coupling process, as applied to elastomers, provides a variety of straightforward tools to manipulate the final rubber properties, while starting from simple, readily available precursors. Softer elastomers result from longer chain length between crosslinks or higher [SiOR]:[SiH] ratios; in the latter case increased surface tackiness is also enhanced as a consequence of more dangling chain ends (Figure 4.3D). Reaction rates can be moderated simply by using crosslinkers comprised of bulkier alkoxysilanes,

less catalyst or more solvent. Crosslink density, in addition to the techniques just mentioned, is also readily tuned by using mixtures of tri- and tetra-functional crosslinkers. Manipulating the mechanical properties of the produced rubbers, most of which have to do with changing the network structure to increase the spacing between crosslinks, can be readily achieved by modifying the relative concentration of alkoxysilane crosslinker to H-PDMS-H silicone chain length. Shore hardness ranging from Shore OO 15, to Shore A 30 are readily available with the process (24 and 25, respectively, Table 4.2).

4.6 Conclusions

Formulators design silicone elastomers around a variety of desired properties: transparency, color, tackiness (for adhesion to a variety of surfaces), hardness, resistance to tear, and so forth. Increasingly, the ultimate fate of the material is also to be considered and, in the case of tin derivatives, there is increasing concern about environmental impact.[10] The process described above for silicone elastomer synthesis exhibits a variety of benefits. First, it avoids the use of metal catalysts entirely, and the concentrations of $B(C_6F_5)_3$[11] necessary for reaction are less than tin catalysts. Second, the process is very rapid, and the kinetics are easily manipulated by a variety of simple strategies. Finally, the process allows elastomers with different properties to be readily prepared using by manipulation of ratios of crosslinker to silicone chain, chain length, steric bulk of the alkoxygroups on the crosslinker, and reagent concentrations.

Silicone elastomers containing comparable or improved properties to the materials formed using tin- (moisture cure) or platinum-catalyzed (hydrosilylation cure) processes have been synthesized. The reaction of alkoxy-functional silane crosslinkers with SiH-functional silicones using small amounts of trispentafluorophenylborane as catalyst is a practical alternative to these metal-catalyzed processes and one that occurs much more rapidly at room temperature. Unless very highly reticulated materials are prepared, the gaseous alkane by-product can be removed from the process by vacuum or by slowing the cure process down using less catalyst or through the addition of solvent. The extent of cure, and hence control over the final consistency of the rubber, is readily achieved through catalyst concentration, crosslinker type and concentration, and MW of the siloxanes.

4.7 Acknowledgements

The authors acknowledge the financial support of the Natural Sciences and Engineering Research Council of Canada and 20/20: NSERC Ophthalmic Materials Network. A.S. Fawcett is grateful for a NSERC CGS-D scholarship and J.B. Grande is grateful for a NSERC PGS-D scholarship. The authors also thank Alexander J. McLaughlin for assistance with preliminary experiments.

4.8 References and Notes

1. Malpass, C. A.; Millsap, K. W.; Sidhu, H.; Gower, L. B. *J. Biomed. Mater. Res.* **2002,** *63* (6), 822-829.
2. Kunzler, J. F. *Trends Polym. Sci.* **1996,** *4* (2), 52-59.
3. Mustoe, T. A. *Aesthetic Plast. Surg.* **2008,** *32* (1), 82-92.
4. Chen, H., Brook, M. A., Sheardown, H. D., Chen, Y., Klenkler, B. *Bioconjugate Chem.* **2006,** *17* (1), 21-28.
5. Brook, M. A. *Silicon in Organic, Organometallic, and Polymer Chemistry*. John Wiley & Sons: Toronto, 2000; p 680.
6. Noll, W. J. *Chemistry and Technology of Silicones*. Academic Press: New York, 1968.
7. Chrusciel, J. J.; Lesniak, E. *J. Appl. Polym. Sci.* **2011,** *119* (3), 1696-1703.
8. Zhang, M. Q.; Desai, T.; Ferrari, M. *Biomaterials* **1998,** *19* (10), 953-960.
9. Clarson, S. J.; Semlyen, J. A. *Siloxane Polymers*. Prentice Hall: Englewood Cliffs, NJ, 1993; p 673.
10. Utracki, L. A. *Polymer Blends Handbook*. Kluwer Academic Publishers : Dordrecht ; Boston, 2002.
11. Grande, J. B.; Thompson, D. B.; Gonzaga, F.; Brook, M. A. *Chem. Commun.* **2010,** *46* (27), 4988-4990.
12. Iza, M.; Bousmina, M.; Jerome, R. *Rheologica Acta* **2001,** *40* (1), 10-22.
13. Brook, M. A.; Thompson, D. B. *J. Am. Chem. Soc.* **2008,** *130* (1), 32-+.
14. Chojnowski, J.; Rubinsztajn, S.; Fortuniak, W.; Kurjata, J. *Macromolecules* **2008,** *41* (20), 7352-7358.
15. Kurjata, J.; Fortuniak, W.; Rubinsztajn, S.; Chojnowski, J. *Eur. Polym. J.* **2009,** *45* (12), 3372-3379.
16. Cella, J.; Rubinsztajn, S. *Macromolecules* **2008,** *41* (19), 6965-6971.
17. Hoque, M. A.; Kakihana, Y.; Shinke, S.; Kawakami, Y. *Macromolecules* **2009,** *42* (9), 3309-3315.
18. Malla, R. B.; Swanson, B. J.; Shaw, M. T. *Constr. Build. Mater.* **2011,** *25* (11), 4132-4143.
19. Safa, K. D.; Tofangdarzadeh, S.; Hassanpour, A. *J. Organomet. Chem.* **2009,** *694* (25), 4107-4115.

20. Grande, J. B.; Gonzaga, F.; Brook, M. A. *Dalton Trans.* **2010,** *39* (39), 9369-9378.
21. Rubinsztajn, S.; Cella, J. A. Silicone Condensation Reaction. US 7,064,173 B2, Jun. 20, 2006, 2006.
22. Grande, J. B.; Fawcett, A. S.; McLaughlin, A. J.; Gonzaga, F.; Bender, T. P.; Brook, M. A. *Polymer* **2012,** *53* (15), 3135-3142.
23. Piers, W. E. The chemistry of perfluoroaryl boranes. In *Advances in Organometallic Chemistry, Vol 52*, West, R.; Hill, A. F., Eds. 2005; Vol. 52, pp 1-76.
24. *We thank a referree for this suggestion.*
25. Rubin, M.; Schwier, T.; Gevorgyan, V. *J. Org. Chem.* **2002,** *67* (6), 1936-1940.
26. Malla, R. B.; Shrestha, M. R.; Shaw, M. T.; Brijmohan, S. B. *J. Mater. Civil Eng.* **2011,** *23* (3), 287-297.
27. Parks, D. J.; Blackwell, J. M.; Piers, W. E. *J. Org. Chem.* **2000,** *65* (10), 3090-3098.

CHAPTER 5: Anhydrous Formation of Foamed Silicone Elastomers using the Piers-Rubinsztajn Reaction[**]

5.1 Abstract

Elastomeric silicone foams are generally produced by the generation of hydrogen through reaction of Si-H groups with active hydrogen compounds, including water and alcohols, in a process catalyzed by platinum or tin complexes. It can be very difficult to control the rate and magnitude of bubble formation, particularly because of adventitious water. Silicone foams in a variety of densities (0.08-0.46 g/cm^3) were obtained using a newly developed Piers-Rubinsztajn reaction by combining α,ω-hydride-terminated poly(dimethylsiloxane) with an alkoxysilane crosslinker such as tetraethyl orthosilicate with catalysis by $B(C_6F_5)_3$. A single reaction leads both to crosslinking and bubble evolution. The reaction is not significantly impacted by humidity: foams are generated by the release of alkane gases derived from the alkoxysilane crosslinker, typically methane or ethane, rather than hydrogen. It was found that crosslinker reactivity and concentration, and silicone molecular weight, can be used to effectively control bubble nucleation, coalescence, viscosity build and, therefore, final foam density and the formation of open or closed cell foams. Better quality foams normally resulted when hexane, which acts as a blowing agent, was added to the pre-foam mixture. In addition to these advantages, and excellent reproducibility, the Piers-Rubinsztajn reaction benefits from a very fast induction time.

[**] This chapter is taken from J.B. Grande, A.S. Fawcett, A.J. McLaughlin, F. Gonzaga, T.P. Bender and M.A. Brook, *Polymer*, **2012**, *53*, 3135-3142, and is reproduced with permission from Wiley Periodicals, 2012. Fawcett contributed equally with Grande to the design and organization of experiments. The initial foam experiments were completed by Grande and McLaughlin, Fawcett contributed to the timing and repetition of all foam reaction experiments. Density measurements were completed by Grande. Fawcett contributed to and edited the manuscript with edits and guidance from Grande and Brook.

5.2 Introduction

Foamed silicone polymers exhibit very unusual properties when compared to organic analogs, which dictate their use in challenging applications ranging from joint sealants,[1, 2] insulators, mechanical shock absorbers in the aerospace, aircraft and transportation industry,[3] to biomaterials for wound dressings.[4, 5] Their high thermal stability, resistance to flame spreading, poor combustibility and electrical resistance are of particular use in transportation applications.

Silicone foam preparations can be classified, chemically, into two categories: (a) heat-activated foams and, (b) room temperature vulcanization (RTV).[3,6] Heat-activated vulcanization usually consists of curing a higher molecular weight vinyl or methyl functionalized silicone polymer using a peroxide-vulcanizing agent[3,6, 7] in the presence of a heat-activated blowing agent that is not affected by silicone cure.[8-13] Alternatively, in RTV systems polycondensation or polyaddition reactions occur between crosslinking agents containing a functional group on a silicon atom and silicone polymers containing hydrosilanes in the presence of a metal catalyst, typically based on platinum[7] or tin.[3,7,14] RTV foam systems are generally available as a two component mixture where, after mixing, elastomer cure occurs simultaneously with gas evolution.

Unlike the orthogonal chemical processes that occur in heat cured foams, RTV systems use the same chemical entity - typically a hydrosilane residue - for cure by hydrosilylation with an alkene and foam generation by reaction with active hydrogen compounds, such as H_2O and ROH, generating H_2 (Figure 5.1A). It remains very challenging to control the density and morphology of RTV silicone foams because of the need to control the kinetics of two separate processes: cure and foam/bubble generation. The most demanding aspect is avoiding adventitious water or other active hydrogen compounds that change both the crosslink density of the elastomeric foam and, more problematically, the relative cure/foam kinetics which lead to changes in foam density and structure (open/closed) from the desired outcome: reproducibility in foam generation can be problematic.

The condensation of alkoxysilanes with hydrosilanes (Figure 5.1B) giving alkane byproducts, catalyzed by $B(C_6F_5)_3$ - the Piers-Rubinsztajn reaction - can be used to create small well-defined silicone structures from simple starting materials.[15-17] This recently discovered reaction has been barely explored in silicone chemistry, particularly for the preparation of high molecular weight polymers. The few literature reports on the Piers-Rubinsztajn reaction suggest that it could have several potential advantages in the formation of silicone foams, including: rapid reaction times even at room temperature;

facile formation of gaseous by-products that could act as blowing agents; very low sensitivity to the presence of water, which will therefore not act as a blowing agent; and the need for relatively low catalyst concentrations. Current RTV technologies use metal-based catalysts that may be disadvantageous on the basis of cost (platinum) or environmental (tin) reasons: the high temperatures required for heat- generated foams can be avoided. *We note that the rapid generation of volatile and flammable byproducts means that particular care should be exercised with this process, particularly at larger scales.*

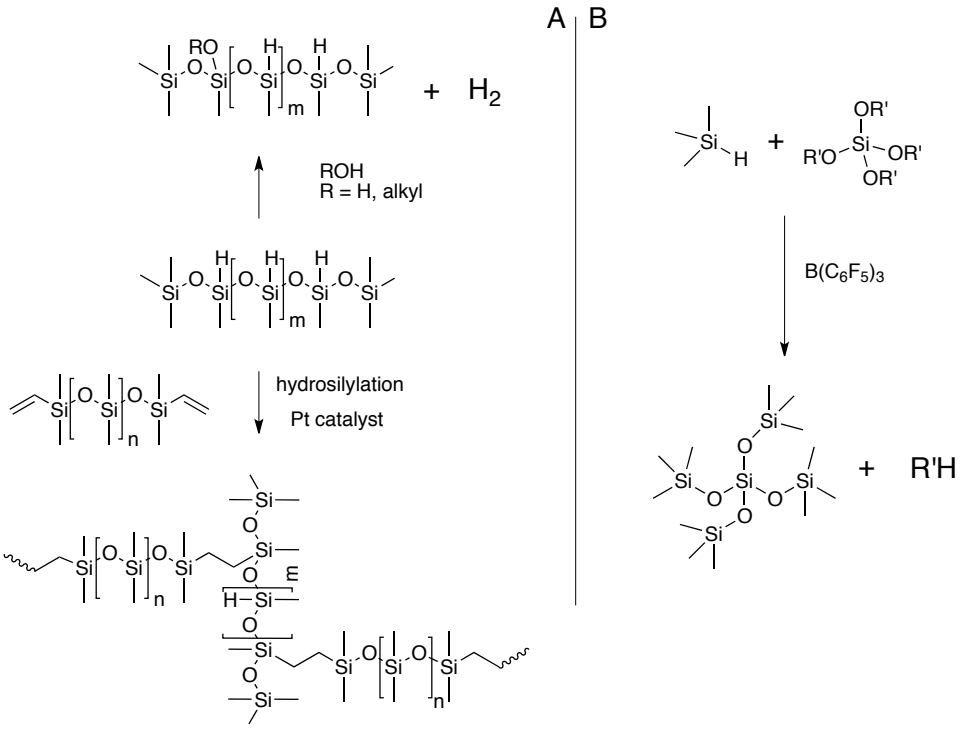

Figure 5.1. A: Gas evolution vs. RTV cure. B: A model Piers-Rubinsztajn reaction. R' = Me, Et, Pr

We have examined the applicability of this unusual condensation reaction as a synthetic route to RTV silicone foams. α,ω-Hydride-terminated poly(dimethylsiloxanes)(PDMS) were cross-linked with tetramethyl orthosilicate ($Si(OMe)_4$), tetraethyl orthosilicate ($Si(OEt)_4$), or tetrapropyl orthosilicate ($Si(O\textit{n}\text{-}Pr)_4$), respectively. The ability to reproducibly crosslink polymers and simultaneously blow silicone foams under these reaction conditions was examined as a function of molecular weight of the starting hydride-terminated PDMS polymer, chemical nature of the alkoxy crosslinker, catalyst concentrations, and the presence and concentration of small amounts of the hydrocarbon

solvent hexane. Foam structures and densities were correlated with the reagents used for foam manufacture.

5.3 Experimental

5.3.1 Materials

Tetramethyl orthosilicate (TMOS), tetraethyl orthosilicate (TEOS), tetrapropyl orthosilicate (TPOS), trifluoromethanesulfonic acid, magnesium oxide and trispentafluorophenylborane $B(C_6F_5)_3$ were purchased from Sigma-Aldrich, and used as received. Octamethylcyclotetrasiloxane (D_4), α,ω–hydride-terminated poly(dimethylsiloxane) (H-PDMS-H) 2-3, 7-10 and 100 centiStokes (cSt, approximate MW 730, 1,190 and 5,000 g mol^{-1}, respectively (silicones are commonly sold by their kinematic viscosity in cSt, which may be converted to viscosity by multiplying by the density of the fluid. 1000 cSt is thus 970 mPa s) were purchased from Gelest. Hexanes, tetrahydrofuran and toluene were purchased from Caledon. Solvents were dried over activated alumina before use.

5.3.2 Methods

Nuclear magnetic resonance spectra were recorded using a Bruker DRX500 or 600 Avance spectrometer. SEM images were obtained using a Philips 515, JEOL 7000F, Focused Ion Beam, Zeiss NVision40 scanning electron microscope.

5.3.3 Synthesis of ~ 2570 g/mol Hydride-terminated H-PDMS-H (poly(dimethylsiloxane))

To a mixture of octamethylcyclotetrasiloxane D_4, (40.0 g, 0.135 mol (Me_2SiO) unit) and 1,1,3,3-tetramethyldisiloxane (2.79 g, 20.8 mmol) was added trifluoromethanesulfonic acid (0.02 ml, 0.038 g, 0.25 mmol) at room temperature. The mixture was then heated at 100°C for 5 h. Once complete, the mixture was cooled to room temperature. Tetrahydrofuran (~ 200 ml) and magnesium oxide (~2-3 g – to quench the triflic acid) were then added to the solution. The mixture was then filtered through a fritted funnel and concentrated under reduced pressure. The residue was purified by removal of small molecular weight molecules using Kugelrohr distillation at 140 °C under vacuum (0.1 mmHg) for 5 hours yielding a colorless oil (yield – 33.2 g).

^1H NMR ($CDCl_3$, 600 MHz): δ 4.70 (m, 2H, $OSi(CH_3)_2H$), 0.18 (s, 12H, $H(CH_3)_2Si(OSi(CH_3)_2)_nOSi(CH_3)_2H$), 0.08 ppm (s, 200 H, $(OSi(CH_3)_2)_nOSi(CH_3)_2H$), ^{13}C

NMR: ($CDCl_3$ 125 MHz) δ 0.90, 0.84, 0.74 ppm; ^{29}Si NMR ($CDCl_3$, 99 MHz, 1 % w/v $Cr(acac)_3$): δ -6.69 (M), -19.68 (M), -21.73 (M) ppm.

Nomenclature: Numbered formulations contained hexane, e.g., **4** unless indicated by addition of 'n', e.g., **14n**, Table 5.1, Appendix Section 8.4.

5.3.4 General Synthesis of Silicone Foam

In a typical synthesis (shown for 7-10 cSt H-PDMS-H with TMOS, 1:1 (eq SiH:SiOMe), (Table 5.1-entry **8**), H-PDMS-H (2.0 g, 1.70 mmol) and TMOS (0.127 g, 0.83 mmol) were placed in a 25.0 mL vial with hexanes (1 mL). The contents of the vial were stirred and $B(C_6F_5)_3$ (20 μL of a 0.078 M solution, 376 ppm) was quickly added. The contents were stirred gently until a few bubbles began to appear, then the mixture was left to complete the reaction (~30 s) during which time the volume of the mass increased by ca. 50%. *There was a relatively large exotherm during the process*. The vial was then broken to remove the foamed silicone elastomer. Alternatively, the foam could be formed in an open vessel by pouring the mixture immediately into a Petri dish that had been lined with Teflon. Table 5.1 (and Appendix Section 8.4) shows the variables that were examined in an effort to correlate reagent types, concentrations and reaction conditions with the ability to form foams. Factors including: solvent volume (concentration of reagents); MW of H-PDMS-H; type of crosslinker; and molar ratio of Si-H to crosslinker ($Si(OR)_4$), were systematically examined. The induction times between mixing of reagents and foam formation were measured, starting the time from the addition of $B(C_6F_5)_3$ to the solution of crosslinker and H-PDMS-H, until the first signs of gas evolution. Total reaction time refers to the total time from the addition of $B(C_6F_5)_3$ to the time a foam has been fully produced and reaction stopped – the evolution of gas ceased. The density of the silicone foams were measured following the procedure laid out by Chruściel *et al*.[3] as follows:

*Density: d = m/V; Volume (V) f*or a cylinder = $h(\pi r^2)$

Where *m* is the mass of the cylindrical sample, h is the height of the cylindrical sample and r is the radius of the sample.

Table 5.1 Experimental foam data

Entry #	Silane MW (g)[a]	x-linker (g)[b]	Ratio[c]	Catalyst (μL/ppm)[d]	Hexane (mL)	Induction Time (s)	Total time (s)	Density (g/cm^3)	Hard-ness[e]	Shore 00
1	730 (1.0)	TM (0.157)	1|1.5	10/345	1.0	13.1 ± 1.2	33.6 ± 0.9	0.23 ± 0.03	0	
2	1190 (2.0)	TM (0.191)	1|1.5	20/365	1.0	21.6 ± 5.7	32.2 ± 2.8	0.17 ± 0.02	0	
3	2570 (2.0)	TM (0.089)	1|1.5	20/382	1.0	16.1 ± 0.7	18.1 ± 1.9	0.32 ± 0.04	3	50
4	5000 (2.0)	TM (0.094)	1|1.5	20/382	1.0	N	-	-		
5	730 (1.0)	TM (0.104)	1|1	10/362	1.0	5.5 ± 2.2	15.9 ± 0.5	0.13 ± 0.03	0	
6	730 (1.0)	TE (0.143)	1|1	10/349	1.0	8.1 ± 2.1	25.4 ± 5.9	0.11 ± 0.01	0	
7	730 (1.0)	TP (0.182)	1|1	10/338	1.0	42.9 ± 5.9	75.7 ± 7.9	0.09 ± 0.01	0	
8	1190 (2.0)	TM (0.127)	1|1	20/376	1.0	10.3 ± 3.4	23.7 ± 1.6	0.17 ± 0.02	0	
9	2570 (2.0)	TM (0.059)	1|1	20/388	1.0	11.3 ± 2.6	14.9 ± 1.4	0.46 ± 0.04	3	51
10	730 (1.0)	TM (0.201)	1|2	10/333	1.0	31.8 ± 5.1	37.5 ± 4.2	0.14 ± 0.02	0	
11	2570 (2.0)	TE (0.162)	1|2	20/370	1.0	37 ± 10	69 ± 12	0.30 ± 0.03	2	31
12	2570 (2.0)	TP (0.205)	1|2	20/362	1.0	186 ± 95	453 ± 220	0.25 ± 0.07	2	35
Solvent Free										
13n	1190 (2.0)	TM (0.127)	1|1	20/376	-	13.6 ± 1.8	19.6 ± 1.9	0.34 ± 0.03	0	
14n	1190 (2.0)	TE (0.174)	1|1	20/367	-	34.5 ± 8.4	43.6 ± 7.7	0.31 ± 0.01	0	
15n	1190 (2.0)	TP (0.222)	1|1	20/360	-	170 ± 21	204 ± 34	0.21 ± 0.02	1	7
vs Solvent										
16	1190 (2.0)	TE (0.174)	1|1	20/367	1.0	12.0 ± 1.1	35.1 ± 2.8	0.13 ± 0.01	0	
17	1190 (2.0)	TP (0.222)	1|1	20/360	1.0	27 ± 11	68.7 ± 5.7	0.15 ± 0.03	0	
Half the solvent										
18	1190 (2.0)	TM (0.127)	1|1	20/376	0.5	15.5 ± 1.2	19.3 ± 2.7	0.19 ± 0.01	1	3
Double the solvent										
19	1190 (2.0)	TM (0.127)	1|1	20/376	2.0	21.2 ± 1.2	24.0 ± 1.6	0.08 ± 0.01	0	

[a] Hydride terminated PDMS: 7-10 cSt (1,190 g mol-1), 2-3 cSt (730 g mol-1).[b] TM: Tetramethyl orthosilicate, TE: Tetraethyl orthosilicate, TP: Tetrapropyl orthosilicate. [c] ratio = PDMS hydride groups : alkoxysilane groups. [d] Catalyst solution: 40 mg of $B(C_5F_5)_3$ in 1 mL of dry toluene. [e] Hardness scale: For those samples for which a Shore 00 hardness could not be obtained we provide an empirical scale clarifying a range of hardness 0 = too soft to measure with Shore 00, 1 = Shore 00 values: 0-20, 2 = Shore 00 values – 20-40, 3 = Shore 00 values – 40-65. Many of the harder foams cracked during measurement.

5.4 Results and Discussion

The formation of a silicone (or any polymeric) foam requires the ability to match the kinetics of two independent processes: silicone crosslinking that builds the viscosity until the system first gels and then is converted into an elastomer; and, kinetics of bubble nucleation, coalescence and migration through the silicone. If too many bubbles are released before the viscosity increases sufficiently, or bubbles are not released until the elastomer is nearly formed, then few bubbles will be trapped and either a foam won't form at all, or the elastomeric material will be relatively bubble free. It was necessary therefore, to examine the relative kinetics of the two processes and vary them by changing both the reagent concentrations and the nature of the crosslinker.

It was previously shown that the Piers-Rubinsztajn reaction was very sensitive to the steric bulk of both the hydrosilane and alkoxysilane reaction partners: the larger the alkoxy group, the slower the reaction.[18] Although final crosslink density of the elastomer formed from H-PDMS-H and a tetraalkyl orthosilicate should not depend on crosslinker type, any reactivity differences between crosslinkers should provide a control element for the relative rates of condensation and gas generation. Therefore, three different alkoxysilanes $Si(OMe)_4$, $Si(OEt)_4$, $Si(O\text{-}nPr)_4$, which exhibit both different reaction rates in the process and which produce gases of different volatility and solubility in the silicone (methane, ethane and propane, respectively), were used to crosslink moderately sized hydride-terminated polydimethylsiloxanes (H-PDMS-H, MW 730-5000). Preliminary experiments demonstrated that addition of the solvent hexane allowed for the generation of more uniform silicone foams. Hexane was therefore added to many of the formulations (hexane-free foams are described below). The reaction parameters were systematically varied to determine the optimal conditions for foam generation. Although we judge the highest value foams to be relatively low density, closed cell foams that have good mechanical stability, others may find different structures of interest and we therefore report all the types of foams prepared. The foams were characterized by density, Shore OO hardness (for selected examples, and an empirical hardness scale for all samples) (Figure 5.2, Table 5.1, Appendix Section 8.4). The preliminary studies demonstrated that the factors which most influenced the mechanical properties of the product elastomers were: chain length (MW) of H-PDMS-H, crosslinker type, cross- linker concentration and solvent volume, each of which will be discussed in turn.

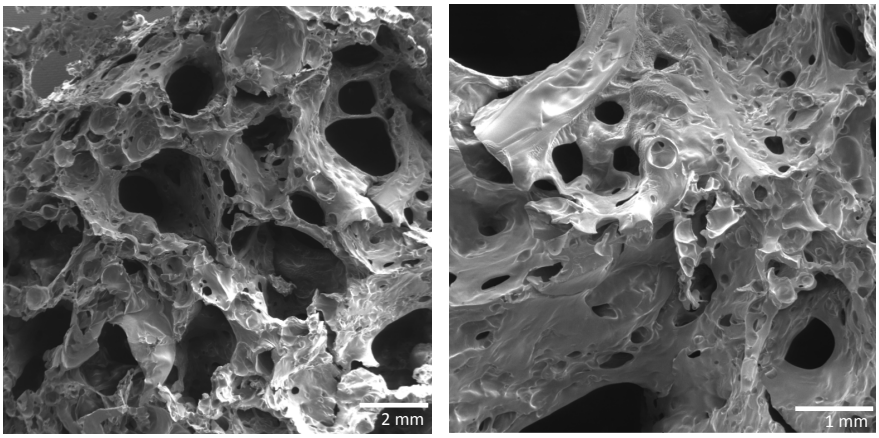

Figure 5.2. Elastomer formation around evolving volatile byproducts resulting in silicone foams **1**. The foam can be characterized in terms of total density, open or closed cell structure and mechanical performance

5.4.1 H-PDMS-H molecular weight

The molecular weight of the H-PMDS-H was systematically increased from ~730 g/mol to ~5000 g/mol while keeping all other variables constant ($Si(OMe)_4$ crosslinker, hexane - 1.0 mL). As expected from polymer theory,[19] which has particularly benefitted from the study of silicones,[20] the distance between crosslinks,[21] which tracks with H-PDMS-H chain length, dramatically affected the resulting foam structure and mechanical properties: we have recorded, where possible, Shore OO hardness and provided an empirical scale for hardness for other samples (Table 5.1). In general, foam hardness tracked with density, but was also affected by bubble size and dispersity. These silicone foams, which were not reinforced by silica fillers, were therefore in some cases friable such that measuring hardness was precluded.

The use of H-PDMS-H MW ~730 g/mol **1**, led to a fairly brittle silicone foam (Figure 5.3A) compared to **2**, in which MW ~ 1190 g/mol was used, which was less rigid and brittle (Figure 5.3B, brittle foams cracked when mechanically bent). Increasing the molecular weight further to MW ~2570 g/mol, such as in foam **3**, led to materials that were more ductile and flexible in nature, and capable of undergoing repeat compressions without any cracking or tearing (Figure 5.3C). If, however, the size of the starting H-PDMS-H was significantly increased, such as in **4** (MW = 5000 g/mol), foams were not produced at all. Instead, virtually bubble free elastomers resulted (Figure 5.3D, Table 5.1, Appendix Section 8.4). Thus, one can tune the properties of the prepared foamed elastomer, depending on the particular application, by simply varying the molecular

weight of the starting hydrosilane. This also allows one to prepare bubble free silicone elastomers.

The effect of the molecular weight of the starting H-PDMS-H on the induction or total times of foam generation was marginal. For example, when lower molecular weight H-PDMS-H (730 g/mol) was used **1**, the induction time was 13.1 ± 1.2 s, with a total reaction time of 33.6 ± 0.9 s. When H-PDMS-H with a molecular weight of 1190 g/mol was used **2**, the induction time the reaction increased only to 21.6 ± 5.7 s with a total reaction time of 32.2 ± 2.8 s. Further increasing the H-PDMS-H molecular weight to ~2570 g/mol **3** led to an induction time of 16.1 ± 0.7 s, and a total reaction time of 18.1± 1.9s.

A B C D

Figure 5.3 Effect of varying starting H-PDMS-H (molecular weight), while keeping all other variables constant. A: (**1**, 730), B: (**2**, 1190), C: (**3**, 2570), D: (**4**, 5000 g/mol), respectively

5.4.2 Effect of the starting crosslinker

The nature of the starting crosslinker had a dramatic effect on the rate of the foaming process and the resulting morphology. The rate of the Piers-Rubinsztajn reaction is affected by the steric demand of the hydrosilane which is invariant in the experiments described here, the concentrations of reagents and, most importantly, the steric demand of the alkoxysilane[16,18]. As the cross-linker was changed from unhindered alkoxysilanes such as $Si(OMe)_4$ to $Si(OEt)_4$ and then to the more sterically congested centers in $Si(O\text{-}nPr)_4$, the reactions occurred more slowly, the resulting silicone foams had larger bubbles, foams were usually lower in density, became more open celled structures and were more brittle (Figure 5.4A-C). There was a larger exotherm in the reactions that exploited $Si(OMe)_4$, when compared to those using $Si(OEt)_4$ or $Si(O\text{-}nPr)_4$.

When a more reactive crosslinker such as $Si(OMe)_4$ was used to prepare silicone foams, regardless of the starting H-PDMS-H molecular weight, both induction times and times for reaction completion were short, usually occurring in less than a minute with a

noticeable exotherm. In these cases, it was expected that the low solubility of generated methane gas in silicone fluid[22-25] coupled with a larger thermal spike due to the highly exothermic nature of the reaction when $Si(OMe)_4$ is used as a crosslinker, and rapid build in viscosity during elastomer cure, would preclude significant coalescence or departure of the methane gas bubbles: closed cell silicone foams with small cell sizes result (Figure 5.4A, Table 5.1, entry 5, Appendix Section 8.4: Table A 2: 7 examples).

The use of $Si(OEt)_4$ as the crosslinker was accompanied by increased induction and total reaction times: the resulting foams were produced in less than 2.5 min (Table 5.1, entry **6**, Appendix Section 8.4: Table A 2: 7 examples) with a slightly lower exotherm. The increase in reaction time apparently gave bubbles more time to coalesce before being locked into the elastomeric matrix. Bubble sizes as judged by optical microscopy for a given formulation, and which differed only in the type of crosslinker used, were about two times larger when $Si(OEt)_4$ rather than $Si(OMe)_4$ was used (Figure 5.4B).

Changing the crosslinker to $Si(O\text{-}nPr)_4$ further enhanced these effects. The resulting reaction mixtures exhibited substantially longer induction times that averaged around 1.5 min and total reaction times about 3-3.5 min. Cell sizes were also significantly larger (about 2.5 times larger than when $Si(OMe)_4$ was used as crosslinker, Table 5.1 entry 7, Appendix Section 8.4: 7 examples) as a consequence of greater opportunity for bubble coalescence over longer time periods. Loss of the alkane by dissolution in the silicone during cure may also play a role, as is discussed below.

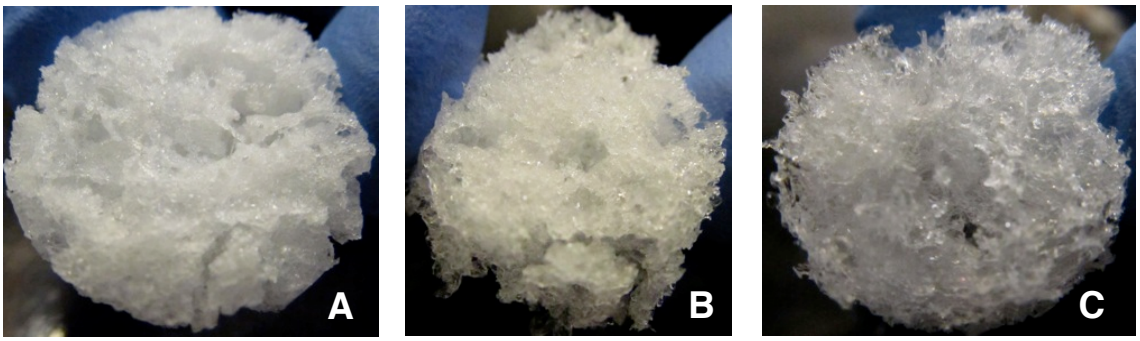

Figure 5.4. Effect of altering the crosslinker in the preparation of silicone foams. A: Crosslinker - TMOS **5**, B: Crosslinker - TEOS **6**, C: Crosslinker - TPOS **7**. Increasing the steric bulk at the alkoxysilane results in silicone foams with larger cell sizes and lower densities.

5.4.3 Effect of the $(RO)_4Si$:H-PDMS-H ratio

The ratio between H-PDMS-H and $Si(OR)_4$ was shown to be a significant factor in both the reaction process and characteristics of the resulting silicone foams. At a SiOR:SiH ratio of 0.5:1, the silicone products were viscous silicone liquids, regardless of the molecular weight of the starting H-PDMS-H and irrespective of the alkoxysilane crosslinker used (Appendix Section 8.4). Presumably, on average, non-crosslinked stars form ($Si(O\text{-}PDMS\text{-}H)_4$).

When the SiOR:SiH ratio was changed to 1:1, fairly brittle foams resulted when H-PDMS-H with a molecular weight of 730 g/mol was used. Increasing the molecular weight to 1190 g/mol at this same SiOR:SiH ratio yielded more ductile foams (cf., MW 730, **5**; MW 1190, **8**, Table 5.1). However, when the starting H-PDMS-H molecular weight was of even higher MW, ~2500 g/mol **9**, very flexible and robust foams were formed[21]. This is to be expected: foam brittleness can be overcome simply by increasing the molecular weight of the H-PDMS-H - the distance between crosslink sites - at a constant SiOR:SiH ratio.[26]

Further increasing the SiOR:SiH ratio to 1.5:1 or 2:1 produced more ductile foams that were also more robust than foams formed with lower amounts of crosslinker: an increase in crosslinker concentration to this range results in fewer crosslink sites, ultimately leading to more elastomeric, less resinous and less brittle materials (Figure 5.5). This was especially evident in foams produced starting from H-PDMS-H with molecular weight of 730 g/mol (**1** - $Si(OMe)_4$:H-PDMS-H = 1.5:1 **10** - $Si(OMe)_4$:H-PDMS-H = 2:1); as the degree of crosslinking decreased, the more flexible the foams became. It should be noted that although very flexible foams were prepared with a SiOR:SiH ratio of 2:1 with a starting H-PDMS-H molecular weight of ~2500 g/mol, foams **11** and **12** remained slightly tacky even after curing. This can be attributed to the relatively large distance between crosslinks at higher SiOR:SiH ratios and to dangling unreacted polymer chains.

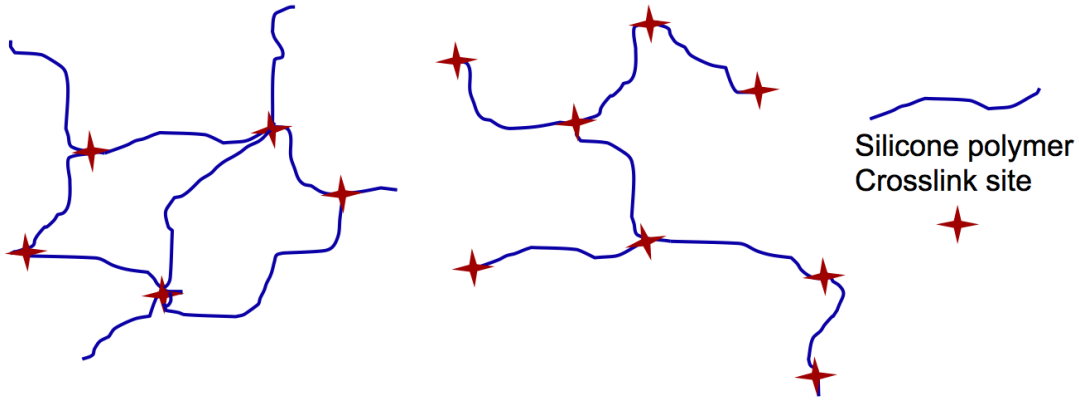

Figure 5.5. Crosslink density changes with an increase in the concentration of alkoxy crosslinker (TMOS). (A) shows a ratio of 1:1 SiOR:SiH, (B) shows a ratio of 2:1, fewer cross-links create a softer silicone foam

5.4.4 Varying the hexane content of silicone Foam formulations

The foams described above were synthesized using hexane (1 ml in a total formulation of ~2 g) to facilitate reagent miscibility, to aid in the preparation of uniform silicone foams, and to also act as a blowing agent. As shown in previous studies[15-18], the Piers-Rubinsztajn reaction is highly exothermic and, in the current reaction, particularly with $Si(OMe)_4$ as crosslinker, can result in fairly high reaction temperatures (> 60°C). The addition of hexane into the formulations acts as a heat sink. As a consequence, however, in addition to the volatile organic byproducts released from the reaction, the hexane can act as a blowing agent (if its boiling point of 68°C is surpassed) depending on the reaction conditions used. Although the use of hexane has largely been beneficial in preparing uniform foams, it was of interest to determine if foams could also be produced from lower VOC formulations that did not benefit from the added blowing effect from the hexane (Table 5.1, Appendix 8.4).

The impact of hexane on the foaming process was readily seen using $Si(OMe)_4$ and H-PDMS-H MW 1190 g/mol prepared with various amounts of hexane: **13n** (0 ml), **18** (0.5 ml), **8** (1 ml), **19** (2.0 ml) (Figure 5.6A). Typical induction times for solvent free reactions were fairly consistent with the silicone foams prepared with hexane, regardless of the crosslinker used. Overall reaction times noted for foams that used $Si(OMe)_4$ as a crosslinker were also similar whether or not hexane was present (**8** 23.7 ± 1.6 v. **13n** 19.6 ± 1.9 s). By contrast, slightly longer reaction times were observed in the absence of hexane when more sterically congested crosslinkers were used, using formulations

containing H-PDMS- H MW of 1192 g/mol with a SiOR:Si-H ratio of 1:1 (TPOS: **15n** 204 ± 34 v. **7** 75.7 ± 7.9s).

As noted, when a sufficiently strong exotherm occurs, hexane can also act as a blowing agent. In the absence of hexane, therefore, higher density foams resulted. For example, **8** has a density of 0.17 ± 0.02 g/cm^3, compared to its solvent free analog **13n**, with a density of 0.34 ± 0.03 g/cm^3. It is also evident that, in the absence of hexane, foams were comprised of smaller pore sizes, and a larger fraction of closed cells (**8** v. **13n**, Figure 5.7). As the concentration of VOCs is increased further in the silicone formulations, more porous, less dense silicone foams result.

General trends for silicone foam densities were similar whether or not hexane was present. For example, foams prepared with formulations containing H-PDMS-H MW of 1190 g/mol and Si(OR):H-PDMS-H ratio's of 1:1, had densities decrease from 0.34 ± 0.03 g/cm^3, to 0.31 ± 0.01 g/cm^3 and 0.21 ± 0.02 g/cm^3 for **13n** (Si(OMe)$_4$), **14n** (Si(OEt)$_4$) and **15n** (Si(O-nPr)$_4$, respectively. These may be compared to the hexane-containing formulations: **8** 0.17 ± 0.02 g/cm^3 (Si(OMe)$_4$), **16** 0.13 ± 0.01 g/cm^3 (Si(OEt)$_4$) and **17** 0.15 ± 0.03 g/cm^3 (Si(O-nPr)$_4$, respectively. These observations can be ascribed to faster elastomer crosslinking with less sterically congested crosslinkers giving to smaller bubble sizes, more bubbles, and ultimately lower density silicone foams.

A

13n **18** **8** **19**

B

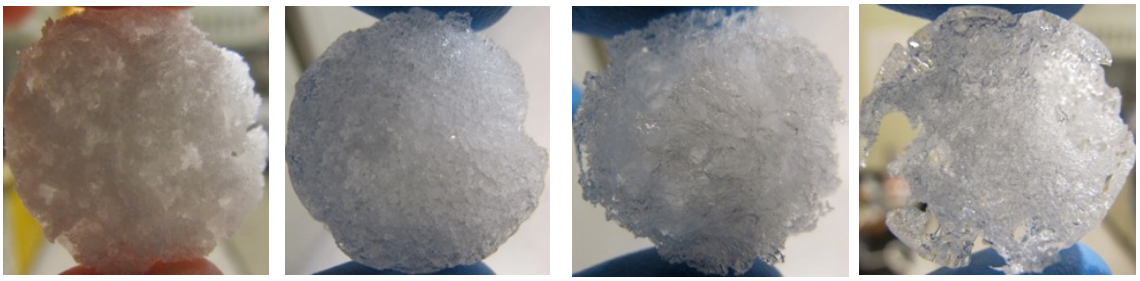

8 **13n** **16** **14n**

Figure 5.6 A: Comparison of foam formulations prepared with four different hexane concentrations (0, 0.5, 1, 2 ml/formulation). B: Comparison of foams created with $Si(OMe)_4$ **8**, and without, **13n** solvent, visually showing a decrease in cell size and an increase in density. Analogous formulation prepared from $Si(OEt)_4$ with, **16** and without, **14n** hexane show the use of more sterically hindered crosslinkers in solvent free conditions leads to less uniform silicone foams

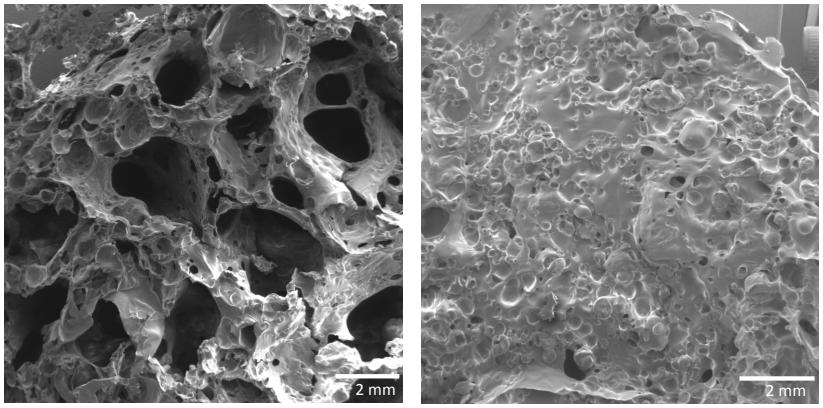

Figure 5.7. SEM images of the surface of foams **8** and **13n**, respectively. Compound **8** shows generally larger pore sizes compared with solvent free analogue **13n**

It was not possible to prepare high quality foams when the more sterically congested alkoxysilane crosslinkers $Si(OEt)_4$ and $Si(O\text{-}nPr)_4$ were used in the absence of hexane. The foams typically exhibited more open cells and, in some cases, contained large voids: there was sufficient time for the volatile byproducts (ethane, propane) to coalesce into larger bubbles, but insufficient time for the majority of the bubbles to leave the matrix before being trapped by cure. With either crosslinker, silicone foams prepared in the absence of solvent were not as uniform as those prepared with solvent. For example, **16** is a uniform foam while its solvent free analog **14n** (H-PDMS-H - 1192 g/mol, Si(OR):Si-H 1:1, crosslinker - $Si(OEt)_4$) contains small areas of elastomer that have no bubbles (Figure 5.6B). This could be due to a higher initial viscosity in the formulation when solvent is

not present, resulting in less efficient mixing and non-uniform foams. More likely, however, the higher solubility's of the evolving gases (ethane, propane vs. methane)[3,22-24] in silicone provide a different mechanism by which gas bubbles can be lost from the system: they dissolve into the surrounding matrix or, through Ostwald ripening,[10] large bubbles increase in size at the expense of smaller bubbles.

The Piers-Rubinsztajn reaction provides several elements to manipulate the formation of foamed structures. Factors that accelerate the kinetics of gas evolution and cure process, including more reactive crosslinkers and use of shorter silicone chains (thus higher [SiH] in the medium), were associated with a higher concentration of small bubbles. By contrast, the use of less reactive crosslinkers and/or longer silicone chains (~5000 g/mol) did not result in foams at all or, in the best cases, very tacky open celled structures.

The key factors to be considered when choosing the brittleness/flexibility of the prepared foams are the H-PDMS-H MW, and the SiOR:SiH ratio: the former is most important. Shorter chain lengths (e.g., H-PDMS-H MW 730 g/mol) result in higher crosslink density, ultimately giving more brittle foams. By lengthening the H-PDMS- H chain, the crosslink density decreases, leading first to more rigid (H-PDMS-H MW 1190 g/mol), and ultimately more flexible and ductile (H-PDMS-H MW 2500 g/mol) silicone foams.

Crosslink density can also be controlled through the manipulation of the SiOR:SiH ratio, and by alteration of the starting H-PDMS-H molecular weight. For example, when the molecular weight of the H-PDMS-H is kept at 730 g/mol and the crosslinker ratio is varied, significant differences in foam structures arise. A ratio of 0.5:1 (Si(OR):SiH) led to no silicone foam generation, and resulted in a viscous silicone liquid. Increasing this ratio to 1:1, allows for a very high crosslink density, ultimately yielding very brittle and ridged foams. Further increasing this ratio to 1.5:1 and then ultimately 2:1, leads to more ductile/flexible materials capable of undergoing repeat compressions without cracking or tearing, because there is a balance between increased crosslinks, and the increasing number dangling polymer chains at higher crosslinker concentrations. These effects of altering the crosslink density by varying the SiOR:SiH ratio hold true for each of the molecular weights used. That is, for each of the given ratios, increasing the molecular weight of the starting H-PDMS-H leads to a decrease in the hardness of the foams (more flexible materials are obtained).

In addition to manipulating the mechanical properties of the prepared silicone foams, one can easily control foam density by addition of solvent, alteration of the H-PDMS-H molecular weight and changing the reactivity of the crosslinker by using crosslinkers with different sterics. However, the interplay between factors to control density is somewhat

more complicated than other parameters. Factors that permit evolved gas to escape from the matrix lead to densification. These include physical escape because gas bubbles are generated and escape faster than being trapped by cure; coalescence of bubbles will change overall density when they located near an external matrix interface and break; and, finally, gas solubility and diffusion from the matrix is more efficient for the alkane byproduct propane > ethane > methane.

In general, although there are exceptions (Table 5.1), higher density foams are achieved through formulations containing less solvent, larger molecular weight H-PDMS-H and less sterically hindered (more reactive e.g., TMOS vs. TPOS) crosslinkers that react more rapidly, which quickly increases the viscosity of the formulation during cure. High reactivity and low foam expansion result in fairly dense materials. The observed hardness generally tracks with density, but is also affected by the average cell sizes and crosslink density. Gradual increases in both solvent concentration and crosslinker sterics ($Si(OEt)_4$ and $Si(O\text{-}nPr)_4$) normally lead to less dense silicone foams.

Cell size is also an important characteristic of silicone foams. Bubble size can be readily manipulated through crosslinker sterics and solvent effects. The cell size is understood to be related to two factors, the speed at which the reaction progresses, and the relative permeability of the volatile gaseous byproducts in the forming silicone elastomer. In general, the less sterically hindered the alkoxysilane crosslinker, the faster the reaction $Si(OMe)_4 > Si(OEt)_4 > Si(OPr)_4$. At higher cure rates, the elastomeric network forms so rapidly that the gaseous byproducts are trapped in high density as small bubbles; there is insufficient time to migrate through the network or coalesce to form larger bubbles. Alternatively, if the reaction kinetics are suppressed, through use of more sterically congested crosslinkers (TEOS, TPOS), the elastomer network forms more slowly, allowing more bubbles to slowly coalesce, leading to larger cell sizes. Ostwald ripening[27] of bubbles based on the silicone soluble ethane/propane byproducts of the latter two crosslinkers provides another mechanism for bubbles to increase in size. As shown in previous studies, condensable gases in silicone polymers that are elastomeric in nature permeate more readily compared to smaller non-condensable gases[23,24.]

Finding formulations that lead solely to open or closed cell silicone foams has been rather challenging. In most cases, silicone foams are produced with both a mixture of open and closed cells. However, it has been determined that if the solvent (hexane) concentration is reduced, and a reactive crosslinker such as TMOS is used, one can produce primarily closed cell silicone foam formulations (Figure 5.6B). With less blowing agent, a more densely packed material results. This coupled with the lower permeability of methane

through the forming silicone network,[22-24] leads to the formation of densely packed, primarily closed cell foams.

The final silicone foam structure, when prepared using the Piers-Rubinsztajn reaction, is readily manipulated by controlling a variety of factors. The first step of foam formation is the initial bubble nucleation, which is controlled by adjusting the rate of gas evolution (crosslinker reactivity). Once the system begins crosslinking the viscosity increases proportionally - diminishing the ability of the nucleated bubbles to move through the elastomeric system. The amount of bubble coalescence then becomes proportional to the viscosity, which is controlled by the crosslink site concentration (the number of crosslink sites per/siloxane unit can be changed with H-PDMS-H MW and the ratio of SiOR:SiH), and to the ability of gases to dissolve into and migrate through the silicone matrix. The final step of foam formation occurs when the elastomeric portion has crosslinked to such an extent that the bubbles can no longer effectively migrate.

Two methods are traditionally used to blow silicone foams. First, foaming agents that play no part in the reaction are used which are activated by various means such as heat. Second, as in the case of most silicone foams, hydrogen gas is released as the result of a competitive reaction to crosslinking via hydrosilylation.[3,6,7,10,13,14] In this case, two separate reactions with two rate constants compete for the same SiH groups. While this process is very efficient, adventitious water or other agents often distort the process by favoring foaming at the expense of crosslinking and compromise reproducibility.

The Piers-Rubinsztajn process for foams avoids the challenges that occur with traditional forming strategies. It is possible to manipulate the outcome of a single process, in which both the blowing agent and crosslinking process occurs, in spite of the fact that a single reaction is required for both bubble generation and crosslinking. Within the process it is straightforward to control bubble nucleation, coalescence and trapping following simple formulation rules. The final foam structure can have a high or low bubble density, which can be further manipulated by the addition of excess blowing agent (hexane) that lowers the viscosity during initial foaming, but nearing the end of the reaction provides an extra source of bubbles before the final elastomer cure. The final mechanical properties of the foam can be controlled using crosslink density.

5.5 Conclusions

A new method has been developed for the preparation of silicone foams. Commercial hydrogen-terminated silicones can be cross-linked in varying ratios using $Si(OR)_4$, where

R = Me, Et, Pr. By varying starting molecular weight of H-PDMS-H, changing the crosslink density and crosslinker/H-PDMS-H ratio, or by controlling solvent effects, the gaseous byproducts can be trapped in the silicone matrix generating foams with varying densities, rigidity, tackiness/brittleness and open or closed cell structure. The process avoids challenges in traditional methods with adventitious water, and generates foams rapidly and in high yield.

5.6 Acknowledgements

We gratefully acknowledge the financial support of the Natural Sciences and Engineering Research Council of Canada. J.B.G and A.S.F would also like to thank NSERC for a PGS-D and CGS-D scholarship, respectively.

5.7 References

1. Malla, R. B.; Shrestha, M. R.; Shaw, M. T.; Brijmohan, S. B. *J. Mater. Civil Eng.* **2011,** *23* (3), 287-297.
2. Malla, R. B.; Swanson, B. J.; Shaw, M. T. *Constr. Build. Mater.* **2011,** *25* (11), 4132-4143.
3. Chrusciel, J. J.; Lesniak, E. *J. Appl. Polym. Sci.* **2011,** *119* (3), 1696-1703.
4. Fawcett, A. S.; So, H. Y.; Brook, M. A. *Soft Matter* **2010,** *6* (6), 1229-1237.
5. Mustoe, T. A. *Aesthetic Plast. Surg.* **2008,** *32* (1), 82-92.
6. Lee, C. L.; Niemi, R. G.; Kelly, K. M. *J. Cell. Plast.* **1977,** *13* (62), 62-67.
7. Noll, W. J. *Chemistry and Technology of Silicones*. Academic Press: New York, 1968.
8. Berridge, C. A. Spongeable polysiloxane composition and process of producing sponge therefrom. 2857343, General Electric Company, 1958.
9. Berridge, C. A. Preparation of sponge rubber from high temperature mixed silicone rubber-silica composition. 2875163, Gerneral Electric Company, 1959.
10. Hoffman, K. R. Siloxane structural foams. 2655485, Dow Corning Corporation, 1953.
11. Wade, R. C.; Blanchard, P. L. Polymer compositions comprising an alkali metal borohydride and stearic acid and preparation of cellular rubber-like articles therefrom. 2951819, Metal Hydrides Incorporated, 1960.
12. Modic, F. J. Foamable organopolysiloxane composition and foamed product obtained therefrom. 3425967, General Electric Company, 1969.
13. Wada, T.; Itoh, K.; Kuga, N. Silicone elastomeric compositions and a method for preparing silicone sponge rubbers therefrom. 3677981, Shinetsu Chemical Company, 1972.

14. Brook, M. A. *Silicon in Organic, Organometallic, and Polymer Chemistry*. John Wiley & Sons: Toronto, 2000; p 680.
15. Brook, M. A.; Grande, J. B.; Ganachaud, F. In *Advances in Polymer Science*, **2010**; Vol. 235, pp 161-83.
16. Grande, J. B.; Gonzaga, F.; Brook, M. A. *Dalton Trans.* **2010,** *39* (39), 9369-9378.
17. Grande, J. B.; Thompson, D. B.; Gonzaga, F.; Brook, M. A. *Chem. Commun.* **2010,** *46* (27), 4988-4990.
18. Brook, M. A.; Thompson, D. B. *J. Am. Chem. Soc.* **2008,** *130* (1), 32-+.
19. Sperling, L. H. *Introduction to Physical Polymer Science*. 4th ed.; Wiley-Interscience: New York, 2005.
20. Mark, J. E.; Erman, B. Polymer Networks: Elastomers. In *Molecular Characterization and Analysis of Polymers*, 1st ed.; Chalmers, J.; Meier, R., Eds. Elsevier Science: 2008; Vol. 53, pp 337-83.
21. Sharaf, M. A.; Mark, J. E.; Ahmed, E. *Colloid Polym. Sci.* **1994,** *272*, 504-515.
22. Economou, I. G.; Makrodimitri, Z. A.; Kontogeorgis, G. M.; Tihic, A. *Mol. Simul.* **2007,** *33*, 851-860.
23. Merkel, T. C.; Bandar, V. I.; Nagal, K.; Freeman, B. D.; Pinnau, I. *J. Polym Sci., Part B: Polym. Phys.* **2000,** *38*, 415-434.
24. Pinnau, I.; He, Z. *J. Membr. Sci.* **2004,** *244*, 227-233.
25. *We thank a referee for this suggestion*.
26. Falender, J. R.; Yeh, G. S. Y.; Mark, J. E. *J. Am. Chem. Soc.* **1979,** *101*, 7353-7356.
27. Tcholakova, S.; Mitrinova, Z.; Golemanov, K.; Denkov, N. D.; Vethamuthu, M.; Ananthapadmanabhan, K. P. *Langmuir 2011* **2011,** *27*, 14807-14819.

CHAPTER 6: Silicone Foams Stabilized by Surfactants Generated *in situ* from Allyl-Functionalized PEG[††]

6.1 Abstract

Silicone foams normally require the use of agents or chemical reactions that blow gases, and a surfactant for bubble stabilization. We have discovered that the presence of monoallyl-functionalized poly(ethylene glycol) (PEG) leads to large increases in the viscosity of silicone pre-elastomers such that stable foams form with bubbles mostly being generated by coalescence of dissolved gases during the normal degassing process. Although silicone elastomer cure may take up to 24 h for completion, the foams remain stable during this time when appropriate concentrations of allyl-PEG and curing catalyst are used. No traditional surfactant is required, but PEG-modified silicone surfactants are formed *in situ* by covalent grafting of the PEG to the silicone matrix, leading to the increase in viscosity. The presence of allyl-PEG decreases elastomer cure efficiency, but this is readily overcome, if necessary, to generate more rigid foams by the use of additional platinum catalyst, in which case foaming occurs both due to loss of dissolved gases and to hydrogen evolution. Foam stabilization with appropriate allyl-PEG compounds is a consequence of an initial viscosity increase.

6.2 Introduction

Silicone elastomers have an excellent reputation as biomaterials: their useful properties include easy preparation in complex shapes; sterilizability; gas transmissibility (important for ophthalmic applications); and hydrophobicity. Hydrophobicity is particularly important in a variety of topical applications including scar remediation and in wound

---

[††] This manuscript is reprinted from A.S. Fawcett, H.Y. So, H. Sheardown, and M.A. Brook, *Soft Matter*, **2010**, *6*, 1229-1237, which has been reproduced with permission from RSC Publications, 2010. Fawcett developed and optimized all experimentation in this chapter. Fawcett also assisted So with rheological characterization of materials and wrote the majority of the manuscript with additions, edits and guidance from So, Sheardown and Brook.

dressings.[1] The latter application makes use of hydrophobic silicone interfaces that do not adhere to (moist) wounds, although they may adhere to skin. However, the very high hydrophobicity can also be problematic. When proteins adsorb on such surfaces, they can undergo denaturation, which in some cases can lead to adverse biological events.[2]

One strategy used to improve the biocompatibility and water wettability of silicone polymers exploits hydrophilic coating materials, such as PEG (poly(ethylene glycol)).[2-5] PEG of an appropriate molecular weight is protein repellent, which in in vitro tests is associated with much 'quieter' biological surfaces. We were interested in developing strategies for the preparation of hydrophilic silicone elastomers that could have utility either topically or internally: PDMS and PEG are both FDA (US Food and Drug Administration) approved for biomedical applications.

Foams are a special type of silicone elastomer used for biomaterials. For example, one treatment for retinal detachment utilizes foamed silicone as scleral buckles. Such materials have sufficient elastomeric properties to constrain movement of the eye, placing it in closer contact with the retina, and are lightweight and biocompatible over extended implantation times.[6] The preparation of foams generally requires an added blowing agent[7] or a chemical reaction leading to gas evolution[8, 9] and, frequently, the presence of a surfactant:[10] foamed structures result when the cure kinetics are matched to those of bubble generation.[11]

PEG-modified silicone surfactants play an important role in the stabilization of foam structures, for example, polyurethane foams.[10] In such cases, small bubbles are prevented from coalescing by the surfactant during urethane cross-linking. We reasoned that PEG-modified silicone surfactants could be used to prepare water wettable PEG-modified silicone elastomer foams. Such foams may have utility in applications that require contact with humans, either topical or sub-cutaneous.

Silicone elastomers are often cured/cross-linked using platinum-catalyzed hydrosilylation (addition cure: $R_3SiH + H2C{=}CHSiR'_3 \rightarrow R_3Si{-}CH_2CH_2SiR'_3$). We considered that the simple addition of allyl-modified PEG to a silicone foam formulation would lead, during cure of the silicone, to the simultaneous grafting of allyl-PEG-grafted via hydrosilylation, generating bubble-stabilizing surfactants *in situ* (Figure 6.1).

Normally, platinum-cured silicone elastomers are degassed (to remove entrained/dissolved air) after mixing the two parts (SiH + Sivinyl), but prior to cure: otherwise, undesired bubbles are frequently found in the cured elastomer.[12] In our hands, mixtures of commercially available Sylgard 184 elastomer (Dow Corning)[2,5,13] and allyl-modified PEG unexpectedly led to highly foamed silicone structures: foams did not result

when allyl-PEG was absent. We discuss below the factors that control foam generation and stability, including PEG molecular weight, concentration, and functionality, as well as catalyst concentration and vacuum strength, and describe the structures of the resulting foams.

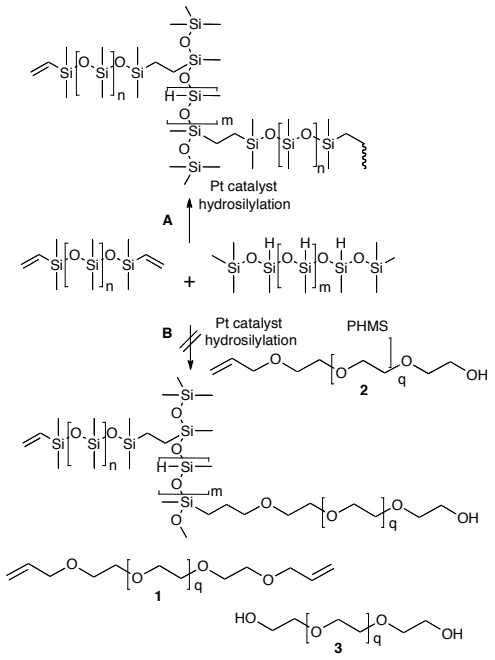

Figure 6.1. Reaction scheme depicting PDMS (A) cross-linking and (B) PEO grafting by hydrosilylation

6.3 Experimental

6.3.1 Materials

Monoallyl-PEGs (M_w 250 and 500 g/mol) were a gift from Clariant. Sodium hydride (in 60% mineral oil), dihydroxy- terminated PEG (M_w 200 and 400), and allyl bromide were purchased from Aldrich. Karstedt's catalyst ($–Pt_2(H_2CCHSi\text{-}Me_2OSiMe_2CHCH_2)_3$, 2.1–2.4% Pt in xylenes) and vinyl-terminated poly(dimethylsiloxane) 4–6 centiStokes (cSt) were purchased from Gelest; the Sylgard 184 kit, D4 (octamethylcyclotetrasiloxane) and poly(hydromethylsiloxane) (PHMS) (DC1107) were obtained from Dow Corning; and vinyl-terminated poly(dimethylsiloxane) 5000 cSt (Mw ~49 000) from United Chemical Technologies, Inc. Hexanes, dichloromethane, diethyl ether, and tetrahydrofuran were purchased from Caledon and dried using pressurized alumina columns.

NMR spectra were recorded using a Bruker Biospin AV200 and a Bruker DRX500 spectrometer (at 200 and 500 MHz, respectively, for protons). Infrared spectra were recorded on a Bio-Rad FTS-40 attenuated total reflection Fourier transform IR using a horizontal cadmium selenide ATR rig. SEM images were obtained using a Philips 515, JEOL 7000F, Focused Ion Beam, Zeiss NVision40 scanning electron microscope.

An ARES 3ARES-9A Rheometer was used to carry out rheological studies to determine the dynamic viscosity of samples. The rheometer was of parallel plate geometry having a plate diameter of 25 mm. Dynamic time sweep tests were performed at relatively low oscillatory frequencies of 5 rad s^{-1} and a strain of 5% to obtain the change in dynamic viscosity as a function of time. Each sample load had an average thickness of 1.3 mm (Figure 6.2).

A JEOL JSM-7000S SEM model was used to obtain images where samples with a diameter of 0.635 cm were prepared by coating with 10 nm of platinum. The internal structure of the material was examined using freeze fracture SEM. Samples were submerged in liquid nitrogen and fractured to attain the internal structure. Energy-dispersive X-ray spectroscopy analysis (SEM- EDX) was performed on samples to acquire elemental analysis on sites of interest.

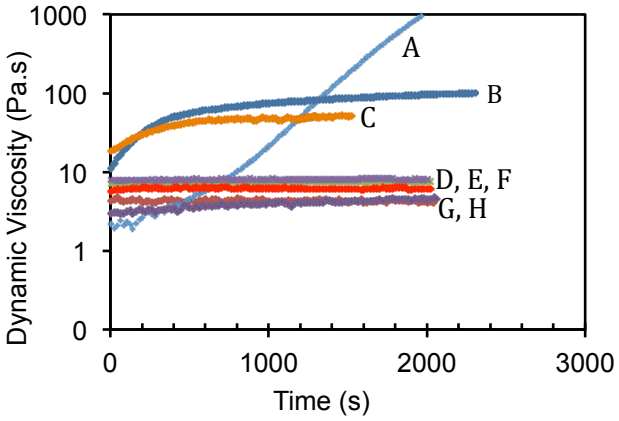

Figure 6.2. Influence of PEG functionality on dynamic viscosity over time of the Sylgard base alone (control) or with 20 wt% 1, 2 or 3, respectively. (A) Sylgard elastomer + PHMS (control, Table A3, entry 1); (B) A + 20% 2 M_w 500(Table A3, entry 2); (C) A + 20% 1 M_w 500 (Table A3, entry 6); (D) A + 20% 3 M_w 400 (Table A3, entry 5); (E) Sylgard base + 20% 3 M_w 400; (F) Sylgard base + 20% 1 M_w 500; (G) Sylgard base; and (H) Sylgard base + 20% 2 M_w 500

6.3.2 Synthesis of diallyl-PEG M_w 500 and 250

In a typical synthesis (shown for PEG M_w 500), monoallyl-PEG (5.00 g, 10 mmol) and THF (50 mL) were combined in a 100 mL round-bottomed flask, and stirred with a magnetic stir bar. Sodium hydride (0.72 g, 12.0 mmol, excess) was slowly added over a period of 5 min and the resulting mixture was left to stir for an additional 1 h. Excess allyl bromide (1.03 mL, 12.0 mmol) was added dropwise and the reaction was stirred overnight at room temperature. The THF was removed from the resulting mixture using a rotary evaporator and the resulting material was diluted with water and washed with diethyl ether, and twice with dichloromethane. The organic solvents were removed using a rotary evaporator. The residue was dissolved in hexanes and run through a silica pad to remove any remaining oil (from the sodium hydride). The silica was then rinsed through with methanol and then dichloromethane (DCM) to collect the diallyl-PEG. The solvent was evaporated at reduced pressure. Residual NaBr was removed by trituration with toluene: filtration and evaporation gave a pure material. Yield M_w 500 (85%, 4.25 g, 8.5 mmol) and M_w 250 (56%, 1.12 g, 4.5 mmol).

M_w 250: ^{1}H NMR ($CDCl_3$) δ = 5.88 (m, 2H); 5.22 (m, 4H); 4.00 (d, 4H, J ¼ 5.8 Hz); 3.64–3.59 (m, 19H).
M_w 550: ^{1}H NMR ($CDCl_3$) δ = 5.87 (m, 2H); 5.19 (m, 4H); 3.99 (d, 4H, J ¼ 5.6 Hz); 3.62–3.53 (m, 39H).

6.3.3 Preparation of SiH-functionalized PDMS—control

In a beaker, Sylgard 184 base (3.1 g), Sylgard 184 curing agent (0.31 g), and DC1107 (0.31 g) were sequentially combined. The mixture was stirred vigorously by hand and 2.0 g were transferred to a 35 mm × 10 mm Petri dish. The dish was placed under vacuum (571 Torr) for one day to degas and cure at room temperature. After initial foaming, the silicone cured to an optically transparent, bubble-free elastomer.

ATR-FTIR: 2961; 2163 (Si-H); 1050 (Si-O-Si); 1070 cm^{-1}.

6.3.4 Non-Sylgard formulations

Vinyl-terminated PDMS (5000 cSt, 1 g), PHMS (DC1107, 0.1 g), Karstedt's catalyst (diluted in $(Me_2SiO)_4$, 60 ppm) and mono-allyl-PEG M_w 500 **2** (0.23 g) were mixed by hand. At these higher catalyst concentrations a soft elastomer foam was blown irrespective of the application of a vacuum (Appendix 8.5: Table A 3, entries 16–19).

6.3.5 Grafting of allyl-PEG to the silicone elastomer: an ^{1}H NMR study

In a beaker Sylgard 184 base (1.5 g), Sylgard 184 curing agent (0.15 g), DC1107 (0.15 g) (10 : 1 : 1—Sylgard Base–curing agent– DC1107), monoallyl-PEG 500 M_w **2** (0.45 g, 20% w/w), and additional Karstedt's catalyst (19 ppm of Pt, in addition to that already present in the Sylgard 184, Table A 3, entry 8) were sequentially combined. The solution was stirred vigorously by hand after which a portion was immediately placed into 15 mL of $CDCl_3$ and ^{1}H NMR spectra were obtained. Simultaneously, the remainder of the mixture was placed in a mixer with no head- space, for 1 h. After this time the cured, or highly viscous, elastomeric mixture was removed from the mixer and placed into 15 mL of $CDCl_3$ at which time a second ^{1}H NMR spectra were obtained. No change was observed.

Before/after: ^{1}H NMR ($CDCl_3$) δ = 5.88 (m, 1H); 5.21 (m, 2H); 4.71 (s, 3H, SiH); 4.00 (d, 2H, *J* = 5.6 Hz); 3.65–3.64 (m, 44H); 0.19–0.06 (m, 146H).

If only very low degrees of grafting were occurring, it would be very difficult to observe grafting by ^{1}H NMR. Therefore, an alternative recipe was examined that exploited Me_3Si-terminated PDMS (5000 cSt, 1 g), which cannot react chemically with the PHMS (0.1 g), Karstedt's catalyst (diluted in $(Me_2SiO)_4$, 80 ppm) and monoallyl-PEG M_w 500 **2** (0.23 g). These materials were mixed by hand. One portion was studied rheologically (see Appendix Section 8.5) and the other was examined by ^{1}H NMR (Appendix 8.5: Table A 3, entry 19) at 1 h and 2 days. The NMR at 1 h showed that about 32% of the allyl group had reacted; complete reaction to allyl-grafted PEG was noted by 2 days.

At 1 h: ^{1}H NMR (500 MHz, $CDCl_3$) δ = 68% unreacted starting materials 5.88 (m, 1H); 5.21 (dd, 2H, *J* = 10.5, 1.5 Hz); 4.71 (s, 3H, SiH); 4.00 (d, 2H, *J* = 5.5 Hz); 3.65–3.64 (m, 44H); 0.19–0.06 (m, 146H).

+32% allyl-grafted PEG: 4.76 (dd, 2H, *J* = 12.5, 6.5 Hz, OCH_2); 4.70 (s, 3H, SiH); 3.65–3.64 (m, 44H); 1.53 (dd, 2H, *J* = 6.7, 1.5 Hz, OCH_2CH_2); 0.89 (t, 2H, *J*= 7.5 Hz, CH_2CH_2Si); 0.19–0.06 (m, 142H).

6.3.6 General synthesis of PDMS-PEG elastomers

In a typical synthesis (shown for monoallyl-PEG M_w 500 **2**, 20% w/w), Sylgard 184 base (3.02 g), Sylgard 184 curing agent (0.32 g), DC1107 (0.31 g), (10 : 1 : 1—Sylgard base–curing agent– DC1107) and monoallyl-PEG (0.02 g) were combined sequentially in a beaker. The solution was stirred vigorously by hand and 2.0 g were transferred to a 35 mm × 10 mm Petri dish (or a 120 × 60 mm Petri dish or a large mouth vial). The dish was

then placed under vacuum (571 Torr, although other pressures were examined) overnight to cure.

Table A 3 shows the variables that were examined in an effort to correlate reagent types, concentrations and reaction conditions with the ability to form and cure a foam. Factors including: vacuum strength, PEG concentration, PEG molecular weight (MW), and PEG functionality, catalyst concentration (a catalyst stock solution, 920 ppm Pt, used to increase catalyst concentration in the elastomers, was prepared by diluting Karstedt's catalyst (40 mL) in either 4–6 cSt vinyl-terminated PDMS or $(Me_2SiO)_4$ (1 mL)), surface area of the container used for cure, and other silicone systems (*i.e.,* in addition to Sylgard 184) were examined. The initial viscosity of the system was observed as well as the final hardness of the elastomer after a reasonable cure-time, typically 24 h in some cases longer cure times were required (48 h).

6.4 Results

6.4.1 Preparation and systematic study of foamed PDMS elastomers

Foamed silicone elastomers were prepared using the Sylgard elastomer kit that consists of two parts, a high viscosity base (5000 cSt, containing vinyl groups and the catalyst) and a liquid curing agent (containing Si–H groups): cure occurs via platinum-catalyzed hydrosilylation (Figure 6.1A). Normally, the two constituents are mixed in a 10 : 1 (base–curing agent) ratio, which provides a matched SiH–Sivinyl stoichiometry. The uncured mixture is then generally degassed to remove both air entrained during mixing and air dissolved in the silicone, such that the formation of bubbles during cure is avoided.

The generation of grafted PEG-rich silicone elastomers required functional tethers on both the silicone and the PEG. Additional SiH functionality was therefore added to the elastomer mixture using poly(hydromethylsiloxane) (PHMS, that is, the usual Sylgard 10 : 1 part ratio was modified with an additional 1 part PHMS). Any loss of SiH groups due to reaction between PEG and the silicone would therefore be compensated for by the presence of excess PHMS.

Three different types of PEG molecules were used to change the hydrophilicity of the silicone: diallyl-**1** or commercially available monoallyl-**2** or dihydroxy-terminated PEG **3**

(Figure 6.1). The hydroxy-modified material cannot chemically bind into the elastomer,[‡‡] while either of the allyl-functional species could in principle undergo hydrosilylation forming propenyl linkages between polyether and silicone (Figure 6.1B).

During a series of survey experiments designed to optimize formulation (Appendix 8.5: Table A 3), it was noted that the allyl-PEG-containing mixtures were notably more viscous than Sylgard + PHMS alone. More significantly, this viscosity was sufficiently high such that some of the foams which formed during degassing did not collapse on release of the vacuum: normally, degassing of silicone produces a temporary foam that collapses while still under vacuum or after the vacuum is removed. The origins of this increased viscosity in the silicone pre-elastomer and the characterization of the resulting foams then became the key objectives of the study.

Controls were developed before the factors that could contribute to foaming were systematically studied. Sylgard 184 that was formulated with additional PHMS but without **1**–**3** cured normally, and did not lead to foams, irrespective of the applied vacuum (Appendix 8.5: Table A 3, entry 1). It was found that the surface area–volume ratio of the container in which the pre-elastomer was placed did not have an effect on foam formation. As seen in Appendix 8.5: Table A 3, entries 2–4, the foaming was not a consequence of inefficient bubble migration in narrow vessels—similar foams were observed in high surface area–volume Petri dishes.

6.4.2 Preparation of foams without concomitant cure

The viscous Sylgard 184 base contains vinyl-modified silicone polymer chains, the platinum catalyst, and silica filler. An additional control experiment examined, using rheology, the ability of various PEG polymers to facilitate foam stabilization with the base alone (i.e., without inclusion of the SiH-containing curing agent, Figure 6.2). The presence of any of compounds **1**–**3** in the Sylgard silicone base led to little change in viscosity when compared with the base itself (Figure 6.2E–H). As importantly, viscosity did not build over time. By contrast, when the SiH- containing curing agent was also added to the mixtures, diallyl-PEG **1** and particularly monoallyl-PEG **2** of the same nominal MW led to increases in viscosity of nearly 2 orders of magnitude. Importantly, the build in viscosity in these two cases occurred much more rapidly than viscosity build caused by cure (Figure 6.2B, C vs. A). Dihydroxy-PEG did not affect the viscosity of the system (Figure 6.2D).

[‡‡] Note that formation of alkoxysilanes by this process is possible, but these linkages are hydrolytically unstable.

6.4.3 PEG functionality and ‘‘foamability’’.

There was a striking effect of the PEG end group on ‘foamability’. Hydroxy-terminated PEG of M_w 200 and 400 (Appendix 8.5: Table A 3, entry 5) did not create a noticeable increase in viscosity (Figure 6.2D), nor did it lead to foams: the presence of the PEG did not noticeably affect cure and cloudy elastomers formed. The presence of diallyl-PEG of 500 M_w (Appendix 8.5: Table A 3, entry 6, Figure 6.2C) led to noticeable increases in viscosity of the initial elastomeric mixture. However, the final elastomers exhibited lower bubble density and higher bubble polydispersity than those formed from monoallyl-PEG-containing materials under otherwise similar conditions (Appendix 8.5: Table A3 entry 2, Figure 6.2B). In addition, the samples were less cured. Thus, the best foams, based on highest bubble density and mono-dispersity, arose from silicone elastomers doped with 20% w/w monoallyl-PEG.

A range of PEG concentrations, 0.5, 5, 20 and 40% w/w, were examined in the foamed elastomers, using M_w 250 and 500 monoallyl-PEG chains (Appendix 8.5: Table A 3, entries 2 and 10–12). Only at higher concentrations (20% w/w) did the mixture become sufficiently viscous that a foam was formed. The relatively mono-disperse bubbles were evenly distributed throughout the material. At higher concentrations (40% w/w, entry 12) the PEG effectively diluted the silicone elastomer mixture to such an extent that the mixture led to a paste containing some bubbles: the silicone did not effectively cure. While the number of entrained bubbles in the elastomers correlated with PEG concentration, the degrees of cure were inversely proportional, as seen from the 5% and 0.5% PEG samples, respectively (entries 11 vs. 10).

With 20% w/w monoallyl-PEG of either MW there were many more bubbles present within the material and the overall volume expansion was much greater than with 5% w/w (entry 2, Figure 6.3C). The concentration of allyl groups thus plays a large role in foam formation. For good foaming, there is a balance between the increase in viscosity created by the allyl-PEG and the inhibition of silicone cross-linking. At lower PEG levels, there is little effect on the cross-linking of the elastomers (i.e., cure is not significantly inhibited), but little foaming was observed due to increased viscosity. With too much PEG, the mixture is diluted by the lower MW material and the viscosities tend to decrease; the materials never cure properly, and contain polydisperse and typically larger bubbles than formulations with less PEG. Therefore, for efficient foaming, the amount of allyl-PEG introduced into the elastomeric mixture must be low enough that cure is not significantly suppressed, yet high enough such that a viscous pre-elastomer captures the bubbles.

6.4.4 Molecular weight

The ability to produce foamed structures was correlated, within the narrow limits examined, with the molecular weight of the PEG oligomers: attempts to use PEG of MW larger than about 500 were unsuccessful because the PEG chains did not dissolve in the silicone matrix nor did they readily disperse. The overall difference between the foams made with M_w 500 and 250 PEG could be seen in the final hardness of the cured elastomers (data not shown). With 500 M_w monoallyl-PEG, the final material is harder or more cured than with the 250 M_w for monoallyl-PEG-containing elastomers with 20% w/w. This is a consequence of suppression of cure by the higher mole fraction of allyl groups in the 250 M_w PEG-containing elastomers.

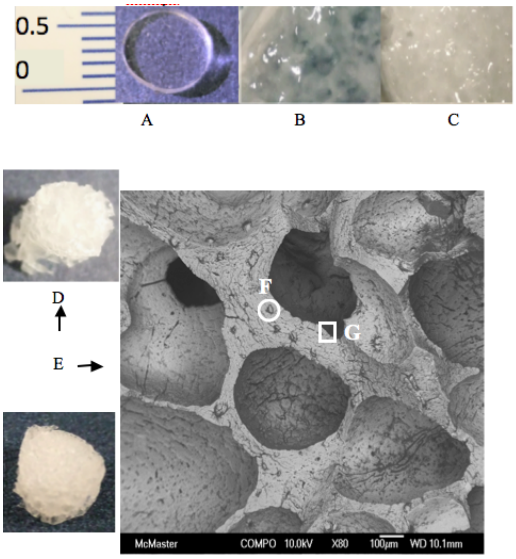

Figure 6.3. (A) Sylgard PDMS with DC1107 (10 : 1 : 1) (Table A3, entry 1); (B) Sylgard PDMS (with DC1107) with monoallyl-PEG M_w 500 40% w/w (entry 12); (C) Sylgard PDMS (with DC1107) with monoallyl-PEG M_w 500 20% w/w (entry 2); (D) Sylgard PDMS (with DC1107) with mono- allyl-PEG M_w 500 20% w/w cured under a vacuum of 176 Torr with excess catalyst (14 ppm Pt) (entry 7). SEM scale bar = 100 mm. (E) Similar formulation as D, prepared without vacuum (entry 9). Optical photographs all at the same scale (see ruler, 0.5 cm). (F) Particulate structure rich in PEG as shown by EDX when compared to, (G) the silicone polymer found in the strut.

6.4.5 Pressure effects

During the normal synthesis of PDMS elastomers, after the components of Sylgard 184 were mixed together, the solution was placed under vacuum to be degassed prior to cure. After initial foaming, the mixture rapidly became clear as the bubbles migrated through

the viscous mixture and then left it. A transparent, bubble-free rubber resulted after curing (Figure 6.3A). The effect of pressure on foam formation was examined by exposing various silicone pre-elastomers to three different levels of vacuum: 'house' vacuum (176 Torr); high vacuum (1×10^{-4} Torr); or room pressure (749 Torr), respectively. When this protocol was followed at various pressures with Sylgard containing excess PHMS, bubble-free elastomers generally resulted, although there were occasionally bubbles found in the materials that had not been exposed to vacuum (Table A3, entries 2, 13 and 14).

The addition of allyl-PEG to this recipe led to mixtures that foamed during degassing and remained as foamed structures at least partially (Figure 6.3B), and generally completely, after curing. The viscosity of the mixture was insufficient to prevent the bubbles from escaping at the highest vacuum. Opaque, cross-linked elastomers resulted in this case, with only adventitious small bubbles of random size located in the matrix. At room pressure the bubbles, which are produced by a combination of dissolved air, air entrained during mechanical mixing and from the reaction of the SiH groups, were very small and relatively monodisperse, were evenly distributed throughout the matrix, and were fixed in place by curing into the material. At moderate vacuum (house vacuum, 176 Torr), the vacuum strength is sufficient to permit the bubbles to expand and partially coalesce, creating a foamed material with larger bubble sizes than those produced at room pressure, but is not strong enough to significantly de-gas the elastomeric mixture. Thus, pressure and catalyst concentration can be manipulated to control the foam density, average bubble size and size distribution.

6.4.6 Origins of viscosity build: the question of chemical grafting of allyl-PEG

^{1}H NMR spectra were obtained on the elastomeric mixture containing Sylgard 184, monoallyl-PEG M_w 500 (20% w/w) and additional catalyst in $CDCl_3$ immediately after mixing (entry 8). The spectrum at that time clearly showed presence of protons of unreacted SiH groups, from Sylgard and added PHMS, and allyl and backbone protons from the PEG: vinyl groups from the Sylgard, which are present in low concentration, could not be directly observed. After mixing for 1 h in a constrained volume mixer with no headspace, a sample of the—by then highly viscous—elastomer was swollen in $CDCl_3$ (see Appendix Section 8.5). After cure, the spectrum showed, as with the spectrum of the freshly mixed material, that the allyl and backbone protons of the PEG were completely intact, initially suggesting that the allyl-PEG had not participated in hydrosilylation.

The concentration of allyl groups at the termini of a 500 M_w polymer is considerably higher than on vinyl groups at the terminus of a 50 000 M_w silicone. In addition, we are

unsure of the specific formulation of Sylgard 184. Therefore, the tests were repeated using commercially available 5000 cSt Me_3Si-terminated PDMS (which cannot cure by traditional means), PHMS (DC1107) and 500 M_w **2** (20% w/w). In this case, it was possible to detect loss of about a third of the allyl groups in the first hour, and the rest underwent hydrosilylation over the next 2 days. The rheological studies (Table A3, entry 20, see Appendix Section 8.5) of this mixture showed a comparable viscosity profile—much faster than curing—similar to that shown in Figure 6.2B, although the magnitude of change was somewhat different. Thus, the observed increase in viscosity is associated, in part, with the presence of PEG-silicone surfactants generated by hydrosilylation of allyl-PEG (Figure 6.1B).

An elastomeric silicone foam could also be generated using three ingredients in place of Sylgard 184, commercially available 5000 cSt vinyl-terminated PDMS, PHMS (DC1107) and 500 M_w **2** (20% w/w): a foam was only observed when **2** was included. When additional catalyst (Table A3, entries 16–18, compared with the control entry 15) was added to the non-Sylgard elastomeric mixture, a stiff, evenly foamed material was formed. Thus, these studies also demonstrate that the presence of monoallyl-PEG will permit standard platinum-cured silicone elastomers to be prepared as foams with controlled density and hardness.

6.4.7 Competing hydrosilylation reactions

Sylgard 184 normally takes a few hours at room temperature after mixing to become tack free, and full cure can require up to 48 h. The presence of additional PHMS increases the curing rate, and leads to an optically clear elastomer (Appendix 8.5: Table A3, entry 1, Figure 6.3A). The addition of HO-terminated PEG to the Sylgard + PHMS reaction mixture (Table A3, entry 5) had no noticeable effect on silicone cure (nor on the magnitude of foaming). By contrast, the presence of mono- or diallyl-PEG was accompanied by a significant suppression of cure (entries 2 and 6) in addition to increased viscosity.

The slower cure could be overcome by the addition of more Karstedt's platinum catalyst (added in various amounts from a stock solution, see Experimental section, Table A3). For example, a foam with uniform bubble size and the consistency of a thick ''paste'' was prepared by adding 20% w/w monoallyl-PEG of 500 M_w to Sylgard (Figure 6.3C, Table A3, entry 2). There was a direct correlation between added catalyst and the magnitude of cure: at higher catalyst loadings, instead of a viscous paste after 48 h, a cured foam

material was produced that was spongy to the touch and returned to its shape after deformation ceased (entry 7).

When extra catalyst was present in the formulation, a foam was blown even if a vacuum was not used. This is a consequence of the reaction between adventitious water and any silanols present in the polymer. The free hydroxy groups on monoallyl-PEG could also participate in such reactions: this reaction is the basis of most commercial silicone foams (SiH + ROH → H_2 + SiOR, R = H, alkyl, aryl).[7] However, the subtle distinctions between foams derived from monoallyl- vs. diallyl-PEG, and the absence of foaming with dihydroxy-PEG argue against this being a significant source of H_2. Thus, it is possible to vary the hardness of the foam while maintaining a uniform bubble size and concentration simply by controlling catalyst concentration. Foaming results from a combination of blowing by hydrogen gas and, primarily, bubbles from dissolved/entrained gases generated by vacuum.

6.4.8 Nature of the foam

A range of foamed materials could be prepared as described in Table A3. It was possible to control bubble density, bubble polydispersity and size by manipulating the formulation: selected photographs representing typical foam structures are shown in Figure 6.3A–E. More detailed examination by SEM (Figure 6.3D, E spots F, G) was made of the sample derived from Sylgard PDMS elastomer containing monoallyl-PEG M_w 500 with excess catalyst (Table A3, entry 9). This sample was chosen because of its high bubble density, the bubbles' relative monodispersity, the even distribution of bubbles throughout the material and for its stiffness, which allowed for better handling ability and easy coating of samples with Pt (for the SEM). Figure 6.3D shows that the bubble diameter ranges from 100–1000 mm with an average size of about 500 mm and an approximate bubble density of 5.5 bubbles mm^{-2}. It was also possible to control the degree of cure, as discussed below, to give foams ranging in hardness from a soft paste, to a rigid foam.

6.4.9 Origins of the viscosity: reinforcing droplets

The micrograph in Figure 6.3 shows small particulate-like structures (Figure 6.3F, O) in the struts (Figure 6.3G, □) between the bubbles (see also the highlighted circle in Figure 6.6). The elemental composition of the particulate objects was compared with silicone struts in the vicinity. Energy-dispersive X-ray (EDX) spectroscopy was used to measure elemental composition of the two spots as shown in Figure 6.3 and Table 6.1. As shown in the table, the particle is highly enriched in carbon, depleted in silicone, and consistent with a composition primarily of PEG.

Table 6.1. Summary of elemental analysis at pore interface on top surface (see Figure 6.3E)

Element	Atomic %	
Spot	Silicone strut (G)	Particle (F)
Carbon	39.81	68.23
Oxygen	30.46	25.68
Silicon	28.74	6.09

6.5 Discussion

Silicone foams must normally be generated by the use of blowing agents or reactions that generate gas from silicone constituents.[7] Maintaining a foam in the elastomers described above was always associated with an increase in viscosity in the pre-elastomer (Figure 6.2). Bubbles could be generated simply by degassing and, additionally, by hydrogen created from the Si–H polymers in the presence of the platinum catalyst. If the combination of vacuum and viscosity was not properly balanced, foams did not reproducibly result. For example, high vacuum and/or lower pre- elastomer viscosities led to bubbles escaping prior to cure: the surface area–volume ratio, which might be associated with the efficiency with which bubbles could escape, did not play a significant role on the ability of various formulations to foam.

The combination of vacuum and viscosity also played a role in bubble size. Higher vacuum or lower viscosity was associated with larger bubbles, as would be expected, due to greater expansion and more efficient coalescence, respectively (cf. Figure 6.3B–D, where nominal bubble size decreased from B ~ 3 mm / C ~ 1.5 mm / D ~ 500 mm).

Although several factors can contribute to viscosity build in the pre-elastomer, the key parameters were associated with the functionality and concentration of PEG: a significant viscosity increase only occurred when SiH-containing polymers were present (no viscosity build or foams were observed in the absence of these materials, Figure 6.2), and allyl-functional PEG was included in the pre-elastomeric mixture, particularly at concentrations around 20% w/w. By contrast, the dihydroxy-terminated PEG had no significant effect on viscosity, and foams were not observed. The diallyl-PEG derivative was initially more efficient than monoallyl-PEG in increasing viscosity of the pre-elastomer (Figure 6.2C vs. B). However, the final foams were much softer because greater concentrations of allyl groups led to lower degrees of cure. The best foams, based on highest bubble density and monodispersity, arose from silicone elastomers doped with

20% monoallyl-PEG. The presence of monoallyl-PEG built significant viscosity in the pre-elastomer, and suppressed cure less than diallyl-PEG.

These observations are captured in a model phase diagram (Figure 6.4). The likelihood of obtaining cured foam correlates with the viscosity of the pre-elastomer, which in turn is directly related to the concentration of allyl groups in the pre-elastomer, and also correlates with the concentration of allyl-PEG. The hardness of the final foam is also linked to the concentration of allyl groups in the mixture, but in an inverse manner. Allyl groups suppress cure by interacting with the platinum catalyst leading to incomplete cure and softer foams. This effect can be overcome by adding additional platinum, restoring levels of cure, and providing a new source of bubbles from hydrogen evolution.

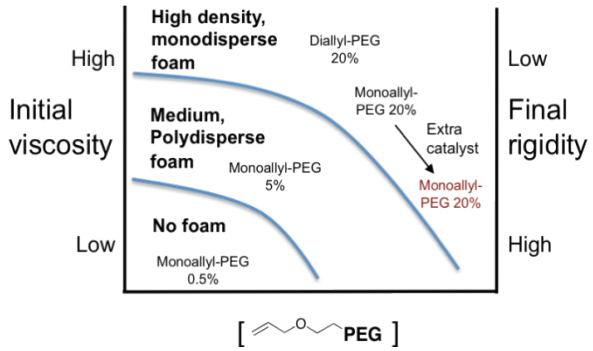

Figure 6.4. Ability to control foam morpholigy through PEG functionality and catalyst concentration

Karstedt's catalyst is a platinum zero species stabilized by three vinyl ligands.[14] When allyl-PEG is present, in addition to the vinylsilicones/SiH silicones, ligand scrambling will introduce PEG chains onto a fraction of the catalyst present through allyl group complexation (Figure 6.5A). The relative insolubility of PEG in silicones will result in reduced catalyst activity; the formation of an active catalyst with Si–H and Si–vinyl groups linked via Pt (Figure 6.5B) is suppressed. The reduction in cross-linking efficiency correlated directly with the concentration of added allyl groups, and was not dependent on the MW of the PEG or whether the allyl compound present was either mono- or diallyl-PEG.

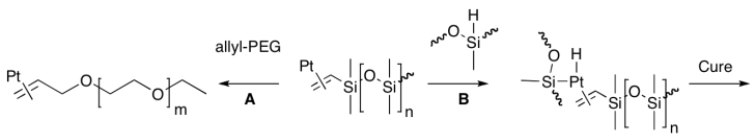

Figure 6.5. Ligand exchange *versus* cure

The origin of 'foamability' is the most interesting aspect of these results. The optimal foams, as defined by a high density of uniformed sized bubbles, occurred with about 20 wt% of mon- oallyl-PEG added to the silicone pre-elastomer. Foams arose during normal degassing, and could be extended by blowing of H_2 gas when additional catalyst was added. The main factor responsible for the maintenance of foams during degassing (or release of H_2) was the increased viscosity when allyl-PEG was present (Table A 3, entries 2–4, 7, 8, 13, 14, and 16–18). Under such conditions, bubbles could form, coalesce to a limited degree, but not readily exit the polymeric matrix. Chemical grafting of the allyl-PEG to the silicone in the early stages of the mixture was demonstrated with model systems.

The PEG-silicone surfactants can act to stabilize dispersed PEG droplets. Similar stabilization by polyether silicone surfactants has been observed in water-in-silicone oil emulsions.[15] As shown in a model structure in Figure 6.6, dispersion of the relatively insoluble PEG can be facilitated both by PEG chains anchored at the perimeter of the droplet, hydroxy groups at the other end of the PEG chain than can self-associate. EDX data showed that these particles (highlighted in Figure 6.6) are primarily comprised of PEG, supporting this model.

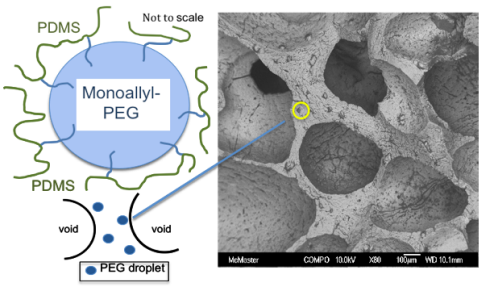

Figure 6.6. Monoallyl-PEG acting as an *in situ* viscosity-modifiying agent (droplet shown inside circle on the SEM photograph).

The addition of fillers to polymer melts, or uncured or pre-cured polymers such as silicones,[16] leads to enormous increases in viscosity,[17] to a degree such that processing frequently becomes problematic.[17] The presence of stabilized allyl-PEG droplets in uncured silicone elastomers, particularly at 20% loading, will similarly increase the viscosity by acting as a filler. The diallyl- PEG compounds led to greater increase in initial viscosity than monoallyl-PEG, perhaps due to the presence of more, smaller droplets that more effectively build viscosity. However, the more convenient formulation used monoallyl-PEG which builds viscosity as a consequence of the approximately 5–10 mm droplets that form in the silicone (Figure 6.6). This viscosity build occurs to a degree

such that the pre-cured material holds bubbles in place until cure occurs. By contrast, insoluble hydroxy-terminated PEG will form large domains in PDMS that do not increase the viscosity to the same degree.

The creation of a foamed elastomer normally requires a subtle balance between the rates of cure and rate of bubble nucleation. Outside of optimal parameters, bubbles either form too quickly and then escape, or are formed after cure is too far advanced. Such parameters are manipulated by controlling the rate of gas evolution, including by the use of blowing agents, viscosity control using fillers, and surfactants to stabilize bubbles as they form. The method described above provides alternative strategies that take advantage of the high solubility of gases in silicones, and by the affinity of allyl-PEG for silicones. Reactions that generate gases (e.g., excess catalyst + PHMS + ROH) can be exploited, but are not necessary. To a significant degree, the rate of gas evolution is irrelevant in these systems, because the viscosity build provided by the dispersion of allyl-PEG in the silicone holds the bubbles in place until cure can be attained.

This process for the preparation of PEG-modified silicone foams is straightforward and the strategy thus holds promise for the preparation of foamed silicone biomaterials, where hydrophilic modification by PEG can be helpful in reducing protein adsorption. Future work will focus on controlling foam density and examining the biostability of such materials.

6.6 Conclusion

Monoallyl-PEG at loadings of ~20 wt% led to significant increases in the viscosity of uncured silicone elastomers. During normal degassing, bubbles formed that remained in place until cure occurred many hours later. The phenomenon is proposed to arise from the formation of PEG-grafted silicone surfactants that can stabilize PEG droplets that act as fillers, which increase the viscosity and decrease the efficiency of bubble coalescence and migration through the silicone matrix. The extent of cure, and hence the final consistency of the foam, can be controlled through the control of catalyst concentration. Such foamed, hydrophilically modified, silicone elastomers may have applications as biomaterials.

6.7 Acknowledgements

We gratefully acknowledge the financial support of the Natural Sciences and Engineering Research Council of Canada and 20/20: NSERC Ophthalmic Materials Network, and thank Clariant for the gift of monoallyl-PEGs.

6.8 References

1. Mustoe, T. A. *Aesthetic Plast. Surg.* **2008,** *32* (1), 82-92.
2. Chen, H., Brook, M. A., Sheardown, H. D., Chen, Y., Klenkler, B. *Bioconjugate Chem.* **2006,** *17* (1), 21-28.
3. Chen, H.; Brook, M. A.; Chen, Y.; Sheardown, H. *Journal of Biomaterials Science-Polymer Edition* **2005,** *16* (4), 531-548.
4. Chen, H.; Brook, M. A.; Sheardown, H. *Biomater.* **2004,** *25* (12), 2273-2282.
5. Chen, H., Chen, Y., Sheardown, H., Brook, M. A. *Biomaterials* **2005,** *26* (35), 7418-7424.
6. Colthurst, M. J., Williams, R. L., Hiscott, P. S., Grierson, I. *Biomaterials* **2000,** *21* (7), 649-65.
7. Liu, P. B.; Liu, D. L.; Zou, H. W.; Fan, P.; Xu, W. *J. Appl. Polym. Sci.* **2009,** *113* (6), 3590-3595.
8. Lee, C. L.; Homan, G. R. *J. Cell. Plast.* **1982,** *18* (4), 233-239.
9. Bauman, T. M.; Dietlein, J. US 4613630, 1986.
10. Zhang, X. D., Macosko, C. W., Davis, H. T., Nikolov, A. D., Wasan, D. T. *J. Coll. Interface Sci.* **1999,** *215* (2), 270-279.
11. Brook, M. A. *Silicon in Organic, Organometallic, and Polymer Chemistry*. John Wiley & Sons: Toronto, 2000; p 680.
12. Thompson, D. B.; Fawcett, A. S.; Brook, M. A. Simple Strategies to Manipulate Hydrophilic Domains in SIlicones. In *Silicon Based Polymers: Advances in Synthesis and Supramolecular Organization*, Ganachaud, F.; Boileau, S.; Boury, B., Eds. Springer: 2008; p 298.
13. Nalayanda, D. D.; Puleo, C. M.; Fulton, W. B.; Wang, T. H.; Abdullah, F. *Exp. Lung Res.* **2007,** *33* (6), 321-335.
14. Hitchcock, P. B.; Lappert, M. F.; Warhurst, N. J. W. *Angew Chem Int Edit* **1991,** *30* (4), 438-440.
15. Zelisko, P. M.; Brook, M. A. *Langmuir* **2002,** *18* (23), 8982-8987.
16. Blair, M. W.; Muenchausen, R. E.; Taylor, R. D.; Labouriau, A.; Cooke, D. W.; Stephens, T. S. *Polym Degrad Stabil* **2008,** *93* (8), 1585-1589.
17. Noll, W. J. *Chemistry and Technology of Silicones*. Academic Press: New York, 1968.

CHAPTER 7: General Conclusions

The unique properties of dimethylsiloxanes are attributed to the molecular construction of the polymer backbone. The flexibility of the Si-O-Si linkages allow for the polymer chains to exhibit a low T_g and high elasticity when crosslinked, while the hydrophobic methyl groups combined with the flexible backbone promote low intermolecular interactions. As a consequence, silicones are normally very surface active. This thesis has focused on the interaction of silicone polymers with each other, and how small structural changes along the polymer backbone can cause substantial changes in the observed materials properties.

In Chapter 2 the thermal click reaction of alkyne-functionalized coumarin molecules onto azide-functionalized PDMS copolymer led to large changes in the mechanical properties of the silicone. Instead of having silicone polymers with a high free volume, the opposite became true – the self-association of coumarin moieties promoted physical crosslinking. The flexibility of the silicone chain allowed for the coumarin molecules to form the preferred orientation for head-to-tail aromatic stacking. The degree of self-association between polymer chains was shown to be directly dependent on the concentration of coumarin along the polymer backbone. When a high concentration of coumarin was present, the materials were very brittle; almost glass-like. At low concentrations of coumarin groups on the silicone backbone the material is more of a waxy solid; however, elastomeric materials can be formed when a concentration of coumarins is in between the two extremes. All of the coumarin-functional silicones had a response to heat that is thermoplastic in nature, a contrast to what is usually observed with chemically crosslinked silicone elastomers. These thermoplastic elastomers could have a wide range of applications as typically silicone thermoplastic elastomers must have a secondary polymer blended in to achieve these properties. The blending of silicones with other thermoplastic polymers disables the advantageous properties of the silicone, by creating a system that utilizes only silicone chains, albeit modified with small molecules, many of the advantageous properties of silicone elastomers can be retained.

In Chapter 3 the physical interaction of the coumarin-siloxane materials examined in Chapter 2 are further investigated by exploiting the photoactive nature of the coumarin to incorporate chemical crosslinks into the material. Once photochemistry is initiated, thermoplastic elastomers are converted into thermosets with reversible chemical crosslinks. Coumarin undergoes dimerization at wavelengths greater than 300 nm and the cyclobutane product photocleaves at wavelength less than 300 nm. A decrease in

viscosity was initially seen between the silicone polymers (containing a lower levels of coumarin groups) when dimerization is initiated. This was ascribed to the need for intermolecular re-organization from the thermal permitted head-to-tail stacked coumarin aromatic groups to an orientation that permits the orbital controlled photocyclization. That is, loss of associative crosslinking is required before photoinduced covalent crosslinking can occur. Once enough covalent links were formed the viscosity began to rise again, with **PC-PDMS-11** having the highest degree of modulus increase. The reversibility of this system could not be monitored on the rheometer due to experimental limitations; however, we can see in solution, through UV-spectroscopy, that a certain degree of reversibility could be achieved: after multiple cycles a photostationary state was achieved. The reversibility of the covalent bonds of coumarin in combination with the self-assembly of coumarin on silicones, creates a unique "two-component crosslinking" system, which may have use in many applications, including self-healing applications.

In Chapter 4 the covalent interactions between silicones are examined, however, in this case non-reversible interactions were key. By controlling the molecular weight of polymers and type of crosslinker used, a variety of silicone elastomers can be synthesized. Taking advantage of the Piers-Rubinsztajn reaction between alkoxysilanes and hydrosilanes allows for precise control of the synthesis of silicone elastomers and their properties. Hydrosilane-terminated PDMS of 1,000 cSt with tetrafunctional crosslinkers (i.e., TEOS) made silicone elastomers using comparable synthetic protocols, and catalyst concentrations to current PDMS elastomer procedures that utilize platinum based curing agents. The properties associated with elastomers prepared using the Piers-Rubinsztajn are similar to elastomers prepared with tin or platinum, however, the main benefit to using this system is the speed of preparation and the low catalyst loadings required. Control of the crosslink density can be obtained, as well as the presentation of functional groups within the elastomer, to enable potential other chemistries to take place, such as S_N2 or 'click' chemistry.

Chapter 5 continues to investigate silicone structures and attempts to further understand how interchain silicone interactions can be used to create novel silicone foams. Through the use of the Piers-Rubinsztajn reaction silicone elastomers were structured into silicone foams by taking advantage of the reactions gaseous alkane byproducts. The reaction could be manipulated to provide *in situ* blowing agents to form a variety of foams with different densities. Control over the foam structure was achieved by controlling the hydrosilane molecular weight and the reactivity of the alkoxysilane crosslinker.

Lastly, Chapter 6 examined the interfacial properties of silicones when blended with other polymers. It was discovered that the incorporation of monoallyl-poly(ethylene glycol)

caused a significant increase in viscosity when combined into the PDMS elastomer formulation. The viscosity increase was enough that when the elastomer was degassed, as usual, a foam was formed, that cured into place. The change of incorporating different functionalities and different molecular weights of PEG into the PDMS elastomer formulation was observed using rheology. It was determined that, with the monoallyl species, the allyl endgroup acted as a hydrophobic head with the hydroxyl endgroup acting as a hydrophilic tail. The hydrophilic PEG groups formed colloids that act as fillers to increase the viscosity, while the allyl groups can react with the hydrophobic silicone. The blending of PEG with PDMS created unique amphiphilic foamed materials, which demonstrates the unique opportunities for controlling the interfaces between two polymers.

In conclusion, this thesis has examined three unique methods of controlling interchain silicone interactions. The first was through physical interactions, and demonstrated how small changes in the silicone polymer structure can completely change how the polymer chains will interact with one another, including in some instances crosslinking to form thermoplastic elastomers. The second examined how elastomeric and foamed elastomeric materials can be created through covalent interactions either through a reversible photoreaction or through the permanent Piers-Rubinsztajn reaction. The effect of creating polymer-polymer interfaces by blending hydrophilic and hydrophobic polymers together to form silicone foams was also examined, which led to the further understanding of silicone structuring. Future work will continue to build on the characterization of the unique physical and chemical interactions between coumarins in a silicone network, to further understand how these materials respond in a variety of environments. By fine-tuning the chemical structure of the silicone polymers it is possible to fine-tune the properties and understand how the silicone chains are interacting with one another.

CHAPTER 8: APPENDIX

8.1 Supporting Information for CHAPTER 2: Self-Association of Pendant Coumarin Groups Converts Silicone Oils into Thermoplastic Silicone Elastomers

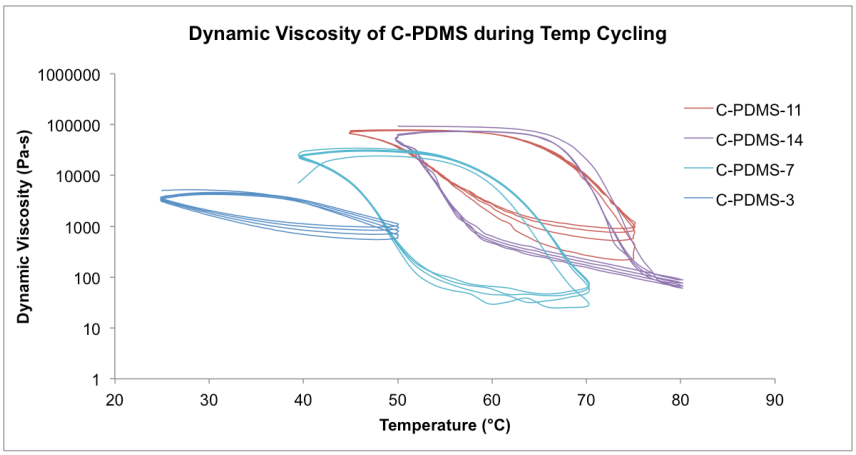

Figure 8.1. Rheological thermal cycling of **C-PDMS-3-14**

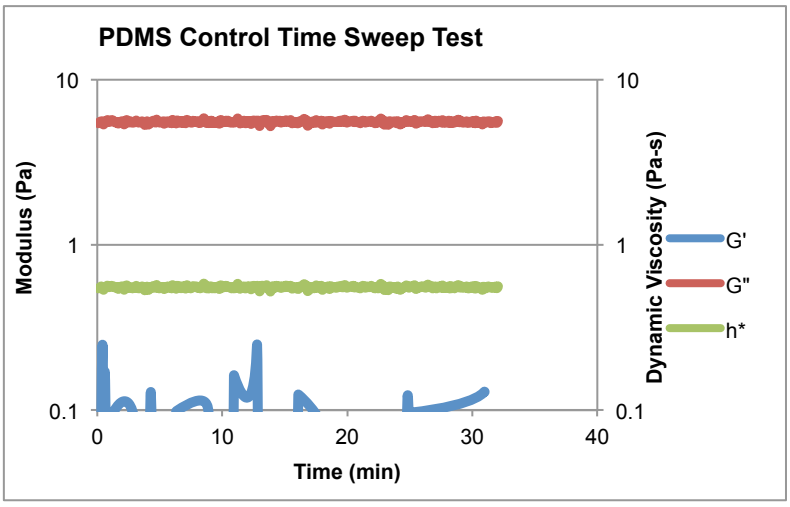

Figure 8.2. Dynamic time sweep test for the cholropropylmethylsiloxy-dimethylsiloxane copolymer. The viscosity is too low for the G' results to be measured accurately on the rheometer.

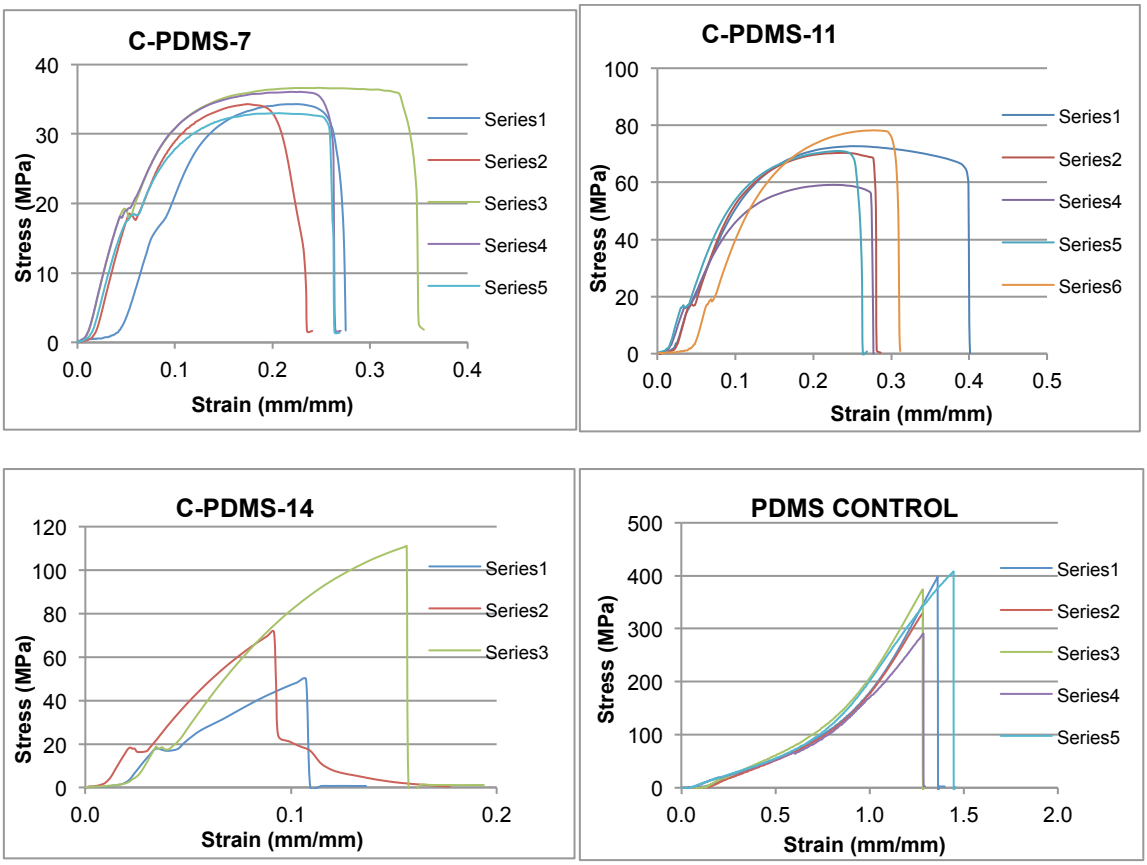

Figure 8.3. Instron Tensile Tests for **C-PDMS-7-14** and the PDMS control

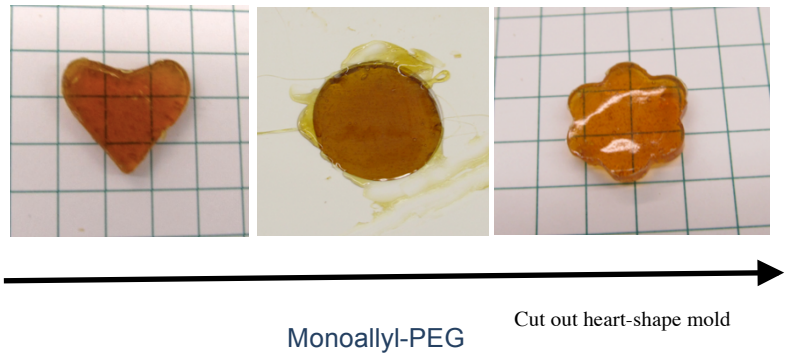

Figure 8.4. Digital photographs of **C-PDMS-7**, demonstrating the thermoplastic nature of the material

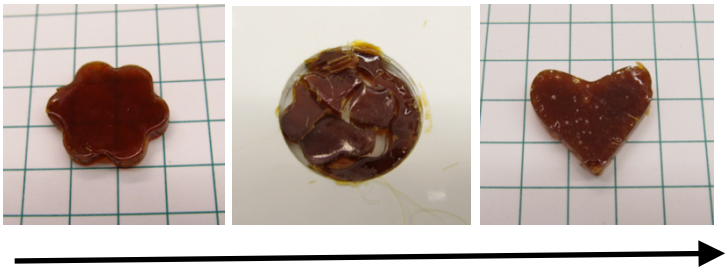

Figure 8.5. Digital photographs of **C-PDMS-14**, demonstrating the thermoplastic nature of the material

8.2 Supporting Information for CHAPTER 3:Phototunable Silicone Crosslinks

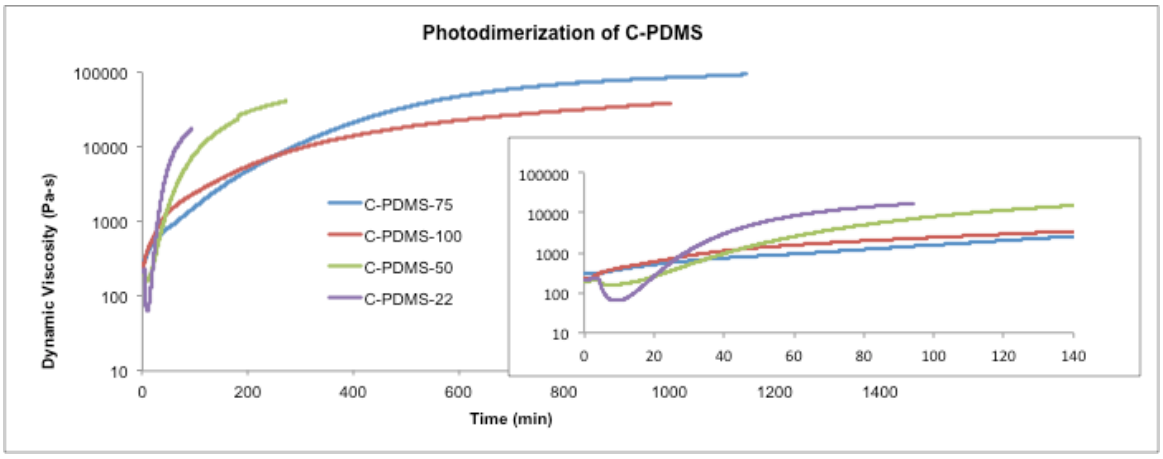

Figure 8.6. Dynamic viscosity during 365 nm irradiation of **C-PDMS**

A 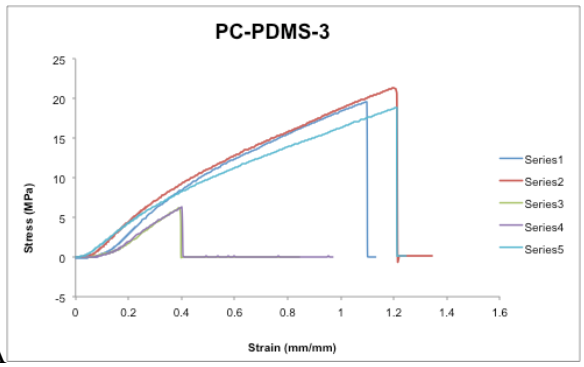

B 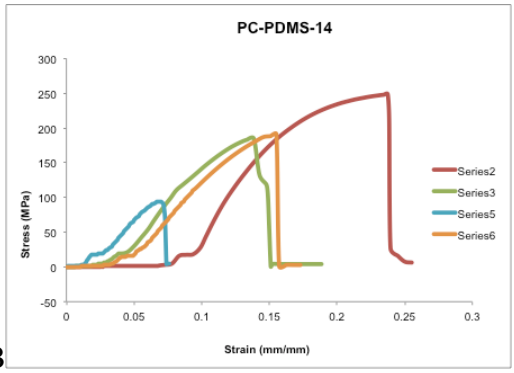

C 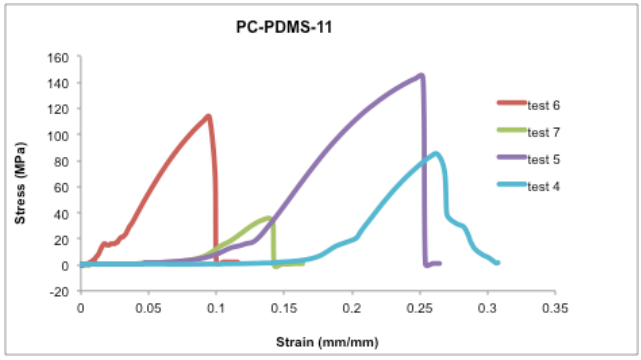

Figure 8.7. Instron tests run on **PC-PDMS** materials

8.3 Supporting Information for CHAPTER 4: Rapid, Metal-Free Room Temperature Vulcanization Produces Silicone Elastomers

Table A 1. Experimental elastomer data

ENTRY #	EXP # In Paper	Silane MW (g)[a]	x-linker (g)[b]	Ratio[c]	Catalyst (µL/ppm)[d]	Hexane (mL)	Rubber (Y/N)	Shore A	Shore OO
				Solvent					
1		28000 (5.0)	Me (0.021)	1|1	30/238	THF 5.0	N	-	-
2		28000 (5.0)	Me (0.021)	1|1	30/238	Hexane 5.0	Y	21	67
3		28000 (5.0)	Me (0.021)	1|1	30/238	Hexane 10.0	Y	10	55
4		28000 (5.0)	Me (0.021)	1|1	30/238	DCM 5.0	Y	10	55
5		28000 (5.0)	Me (0.021)	1|1	30/238	D_4 5.0	Y	9	51
6		28000 (5.0)	Me(0.021)	1|1	30/238	D_4 1.0	N	-	-
				0.5:1					
7	10	28000 (2.5)	Me (0.005)	0.5|1	15/239	2.0	Y	20	78
8		28000 (2.5)	TM (0.003)	0.5|1	15/239	2.0	Y	14	66
9		28000 (2.5)	TE (0.005)	0.5|1	15/239	2.0	Y	17	66
10		28000 (2.5)	TP (0.006)	0.5|1	15/239	2.0	Y	16	66
11		16000 (2.5)	Me (0.009)	0.5|1	15/239	2.0	N		
12		16000 (2.5)	TM (0.006)	0.5|1	15/239	2.0	N		
13	12	16000 (2.5)	TE (0.008)	0.5|1	15/239	2.0	N		
14		16000 (2.5)	TP (0.010)	0.5|1	15/239	2.0	N		
15		5900 (2.5)	Me (0.025)	0.5|1	15/238	2.0	Y	20	70

16	22	5900 (2.5)	TM (0.016)	0.5|1	15/238	2.0	N		
17	23	5900 (2.5)	TM (0.016)	0.5|1	9/143	5.0	Y		11
18	11	5900 (2.5)	TE (0.022)	0.5|1	15/237	2.0	N		
19		5900 (2.5)	TP (0.028)	0.5|1	15/237	2.0	N		
				1:1					
20	13	28000 (2.5)	Me (0.0011)	1|1	15/239	2.0	Y	21	67
21		28000 (2.5)	TM (0.007)	1|1	15/239	2.0	Y	18	67
22	6	28000 (2.5)	TE (0.009)	1|1	15/239	2.0	Y	18	67
23		28000 (2.5)	TP (0.012)	1|1	15/238	2.0	Y	20	66
24		16000 (2.5)	Me (0.0018)	1|1	15/238	2.0	Y	22	67
25		16000 (2.5)	TM (0.012)	1|1	15/238	2.0	N	-	-
26		16000 (2.5)	TE (0.016)	1|1	15/238	2.0	Y	20	68
27		16000 (2.5)	TP (0.020)	1|1	15/238	2.0	Y	28	71
28		5900 (2.5)	Me (0.050)	1|1	15/236	2.0	N	-	-
29	26, 1-5[f]	5900 (2.5)	TM (0.032)	1|1	15/236	2.0	Y	22	75
30	27	5900 (2.5)	TM (0.032)	1|1	1.9/30	2.0	Y	22	78
31		5900 (2.5)	TE (0.044)	1|1	15/236	2.0	Y	11	47
32		5900 (2.5)	TP (0.056)	1|1	15/235	2.0	Y	22	61
				1.5:1					
33	14	28000 (2.5)	Me (0.016)	1.5|1	15/238	2.0	Y	18	62
34		28000 (2.5)	TM (0.010)	1.5|1	15/239	2.0	Y	8	58
35	7	28000 (2.5)	TE (0.014)	1.5|1	15/238	2.0	Y	13	63
36		28000 (2.5)	TP (0.018)	1.5|1	15/238	2.0	Y	16	61
37	19	16000 (2.5)	Me (0.028)	1.5|1	15/238	2.0	Y	18	65
38	16	16000 (2.5)	TM (0.018)	1.5|1	15/238	2.0	Y	23	70
39	8	16000 (2.5)	TE (0.024)	1.5|1	15/238	2.0	Y	21	70

40	18	16000 (2.5)	TP (0.031)	1.5|1	15/237	2.0	Y	18	63
41	25	5900 (2.5)	Me (0.075)	1.5|1	15/235	2.0	Y	30	80
42		5900 (2.5)	TM (0.048)	1.5|1	15/235	2.0	Y	25	69
43	9	5900 (2.5)	TE (0.066)	1.5|1	15/234	2.0	Y	25	68
44		5900 (2.5)	TP (0.084)	1.5|1	15/232	2.0	Y	22	71
				2:1					
45	15	28000 (2.5)	Me (0.021)	2|1	15/238	2.0	Y	10	53
46		28000 (2.5)	TM (0.013)	2|1	15/238	2.0	Y	22	68
47		28000 (2.5)	TE (0.018)	2|1	15/238	2.0	Y	20	68
48		28000 (2.5)	TP (0.024)	2|1	15/238	2.0	Y	5	49
49		16000 (2.5)	Me (0.037)	2|1	15/237	2.0	Y	8	52
50	17	16000 (2.5)	TM (0.023)	2|1	15/238	2.0	Y	14	51
51		16000 (2.5)	TE (0.032)	2|1	15/237	2.0	Y	21	71
52	24	16000 (2.5)	TP (0.041)	2|1	15/236	2.0	Y	-	15
53	12	5900 (2.5)	Me (0.100)	2|1	15/233	2.0	Y	13	51
54		5900 (2.5)	TM (0.064)	2|1	15/234	2.0	Y	18	67
55		5900 (2.5)	TE (0.088)	2|1	15/232	2.0	Y	22	54
56		5900 (2.5)	TP (0.112)	2|1	15/229	2.0	Y		
		Functional Elastomers							
57	21	5900 (2.5)	IT (0.163)	2|1	15/225	2.0	Y	21	66
58	20	5900 (2.5)	VT (0.083)	2|1	15/232	2.0	Y	15	68
59	28	28000 (2.5)	TM (0.009)	1.5|1	15/239	2.0[e]	Y	8	60

[a] Hydride-terminated PDMS: 7-10 cSt (1,190 g mol-1), 2-3 cSt (730 g mol-1).[b] Me: Methyltriethoxysilane, TM: Tetramethyl orthosilicate, TE: Tetraethyl orthosilicate, TP: Tetrapropyl orthosilicate.[c] ratio = alkoxysilane groups : PDMS hydride groups. [d] Catalyst solution: 40 mg of $B(C_5F_5)_3$ in 1 mL of dry toluene. [e] 1.4 mL hexane with 0.6 mL toluene + 1-pyrenemethanol (0.001 g). [f] Table 1 in paper, vary solvent from 0 – 2 mL.

8.4 Supporting Information for CHAPTER 5:Anhydrous Formation of Foamed Silicone Elastomers using the Piers-Rubinsztajn Reaction

Table A 2. Experimental foam data

ENTRY #	EXP # In Paper	Silane MW (g)[a]	x-linker (g)[b]	Ratio[c]	Catalyst (µL/ppm)[d]	Hexane (mL)	Induction Time (s)	Induction st dev	Total time (s)	Totaltime St dev	Density (g/cm^3)	Density St dev
				1:0.5								
F1		730 (1.0)	TM (0.052)	1|0.5	10/380	1.0	-	-		-		
F2		730 (1.0)	TE (0.071)	1|0.5	10/373	1.0	-	-		-		
F3		730 (1.0)	TP (0.091)	1|0.5	10/366	1.0	-	-		-		
F4		1190 (2.0)	TM (0.063)	1|0.5	20/387	1.0	-	-				
F5		1190 (2.0)	TE (0.087)	1|0.5	20/383	1.0	-	-		-		
F6		1190 (2.0)	TP (0.110)	1|0.5	20/379	1.0	-	-		-		
F7		5000 (2.0)	TM (0.012)	1|0.5	20/397	1.0	-	-		-		
F8		5000 (2.0)	TE (0.017)	1|0.5	20/396	1.0	-	-		-		
F9		5000 (2.0)	TP (0.022)	1|0.5	20/395	1.0	-	-		-		
				1:1								
F10	**5**	730 (1.0)	TM (0.104)	1|1	10/362	1.0	5.47	2.17	15.97	0.45	0.128	0.024
F11	**6**	730 (1.0)	TE (0.143)	1|1	10/349	1.0	8.07	2.12	25.40	5.89	1.07	0.012
F12	**7**	730 (1.0)	TP (0.182)	1|1	10/338	1.0	42.97	5.86	75.73	7.94	0.086	0.006
F13	**8**	1190 (2.0)	TM (0.127)	1|1	20/376	1.0	10.30	3.44	23.70	1.60	0.172	0.017
F14	**19**	1190 (2.0)	TE (0.174)	1|1	20/367	1.0	12.03	1.10	35.07	2.85	0.127	0.007
F15	**17**	1190 (2.0)	TP (0.222)	1|1	20/360	1.0	27.43	11.12	68.67	5.71	0.147	0.028
F16	**9**	2570 (2.0)	TM (0.059)	1|1	20/388	1.0	11.33	2.64	14.97	1.36	0.461	0.043
F17		2570 (2.0)	TE (0.081)	1|1	20/384	1.0		17.7		23.5	0.382	

F18		2570 (2.0)	TP (0.103)	1|1	20/380	1.0		36.3		47.6	0.272	
F19		5000 (2.0)	TM (0.024)	1|1	20/395	1.0	N	-		-	-	
F20		5000 (2.0)	TE (0.036)	1|1	20/393	1.0		-		-	-	
F21		5000 (2.0)	TP (0.044)	1|1	20/391	1.0		-		-	-	
				1:1.5								
F22	**1**	730 (1.0)	TM (0.157)	1|1.5	10/345	1.0	13.3	1.21	33.60	0.84	0.227	0.028
F23		730 (1.0)	TE (0.215)	1|1.5	10/329	1.0	52.9	4.05	73.57	6.05	0.156	0.016
F24		730 (1.0)	TP (0.274)	1|1.5	10/314	1.0	194.90	6.30	210.84	10.73	0.146	0.036
F25	**2**	1190 (2.0)	TM (0.191)	1|1.5	20/365	1.0	21.58	5.72	32.15	2.84	0.271	
F26		1190 (2.0)	TE (0.262)	1|1.5	20/353	1.0	26.03	18.17	39.06	23.17	0.184	0.005
F27		1190 (2.0)	TP (0.333)	1|1.5	20/342	1.0	72.99	33.03	155.19	21.56	0.201	0.015
F28	**3**	2570 (2.0)	TM (0.089)	1|1.5	20/382	1.0	16.10	0.71	18.10	1.98	0.315	0.037
F29		2570 (2.0)	TE (0.121)	1|1.5	20/377	1.0		32.2		47.2	0.415	
F30		2570 (2.0)	TP (0.154)	1|1.5	20/371	1.0	144.0	29.51	215.33	26.69	0.294	0.024
F31	**4**	5000 (2.0)	TM (0.094)	1|1.5	20/382	1.0	N	-		-	-	
F32		5000 (2.0)	TE (0.129)	1|1.5	20/375	1.0	N	-		-	-	
F33		5000 (2.0)	TP (0.170)	1|1.5	20/368	1.0	N	-		-	-	
				1:2								
F34	**10**	730 (1.0)	TM (0.201)	1|2	10/333	1.0	31.80	5.15	37.50	4.20	0.140	0.016
F35		730 (1.0)	TE (0.287)	1|2	10/310	1.0	49.23	5.29	79.87	3.11	0.146	0.006
F36		730 (1.0)	TP (0.364)	1|2	10/293	1.0		155		316	0.118	
F37		1192 (2.0)	TM (0.256)	1|2	20/354	1.0	50.94	4.13	60.36	7.98	0.232	0.032
F38		1190 (2.0)	TE (0.350)	1|2	20/340	1.0	62.17	58.86	80.03	133.19	0.187	
F39		1190 (2.0)	TP (0.444)	1|2	20/327	1.0		152.9		243.19	0.27	
F40		2570 (2.0)	TM (0.118)	1|2	20/377	1.0						
F41	**11**	2570 (2.0)	TE (0.162)	1|2	20/370	1.0						

F42	**12**	2570 (2.0)	TP (0.205)	1|2	20/362	1.0					
F43		5000 (2.0)	TM (0.052)	1|2	20/389	1.0	N	-		-	-
F44		5000 (2.0)	TE (0.070)	1|2	20/386	1.0	N	-		-	-
F45		5000 (2.0)	TP (0.090)	1|2	20/382	1.0	N	-		-	-
		Solvent Free									
F46	**13n**	1190 (2.0)	TM (0.127)	1|1	20/376	-		11.68		21.8	0.351
F47	**18n**	1190 (2.0)	TE (0.174)	1|1	20/367	-	Y	16.64		86.89	0.302
F48	**16n**	1190 (2.0)	TP (0.222)	1|1	20/360	-	Y	22.45		418.86	0.23
F49		1190 (2.0)	TM (0.191)	1|1.5	20/365	-	Y	20.56		45.14	0.456
F50		1190 (2.0)	TE (0.262)	1|1.5	20/353	-	Y	25.56		115.02	0.282
F51		1190 (2.0)	TP (0.333)	1|1.5	20/342	-	Y	39.13		556.48	0.243
F52		1190 (2.0)	TE (0.349)	1|2	20/340	-	Y	42.87		171.05	0.32
F53		1190 (2.0)	TM (0.256)	1|2	20/354	-	Y	23.19		72.9	0.329
F54		1190 (2.0)	TP (0.444)	1|2	20/327	-	Y	115.02		759.02	0.298
		Half the solvent									
F55	**14**	1190 (2.0)	TM (0.127)	1|1	20/376	0.5	15.5	1.21	19.33	2.67	0.195
F56		1190 (2.0)	TE (0.174)	1|1	20/367	0.5	Y	28.3		33.4	0.271
F57		1190 (2.0)	TP (0.222)	1|1	20/360	0.5	Y	79		148.0	0.221
		Double the solvent									
F58	**15**	1190 (2.0)	TM (0.127)	1|1	20/376	2.0	21.17	1.16	24.00	1.59	0.082
F59		1190 (2.0)	TE (0.174)	1|1	20/367	2.0	Y	29.6		37.0	0.123
F60		1190 (2.0)	TP (0.222)	1|1	20/360	2.0	Y	85.86		122.0	--

[a] hydride terminated PDMS: 7-10 cst (1,190 g mol^{-1}), 2-3 cst (730 g mol^{-1}). [b] TM: Tetramethylorthosilicate, TE: Tetraethylorthosilicate, TP: Terapropylorthosilicate. [c] ratio = PDMS hydride groups : alkoxysilane groups. [d] Catalyst solution: 40 mg of $B(C_5F_5)_3$ in 1 mL of dry toluene.

8.5 Supporting Information for CHAPTER 6: Silicone foams stabilized by surfactants generated in situ from allyl-functionalized PEG

Table A 3. Variables examined in preparation of foamed PEG-Silicone elastomers

	Parameters							**Outcome**		
Entry	PDMS+ PHMS/g	Added Pt ppm	PEG (g)	Functi-onality[j]	Vacuum (Torr)	PEG M_W	Curing vessel	Viscosity increase	Hardness[g,k]	Foam
1	3.72[a]	----	0	----	176	----	Petri[b]	N	4	N
	Surface/volume ratio									
2	4.08[a]	----	1.0 (20% w/w)	**2**	176	500[d]	Petri[b]	Y	2	Y
3	1.21[a]	----	0.32 (20% w/w)	**2**	176	500	Vial[c]	Y	2	Y
4	8.40[a]	----	2.1 (20% w/w)	**2**	176	500	Petri[d]	Y	2	Y
	Functionality									
5	3.60[a]	----	0.89 (20% w/w)	**3**	176	400[e]	Petri[b]	N	4	N
6	3.72[a]	----	0.94 (20% w/w)	**1**	176	500	Petri[b]	Y	2	Y, less than entry 2
	Additional catalyst									
7	2.42[a]	14	0.61 (20% w/w)	**2**	176	500	Petri[b]	Y	3	Y
8	1.80[a]	19	0.45 (20% w/w)	**2**	749	500	Petri[b]	Y	3	Y
9	1.51[a]	22	0.39 (20% w/w)	**2**	749	500	Petri[b]	Y	3	Y
	PEG Concentration									
10	3.65[a]	----	0.02 (0.5% w/w)	**2**	176	500[d]	Petri[b]	N	4	N
11	4.30[a]	----	0.25 (5.5% w/w)	**2**	176	500[d]	Petri[b]	Slight	2	N, only a few bubbles
12	4.42[a]	----	3.0 (40% w/w)	**2**	176	500	Petri[b]	N	2	Y, large bubble size, 0.5-3 mm
	Pressure Effects									
13	3.36[a]	----	0.85 (20% w/w)	**2**	749	500	Petri[b]	Y	2	Y, very small bubble size, 100 μm
14	3.96[a]	----	0.99 (20% w/w)	**2**	$1x10^{-4}$	500	Petri[b]	Y	2	N

Non-Sylgard PDMS										
15	1.77[f]	48	----	----	749	----	Vial[c]	Slight	4	N[g]
16	2.53	26	0.65 (20% w/w)	**2**	176	500	Vial[c]	Y	3	Y, large bubble size, 5 mm
17	1.98	34	0.52 (20% w/w)	**2**	749	500	Vial[c]	Y	3	Y
18	1.69	60[h]	0.42 (20%w/w)	**2**	749	500	Vial[c]	Y	3	Y
19	1.1[i]	80	0.27	**2**						NMR data

[a]Includes both Sylgard base and curing agent portions in a 10:1 ratio. [b] 35 mm x 10 mm. [c] 20 mL vial, 27 mm diameter. [D] 65 mm x 120 mm. [e] Indicates results were the same with 200 M_w PEG. [f] Vinyl-terminated PDMS of the same viscosity as Sylgard base was used, 5000 cSt (approx. 50 000 M_w). [g] To keep the control to be systematic with the conditions with PEG, a large excess of catalyst was used, this amount for the control containing no PEG caused the material to cure within minutes, and hence, no vacuum was used due to time constraints, and bubbles became entrained in the material. [h]Catalyst solution comprised of 40 mL Pt catalyst, 920 ppm Pt, diluted into 1 mL D4 (octamethylcyclotetrasiloxane, 2.5 cSt). [i] Me_3Si-terminated PDMS of the same viscosity as Sylgard base was used, 5000 cSt (approx. 50 000 M_w). [j] **1**-Diallyl-terminated PEG, **2**-Monoallyl-terminated PEG, **3**-dihydroxy-terminated PEG. [k] 1: oil (honey); 2: gel (toothpaste); 3: soft elastomer (shore A hardness 10); and 4: hard elastomer (shore A hardness 60).